Cavity QED with many atoms

Dissertation an der Fakultät für Physik der
Ludwig-Maximilians-Universität München, vorgelegt von

Ullrich Martini
aus München

February 17, 2000

Contents

Chapter 1

Introduction

Many modern quantum optical experiments examine the interaction of one or a few atoms with a quantized resonator mode of a cavity of very high quality. These experiments allow one to study the coupling of radiation and matter in great detail [10, 6, 38, 21]. The results of these experiments include the demonstration of the quantum nature of light , the modification of spontaneous emission rates by the resonant cavity and the production of light with nonclassical photon counting statistics [32, 33] and even laser operation with one or a few atoms as active laser medium [1].

If the atoms cross the resonator in an atomic beam there is always a nonvanishing probability to find two or more atoms in the resonator. Furthermore, the interaction of a cluster of atoms with the resonator mode is much stronger than that of a single atom. Therefore it is highly desirable to be able to describe the interaction of many atoms with a resonator mode fully quantum mechanically.

The theory of the interaction of many atoms with a quantized resonator mode was originated by the work of Jaynes and Cummings [20] and extended by Tavis and Cummings [36] to the case of many atoms. A collection of two-level-atoms may be described conveniently by regarding the atoms as spin-$\frac{1}{2}$ particles and using Clebsch-Gordan coefficients to couple the atoms to a collective angular momentum, as proposed by Dicke [11]. In his original publication Dicke considered only the totally symmetric coupling, which corresponds to maximum angular momentum. This is appropriate for systems without the influence of dissipative processes, as will be shown here. Because the interaction Hamiltonian has the form of an angular momentum ladder operator the Dicke states simplify the description of a many-atom problem considerably.

In the marginal case of infinitely many atoms the problems has been solved by Davies [12] with the result that the light emitted by an infinite number of atoms is a coherent state in the sense of Glauber [18, 17]. This raises the question of

how many atoms are sufficient to treat the number as approximately infinite.

The situation becomes much more difficult if dissipative processes like spontaneous emission are considered. It is very common in maser theory to treat the interaction time of the atoms with the maser mode as infinitely short. In this treatment atomic dissipation is neglected. This is impossible when systems are considered where the interaction of the atoms with the mode is not intermitted by periods without atoms like it is the case if the flux of atoms is very large or in the case of a ion-trap-laser. Here one has to treat the dissipative processes and the interaction of the atoms with the resonator mode simultaneously.

At this point spontaneous emission causes a difficulty: The action of spontaneous emission of photons on the eigenstates of angular momentum is quite complicated and it seems that the presence of spontaneous emission makes it impossible to use the angular momentum and its projection quantum numbers as collective atomic variables.

The purpose of this work is to show that the collective atomic variables are in fact compatible with the effects of spontaneous emission. This will make it possible to describe experimental results like those of [32] where the interaction of twenty to hundred atoms with a resonator cavity was used to obtain a light source with interesting nonclassical properties. In this experiment the resonator was permanently populated with atoms so that the neglection of spontaneous emission becomes impossible.

The previous theoretical descriptions of this experiment are either restricted to very low numbers of photons [7, 32, 3] oder very low numbers of atoms [26] if a full quantum description of dissipative processes is required. Because the dimension of the state space increases exponentially with the number of atoms it is impossible to treat systems with five or more atoms without resorting to symmetrization. Some work has been done on many-atom laser theory [15, 34, 35]. Here the problem of the dimension of the state space arises also.

Using the theory developed here we will be able to lift these restrictions. This makes it possible to treat systems with significant mean photon numbers as well as large atom numbers.

A common approach to multi-atom problems of this kind is to eliminate the atoms from the dynamics in order to obtain an approximate equation for the resonator mode. This has been done for a classical resonator mode [19] as well as for a quantized description of the resonator mode [13] only. In this approximation one obtains the result that the atoms may be replaced by a single atom whose coupling constant to the resonator mode has been multiplied by the square root of the number of atoms. Other parameters like the intensity of the driving field have to be scaled as well. This scaling behavior has also been observed experimentally [32]. Using the techniques developed here we will compare exact multi-atom

calculations with results obtained from those approximations in order to obtain the range of validity of the approximation used in the elimination of the atoms.

Another approach is to restrict the number of photons in the resonator so that only the lowest states of the atomic ensemble can be excited, as proposed by H.J. Carmichael et al. [7]. They allowed up to two photons, because at least two photons are necessary to obtain the conditional probability of detection a second photon after a first photon has been detected. We will show that this weak field limit is indeed justified, but only for very low values of the mean photon number.

The model (2.1) is not restricted to the interaction of atoms with photons. An example of a different physical system which is described by the same master equation is an array of quantum dots which interacts with phonons. This system has been studied in the special case of four quantum dots by P. Zanardi et al. [40]. Here one is interested in minimizing the coupling constant between the dots and the phonons. This could be achieved by coupling the dots together in order to obtain a dark state which is characterized by zero angular momentum. In the correspondence between this system and the quantum optical system the quantum dots take the place of the atoms and the phonons take the place of the resonator mode. In a similar work it has been proposed [2] to use the symmetric subspace under consideration in this manuscript to reduce the error rate in quantum computation and quantum state storage.

An interesting quantum optical experiment is a micromaser which is pumped not by single atoms but by clusters of atoms. We examine collective effects in micromaser theory, especially on the trapped states. Here one has to distinguish between theories that allow arbitrary atom entrance times [8, 22, 39] and theories that assume that the atoms enter the maser in clusters. Theories of the first type are restricted to very low numbers of atoms. Due to the symmetrization used throughout this work we will focus on masers pumped by atoms arriving in clusters. We will confirm that fluctuations of the atom number of the driving clusters wash out the zero-photon trapped states [39]. In addition we will show that masers which are pumped by large clusters of weakly excited atoms exhibit a very regular behavior.

1.1 Overview

The difficulty in modeling a many-atom system exactly arises from the large state space that is necessary to describe such a system. The main purpose of this work is to show that if all atoms are coupled to the light mode with the same coupling strength a collective description of the atoms is possible and the dimension of the state space is $\frac{1}{6}(Z+1)(Z+2)(Z+3)$, even if all atoms are coupled to individual

reservoirs. This is in contrast to the 4^Z dimensional space needed to describe the Z-Atom system without symmetrization.

The symmetrization procedure drops the information about which atom is excited and which is not excited and keeps only the information about the number of excited atoms. This is exactly the symmetrization procedure required for bosons, but since the atoms can still be distinguished by their position, the spin-statistics theorem does not apply here. Therefore we may apply this symmetrization if the spin of the atoms is half-integer as well.

Assuming resonance between the atoms and the resonator mode the energy contained in the system may appear as photons or excited states. If the number of atoms is larger than the number of energy quanta and resonance is assumed, the number of possible atomic states is no longer restricted by the number of atoms, since there is not enough energy available to excite all atoms. The dimension of the vector space therefore depends only on the total energy of the system.

Since the atoms have two states, excited or not excited, each of the atoms may be described as a spin-$\frac{1}{2}$-system. This spin will be referred to as angular momentum in the following. These spins may be coupled to an collective angular momentum. The eigenvectors of this angular momentum are called Dicke states. It is important to note that all Dicke vectors but the one with the largest possible angular momentum are degenerate.

In analogy with angular momentum we introduce the collective operator L^2 which is constructed from the Z two-level-atoms in the same way as the angular momentum operator describing Z spin-$\frac{1}{2}$-particles. In contrast to the usual angular momentum operator L^2 is dimensionless.

In order to describe spontaneous emission, one needs a dissipative generalization of the Dicke vectors. We replace eigenvectors of L^2 by operators $\hat{\xi}_l$ which are simultaneous left and right eigenstates of L^2 in the sense that $\hat{\xi}_l L^2 = L^2 \hat{\xi}_l = l(l+1)\hat{\xi}_l$. In analogy with Dicke states the quantum number l gives the symmetry of the coupling of the individual spins.

In this basis the matrix elements of the Hamiltonian are calculated easily, since the Hamiltonian has the form of an angular momentum ladder operator. In contrast, the calculation of the matrix elements of the Lindblad operator used to describe atomic baths and spontaneous emission is quite complicated.

The outline of this manuscript is the following: First, we solve the Hamiltonian problem without dissipation in the marginal cases $Z \ll M$ and $Z \gg M$ where Z is the number of atoms and M the number of energy quanta, i.e. the number of photons plus the number of excited atoms. Since we restrict ourselves to exact resonance between the atoms and the resonator mode the energy is determined by the value of M. We will show that in the second case the many-atom sys-

tem indeed corresponds to a one-atom system where the coupling constant g is replaced by $\sqrt{Z}g$, while in the case $Z \ll M$ the correct scaling is $\sqrt{M}g$. In the case $Z \ll M$ one has to scale by the energy, not the atom number.

The case $M \approx Z$ can be treated with good accuracy if higher orders of the perturbation expansion in $\frac{Z}{M}$ respectively $\frac{M}{Z}$ are included. These higher orders do not exhibit any scaling behavior.

The inclusion of dissipative processes, especially of the spontaneous emission of the atoms requires the introduction of a new set of basis states which is suitable to the description of the interaction of the atoms with the resonator mode as well as to the atomic dissipation. We will introduce three new sets of basis states. One of these sets is a generalization of the Dicke vectors and the other two of these sets are ancillary basis sets used to determine the properties of the generalized Dicke vectors.

The first basis consists of eigenstates of the atomic dissipation. This set is only used to determine the dimension of the minimal symmetric atomic subspace which is closed under the action of the spontaneous emission. Unfortunately, these states are not well suited for the description of the interaction of the atoms with the resonator mode.

The second basis is a generalization of the Dicke states. This set of basis states is very well suited to the description of the interaction of the atoms with the resonator mode as well as the spontaneous emission of photons. Using these basis states we will establish selection rules restricting the matrix elements of the atomic dissipation with respect to these basis states.

The third basis is an auxiliary basis needed to make use of the permutation symmetry of the atoms in the calculation of the matrix elements of spontaneous emission. Using this basis we will derive and solve a recurrence relation for the matrix elements of the spontaneous emission with respect to the Dicke states. These matrix elements assume a simple form, despite their rather complicated calculation.

The theory is applied to a micromaser which is pumped not by single atoms but instead by a cluster of atoms. It will be shown that the irregular dependence of the mean photon number on the velocity of the atoms turns into a regular behavior where the time the atoms spend in the resonator is scaled by the square root of the photon number under the condition that the number of atoms is considerably larger than the mean number of photons. The effect of fluctuations of the atom numbers in the driving clusters will be discussed.

Finally, we apply the theory to a system driven by a classical light field. It will be shown that the theory reproduces experimentally measured intensity correlation functions $g^{(2)}$. We determine the dependence of the stationary mean photon

number and the correlation function on the intensity of the driving field. If the driving field is very low the correlation function does not depend on the intensity of the driving field. The experiment [32] used a driving field beyond this limit.

Our exact solution makes it possible to test an approximate theory where the atoms are adiabatically eliminated and the coupling constant and the intensity of the driving field are scaled by the square root of the number of atoms. We will give the range of validity of this approximation. Because of the scaling of the driving field it is expected that the approximation fails at large numbers of atoms. Our results show that it fails at low numbers of atoms, too. Investigating the spectra of the resonator mode we find that the adiabatic elimination of the atoms is only possible if the spectrum is essentially the spectrum of a single atom interacting with the cavity.

Chapter 2

The Model

The theoretical model we use to describe the interaction of the atoms with the resonator mode is the many-atom Jaynes-Cummings model. It consists of an arbitrary number of two-level atoms which are in exact resonance with a quantized resonator mode. All atoms and the resonator mode are coupled to heat baths.

The derivation of the Hamilton operator describing the interaction between the atoms and the mode uses the dipole approximation and the rotating wave approximation. The dipole approximation requires that the wavelength of the electro magnetic field is much larger than the atomic dimensions such that the atom may be replaced by its dipole moment. The rotating wave approximation takes into account only the circular polarized component that couples dominantly to the two-level system and neglects the other component. This is consistent with the two-level description of the atom. For an introduction into the theory of the interaction of atoms with an electromagnetic field see e.g. [25, 9, 27].

Since the model includes losses through the cavity mirrors and spontaneous emission we have to use a master equation in order to describe the time evolution instead of a Schrödinger equation. The dissipative part of the dynamics is then described by Lindblad operators [24]. The atoms are coupled to individual heat baths. This is necessary since we have assumed that the atoms are distinguishable by their position. We assume that the fluctuations of the environments of the atoms and the resonator mode are uncorrelated at different times and that the internal states of the baths are not altered by the interaction with the atoms. Under these assumptions the equation of motion may be formulated as a master equation [28, 41].

All atoms couple to the resonator mode with the same coupling constant and have the same spontaneous emission lifetimes.

It is not necessary that all atoms are located at the same place, since a flat

resonator mode also gives the same coupling constants for all atoms. Also the symmetrization postulate does not enter here, since the atoms are assumed to be distinguishable by position. In particular we do not assume that the atomic densities are sufficient for Bose-Einstein Condensation. Hence it is possible to consider the symmetric atomic variables only, given that the initial condition is symmetric.

If the temperature of the heat baths is zero, the stationary state of the system is trivial with no photons in the resonator mode and no excited atoms. Therefore we will include pump processes like a classical light source coupled into the resonator through the mirrors or the maser pump process where atoms enter the resonator in the upper state.

2.1 The Equation of Motion

Because of dissipation we have to describe the system with density operators instead of wave functions. The appropriate generalization of the Schrödinger equation is the master equation (For an introduction to master equations see e.g. [14, 27]).

The model we discuss here is characterized by the master equation $\dot{\hat{\rho}} = \mathcal{L}\hat{\rho}$ for the density operator $\hat{\rho}$ in Lindblad form [24], where

$$\mathcal{L}\hat{\rho} = \frac{1}{i\hbar}[H, \hat{\rho}] + \mathcal{L}_a\hat{\rho} + \mathcal{L}_f\hat{\rho} \tag{2.1}$$

with the Hamilton operator

$$H = \hbar\omega a^\dagger a + \frac{\hbar\Omega}{2}\sum_i \sigma_z^{(i)} - \frac{\hbar g}{2}\sum_i (a^\dagger\sigma_-^{(i)} + a\sigma_+^{(i)}) - \frac{\hbar\epsilon}{2}(\mathrm{e}^{iwt}a + \mathrm{e}^{-iwt}a^\dagger) \tag{2.2}$$

the resonator mode dissipation

$$\begin{aligned}\mathcal{L}_f\hat{\rho} &= -\frac{A}{2}(1+\nu)(a^\dagger a\hat{\rho} + \hat{\rho}a^\dagger a - 2a\hat{\rho}a^\dagger) \\ &- \frac{A}{2}\nu(aa^\dagger\hat{\rho} + aa^\dagger\hat{\rho} - 2a^\dagger\hat{\rho}a)\end{aligned} \tag{2.3}$$

and the atomic dissipation

$$\begin{aligned}\mathcal{L}_a\hat{\rho} &= -\frac{B}{8}(1-s)\sum_i(\sigma_+^{(i)}\sigma_-^{(i)}\hat{\rho} + \hat{\rho}\sigma_+^{(i)}\sigma_-^{(i)} - 2\sigma_-^{(i)}\hat{\rho}\sigma_+^{(i)}) \\ &-\frac{B}{8}s\sum_i(\sigma_-^{(i)}\sigma_+^{(i)}\hat{\rho} + \hat{\rho}\sigma_-^{(i)}\sigma_+^{(i)} - 2\sigma_+^{(i)}\hat{\rho}\sigma_-^{(i)}).\end{aligned} \tag{2.4}$$

$a^\dagger$ and a are the resonator mode annihilation and creation operators, $\sigma_z^{(i)}$ and ${\sigma_\pm}^{(i)} = \sigma_x^{(i)} \pm \sigma_y^{(i)}$ are the atomic Pauli operators, and ϵ is the amplitude of a classical light field used to drive the system.

The first three terms represent the commutator of the density operator with the Hamiltonian of the system which contains the energy of the light mode, of the atoms and their interaction. The terms proportional to A describe the damping of the light mode caused by an imperfect cavity and the two last terms proportional to B describe spontaneous emission of the atoms. Each atom is coupled to an individual reservoir. The parameter s was introduced to allow for an inverted atomic bath which might be used to obtain laser behavior For $s > \frac{1}{2}$ the atoms are inverted.

The second to last term proportional to $B(1-s)$ will be referred to as $\mathcal{L}_{a,-}$ since it is the atomic loss term and correspondingly the term proportional to Bs as $\mathcal{L}_{a,+}$ This term describes an atomic pump process, since the stationary state of an atom with $s > 0$ describes an excited atom [16].

From now on a rotating frame will be used to eliminate the self-energy terms. The dephasing term has been dropped, which amounts to the assumption $B_\parallel = 2B_\perp$. The method developed here could easily be generalized to include the dephasing term.

It is possible to parameterize the spontaneous emission differently in order to describe the interaction of the atoms with a vacuum containing ν thermal photons:

$$\mathcal{L}_\nu\hat{\rho} = -\frac{B}{8}(1+\nu)\sum_i(\sigma_+^{(i)}\sigma_-^{(i)}\hat{\rho} + \hat{\rho}\sigma_+^{(i)}\sigma_-^{(i)} - 2\sigma_-^{(i)}\hat{\rho}\sigma_+^{(i)}) \tag{2.5}$$

$$-\frac{B}{8}\nu\sum_i(\sigma_+^{(i)}\sigma_-^{(i)}\hat{\rho} + \hat{\rho}\sigma_+^{(i)}\sigma_-^{(i)} - 2\sigma_+^{(i)}\hat{\rho}\sigma_-^{(i)}). \tag{2.6}$$

The terms $\mathcal{L}_{-,\mathrm{nd}}\hat{\rho} = \sigma_+^{(i)}\hat{\rho}\sigma_-^{(i)}$ and $\mathcal{L}_{+,\mathrm{nd}}\hat{\rho} = \sigma_-^{(i)}\hat{\rho}\sigma_+^{(i)}$ make it difficult to describe the system in a basis constructed from symmetrized state vectors, since the action of these operators on symmetrized state vectors destroys the symmetry of the vectors completely. The main purpose of this work is to show how this problem can be solved.

The effect of spontaneous emission of one atom on the tensor product of Dicke states leads to complicated expressions which contain explicitly the Clebsch-Gordan-Coefficients. In order to avoid these involved expressions it is useful to look for expressions that make no reference to an individual atom.

2.2 Collective Damping of the Atoms

If one assumes that atomic dissipation does not occur as spontaneous emission by individual atoms but as a collective process, one can write down the atomic Liouville operator using the collective operators $S_\pm = \sum_i \sigma_\pm(i)$ as

$$-\frac{D}{8}(1+\nu)\left(S_+S_-\hat{\rho} + \hat{\rho}S_+S_- - 2S_-\hat{\rho}S_+\right) \\ -\frac{D}{8}\nu\left(S_+S_-\hat{\rho} + \hat{\rho}S_+S_- - 2S_-\hat{\rho}S_+\right). \tag{2.7}$$

This Liouville operator is very different from the atomic part of (2.1) because in contrast to that model of the spontaneous the collective damping of the atoms does not alter the symmetry of the atoms. In order to formalize this argument we use the collective operator $L^2 = \left(\sum_i \sigma^{(i)}\right)^2$. Because the individual atoms can be described as spin-$\frac{1}{2}$-systems L^2 is formally analogous to an angular momentum operator. In analogy with angular momentum we may use the operator L^2 to describe the symmetry of a state. Eigenstates of L^2 with a large eigenvalue are highly symmetric, while eigenstates of L^2 with a small eigenvalue are unsymmetric.

The collective damping operator (2.7) commutes with the angular momentum operator L^2 while the individual damping operator (2.1) does not.

Because of this property the diagonalization of a Liouville operator containing only collective atomic dissipation is much simpler than the treatment of individual atomic spontaneous emissions. Yet, it is not clear which physical system is properly described by (2.7) and this Liouville operator will not be treated in detail.

2.3 The Eigenvalue Problem

The equation of motion $\dot{\rho} = \mathcal{L}\rho$ (2.1) can be interpreted as an eigenvalue problem: We have to find $\lambda_i, \hat{\rho}_i$ and $\check{\rho}_i$ such that

$$\begin{aligned} \mathcal{L}\hat{\rho}_i &= \lambda_i\hat{\rho}_i, \\ \check{\mathcal{L}}\check{\rho}_i &= \lambda_i\check{\rho}_i \end{aligned} \tag{2.8}$$

where the adjoint Liouville operator $\check{\mathcal{L}}$ is defined by its action on an arbitrary observable $\mathcal{O}$:

$$\mathrm{tr}\left((\check{\mathcal{L}}\mathcal{O})\hat{\rho}\right) = \mathrm{tr}\left(\mathcal{O}(\mathcal{L}\hat{\rho})\right). \tag{2.9}$$

This is the definition of the adjoint of a linear operator on a Hilbert Space. For an introduction to the theory of operators on Hilbert spaces see e. g. [31].

For simplicity we will denote the $\hat{\rho}_i$ and $\check{\rho}_i$ as "right and left eigenstates" of $\mathcal{L}$ or short as "states", although the precise wording would be "eigenoperators and eigenobservables". Likewise we will denote objects like $\mathcal{L}$ that act linearly on the states $\hat{\rho}_i$ or $\check{\rho}_i$ as operators and not as superoperators, as it would be appropriate for objects that operate on operators.

Once these eigenvalues and eigenstates are known, all stationary and dynamic properties of the system may be calculated easily.

Chapter 3

Eigenvalues of the Hamilton Operator

Before examining the full Liouville operator with the dissipative and driving terms we first determine the eigenvalues of the interaction Hamiltonian only. We will find that the scaling of g with the square root of the number of atoms Z does not give correct results if M, the sum of photons and excited atoms, is larger than Z. From this result we expect that in this regime the scaling will not give correct results later when the dissipation and the driving field are included, as we will confirm in chapter 8.

In this chapter we will derive approximative expressions for the eigenvalues of the interaction Hamiltonian from (2.1) in the two marginal cases $Z \ll M$ and $Z \gg M$, where Z is the number of atoms and M is the number of photons plus the number of excited atoms. We will derive an approximation for the eigenvalues that is useful even if $M \approx Z$. The analytical expressions will be used to examine the validity of the system size scaling where one replaces a system consisting of Z atoms interacting with the radiation field by a system with one atom. The multitude of atoms is accounted for by scaling the coupling constant $g \to g\sqrt{Z}$. It will be shown that this scaling holds only for the largest eigenvalues and if $Z \gg M$. If $Z \ll M$ it is shown that the scaling parameter is not Z but M.

In contrast to the one-atom case, the Jaynes-Cummings-model, there is no analytical expression for the eigenvalues of the Liouville Operator (2.1) if the number of atoms is larger than two. This is because the matrices whose eigenvalues and eigenvectors are needed, are $Z+1$-dimensional if there is enough energy present to excite all atoms.

If A, B, and ϵ are zero and the atoms are in resonance with the resonator mode the eigenstates are characterized by a parameter $n_a + n_f = M$ which gives the total energy of the resonator mode and the atoms, in other words the sum of

photons n_f and exited atoms n_a. If M is fixed, n_f is determined by n_a.

The remainder of the Hamilton operator in the case $\epsilon = 0$ does not couple states with different values of M. In order to simplify the notation we introduce the operator H_M which acts only on the subspace with total energy M and the interaction Hamiltonian H_o which contains all terms of 2.1 proportional to g.

In the marginal cases $M \gg Z$ or $M \ll Z$ one can approximate H_M by an operator that can be identified with the $z-$component of an angular momentum operator[1]. We will see that another component of this operator is diagonal such that the diagonalization may be performed by a simple rotation. For the case that $Z \gg M$ this has been discussed by M. Kozierowski et al. [23]. Their work will be generalized to the complementary case $Z \ll M$ here.

The accuracy of the eigenvalues obtained by that procedure will be improved using perturbation theory.

3.1 Dicke Vectors

In analogy to the collective angular momentum of a sample of spin-$\frac{1}{2}$-particles a cluster of two-level-atoms can be described collectively. The eigenstates of the operator $L^2 = \left(\sum_i \sigma^{(i)}\right)^2$ are represented by Dicke vectors $|Z, l, m, r\rangle$ as introduced by R. Dicke in [11]. The quantum number l parametrises the eigenvalues of L^2:

$$L^2 |Z, l, m, r\rangle = l(l+1) |Z, l, m, r\rangle . \tag{3.1}$$

The quantum number r is necessary because the coupling of the atoms is not unique. This ambiguity has no effect on the eigenvalues of the Hamiltonian, but it will later be important for the calculation of the matrix elements of the Liouville operator.

The projection quantum number m runs from $-l$ to l. It is related to the number n_a of excited atoms by

$$n_a = \frac{Z}{2} + m. \tag{3.2}$$

We recognise the atomic parts of the Hamiltonian, $\sum_i \sigma_\pm^{(i)}$, as the ladder operators from angular momentum theory. Using the analogy to angular momentum we can

[1] This angular momentum operator has no direct connection to the angular momentum from the Dicke states, since the procedure leading to the Dicke states is exact in contrast to the approximation described here.

easily determine the matrix elements of the Hamilton operator: In the general case $l < \frac{Z}{2}$ the atomic matrix elements become

$$\begin{aligned} \langle Z, l, m-1, r| \langle n_f + 1| \quad H \quad |n_f\rangle |Z, l, m, r\rangle & \\ = \quad \frac{\hbar g}{2}\sqrt{(l-m+1)(Z+m-l)(n_f+1)}, & \quad (3.3) \\ \langle Z, l, m+1, r| \langle n_f - 1| \quad H \quad |n_f\rangle |Z, l, m, r\rangle & \\ = \quad \frac{\hbar g}{2}\sqrt{(l-m)(Z+m+1-l)(n_f+1)}, & \quad (3.4) \end{aligned}$$

where $|n_f\rangle$ denotes n_f-photon Fock states of the resonator mode. Matrix elements with $|\Delta m| \neq 1$ are zero.

We will now focus on the case $l = \frac{Z}{2}$.

3.2 Lowest Order Perturbation Theory

The nonvanishing matrix elements of H in the case $l = \frac{Z}{2}$

$$\begin{aligned} \langle n_a - 1| \langle n_f + 1| H |n_f\rangle |n_a\rangle &= \frac{\hbar g}{2}\sqrt{(Z-n_a+1)n_a(n_f+1)}, & (3.5) \\ \langle n_a + 1| \langle n_f - 1| H |n_f\rangle_N |n_a\rangle &= \frac{\hbar g}{2}\sqrt{(Z-n_a)(n_a+1)n_f} & (3.6) \end{aligned}$$

may be expanded in a Taylor series

$$\sqrt{1+x} \approx 1 + \frac{1}{2}x - \frac{1}{8}x^2. \quad (3.7)$$

The states $|n_a\rangle$ are shorthand for Dicke vectors [11]. The Dicke vectors are eigenvectors of the angular momentum operator which results from the coupling of the Z spin-$\frac{1}{2}$ operators representing the individual atoms to a collective angular momentum operator. Here all the Dicke vectors have the same maximal angular momentum $l = \frac{Z}{2}$. This restriction is only possible if no atomic spontaneous emission occurs, as is the case considered in this chapter.

This approximated matrix element will be expressed in terms of the three components of the angular momentum operator so that they can easily be rotated.

If $M \gg Z$ the energy must be predominantly stored in the resonator mode such that $n_a \ll n_f < M$. In this case we approximate

$$\begin{aligned} \sqrt{n_f+1} = \sqrt{M-n_a+1} &= \sqrt{M}\sqrt{1-\frac{n_a-1}{M}} \\ &\approx \sqrt{M}\left(1 - \frac{n_a-1}{2M} + \frac{(n_a-1)^2}{8M^2}\right). \quad (3.8) \end{aligned}$$

If $M \ll Z$ mean excitation of the atoms will be low such that $n_a \ll Z$. In this case we approximate (3.6) by

$$\sqrt{Z - n_a + 1} = \sqrt{Z}\sqrt{1 - \frac{n_a - 1}{Z}} \approx \sqrt{Z}\left(1 - \frac{n_a - 1}{2Z} + \frac{(n_a - 1)^2}{8Z^2}\right). \tag{3.9}$$

In the first approximation we keep only the leading term of the expansion of the square root. Hence, H_M is approximated in the case of $M \gg Z$ by the operator $H_M^{(3)}$ whose nonvanishing matrix elements are

$$\begin{aligned} \langle n_f + 1| \langle n_a - 1| H_M^{(3)} |n_f\rangle |n_a\rangle &= \frac{\hbar g}{2}\sqrt{M}\sqrt{n_a(Z - n_a + 1)}, \\ \langle n_a| \langle n_f| H_M^{(3)} |n_f + 1\rangle |n_a - 1\rangle &= \frac{\hbar g}{2}\sqrt{M}\sqrt{n_a(Z - n_a + 1)}, \end{aligned} \tag{3.10}$$

and in the case $M \ll Z$ by

$$\begin{aligned} \langle n_f + 1| \langle n_a - 1| H_M^{(3)} |n_f\rangle |n_a\rangle &= \frac{\hbar g}{2}\sqrt{Z}\sqrt{n_a(M - n_a + 1)}, \\ \langle n_f| \langle n_a| H_M^{(3)} |n_f - 1\rangle |n_a - 1\rangle &= \frac{\hbar g}{2}\sqrt{Z}\sqrt{n_a(M - n_a + 1)}. \end{aligned} \tag{3.11}$$

This approximation gives reasonable results for $M \gtrsim 2Z$ respectively $Z \gtrsim 2M$.

The dimension of $H_M^{(3)}$ depends on the number of energy quanta M, if $M < Z$ and on the number of atoms Z, if $M > Z$. In the case $M \gg Z$ the only effect of M is a scaling of g, and similarly the only effect of Z in the case $Z \gg M$ is a scaling of g. The determination of the eigenvalues is completely analogous. In the following we will focus on the case $Z \gg M$.

The eigenvalues and eigenvectors $H_M^{(3)}$ can be easily determined with the help of the algebraic properties of $H^{(3)}$. We will show that there are two additional operators, $H_M^{(1)}$ and $H_M^{(2)}$ that form together with $H_M^{(3)}$ the angular momentum commutation algebra. In other words, these three operators fulfill the same commutation relations as the three components of the angular momentum operator L_x, L_y and L_z. It is well-known from the quantum theory of angular momentum that this property alone is sufficient to determine the eigenvalues and eigenstates of $H_M^{(3)}$ (See any textbook on quantum mechanics, for a thorough introduction to the quantum theory of angular momentum see [5]).

We define for $Z > M$ additional hermitian operators $H_M^{(1)}$ and $H_M^{(2)}$ by

$$\begin{aligned} {}_{Z,M}\langle n_a - 1| H_M^{(1)} |n_a\rangle_{Z,M} &= i\frac{\hbar g}{2}\sqrt{Z}\sqrt{n_a(M - n_a + 1)}, \\ {}_{Z,M}\langle n_a| H_M^{(1)} |n_a - 1\rangle_{Z,M} &= -i\frac{\hbar g}{2}\sqrt{Z}\sqrt{n_a(M - n_a + 1)}, \\ {}_{Z,M}\langle n_a| H_M^{(2)} |n_a\rangle_{Z,M} &= \frac{\hbar g}{2}\sqrt{Z}\,(-M + 2n_a)\,. \end{aligned} \tag{3.12}$$

The other matrix elements of $H_M^{(2)}$ and $H_M^{(1)}$ are zero. We use the notation $|n_a\rangle_{Z,M} = |n_a\rangle\,|n_f = M - n_a\rangle$.

Since the matrix elements of $H_M^{(2)}$ contain the number n_a of excited atoms in a very simple form we can write any operator whose matrix elements are given as a function of n_a as an operator function of $H_M^{(2)}$. In this way we obtain a representation of the approximated Hamiltonian which is independent of the basis in use.

In the following we will see that there are unitary transformations that permute the $H_M^{(i)}, i = 1, 2, 3$. Therefore, these operators are different representations of the same operator using different basis sets.

The commutation relation between the operators $H_M^{(1)}, H_M^{(2)}$ and $H_M^{(3)}$ are

$$\left[H_M^{(i)}, H_M^{(j)}\right] = i\hbar g\sqrt{Z}\epsilon_{ijk}H_M^{(k)}. \tag{3.13}$$

These commutation relations are exactly the commutation relations of angular momentum. The number of atoms and the coupling constant appear here in the form $g\sqrt{Z}$. This means that for the eigenvalues of $H_M^{(3)}$ the scaling of the coupling constant is exact.

From the theory of angular momentum we obtain immediately the eigenvalues of the approximated Hamilton operator:

$$\frac{\hbar g}{2}\sqrt{Z}k, k = -M, -M+2, \ldots, M. \tag{3.14}$$

The eigenvectors of $H_M^{(3)}$ remain to be determined. Since $H_M^{(2)}$ is diagonal the eigenstates of $H_M^{(2)}$ are the Dicke vectors. The eigenstates of $H_M^{(3)}$ are then found by applying a rotation that maps $H_M^{(2)}$ onto $H_M^{(3)}$.

We choose an unitary transformation U_{MZ} such that:

$$\begin{aligned} U_{MZ}^\dagger H_M^{(1)} U_{MZ} &= H_M^{(1)}, \\ U_{MZ}^\dagger H_M^{(2)} U_{MZ} &= -H_M^{(3)}, \\ U_{MZ}^\dagger H_M^{(3)} U_{MZ} &= H_M^{(2)}. \end{aligned} \tag{3.15}$$

Since the $H_M^{(1)}, H_M^{(2)}$ and $H_M^{(3)}$ are generators of the rotations in the space of the Dicke vectors, we could express U_{MZ} in terms of $H_M^{(1)}, H_M^{(2)}$ and $H_M^{(3)}$.

There is another transformation that permutes the operators cyclically. This transformation could be used here as well.

Figure 3.1 shows the approximate and exact eigenvalues for $Z \approx M = 4$. The exact eigenvalues have been obtained numerically. For $Z < 4$ there is qualitative

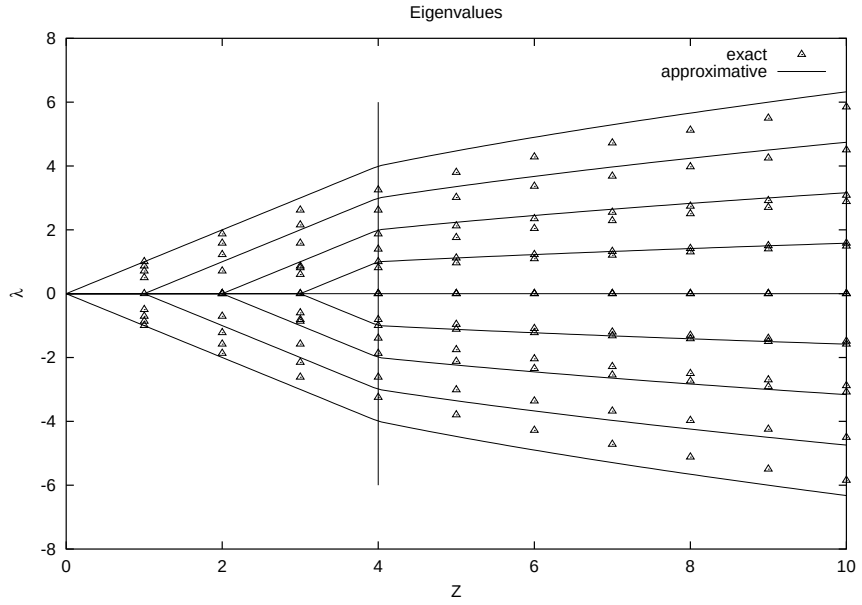

Figure 3.1: The exact eigenvalues (triangles) and the approximative eigenvalues from lowest order perturbation theory (lines) for $M = 4$, $1 \leq Z \leq 4$ and $l = \frac{Z}{2}$

accordance between the exact and the approximative eigenvalues, but the errors of the eigenvalues are of the order of the distance of the eigenvalues. For $Z > 4$ the lowest eigenvalues are in good agreement with the linear approximation while the error of the approximation of the largest eigenvalues is of the order of the distance of the eigenvalues. The vertical line marks the value of $Z = M = 4$ where the two approximations both become invalid. Even at this value of Z the approximations do not diverge.

The exact eigenvalues and their lowest-order approximations for even atom numbers are displayed in figure 3.2 and the corresponding eigenvalues for odd atom numbers in figure 3.3. The approximate expressions for the odd and even eigenvalues are the same. Here the eigenvalues for $l < \frac{Z}{2}$ are displayed also. While the error is of the order of 10% at $Z \approx M = 4$ the approximation is very good for $Z \gg M$.

Obviously, (3.14) describes the eigenvalues very well if $Z > 2M$. Because g and Z enter (3.14) only in the combination $g\sqrt{Z}$ this means that the scaling describes the eigenvalues correctly. On the other hand, if $Z < 2M$ the scaling of g by the square root of the number of atoms fails.

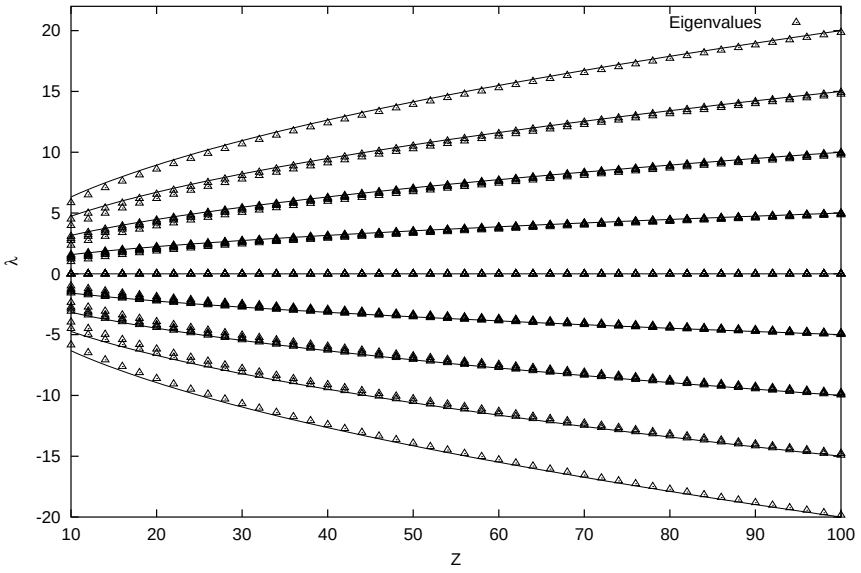

Figure 3.2: All eigenvalues corresponding to even numbers of atoms (triangles) and the approximative eigenvalues from linearization (lines) for $M = 4$, $Z \geq 10$

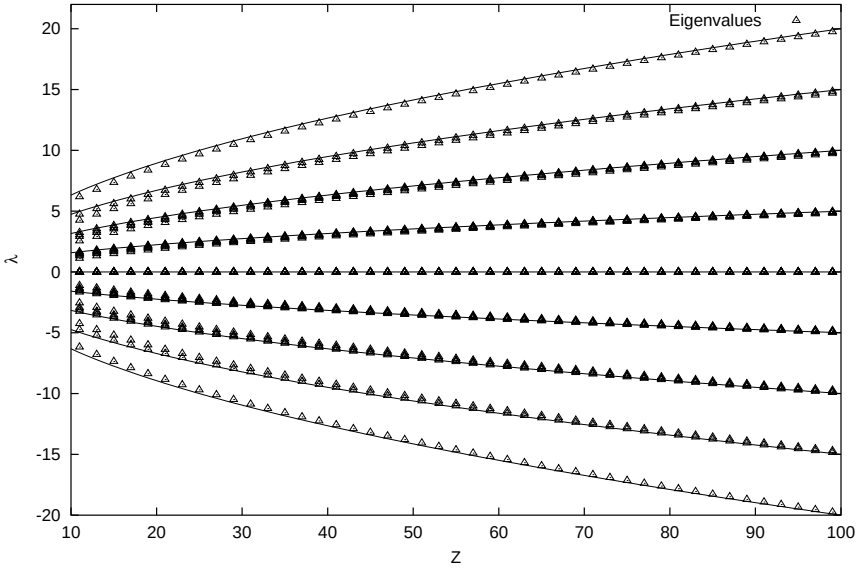

Figure 3.3: All eigenvalues corresponding to odd numbers of atoms (triangles) and the approximative eigenvalues from linearisation (lines) for $M = 4$, $Z \geq 10$

3.3 First Order Perturbation Theory

Now we proceed to improve the eigenvalues by a higher order of perturbation theory. The expansion (3.8) respectively (3.9) can be used to expand the Hamilton

in a Taylor series whose leading term is proportional to $H_M^{(3)}$. Using this expansion we can approximate the eigenvalues to the second order of $\frac{M}{Z}$ respectively $\frac{Z}{M}$.

All nonzero matrix elements of H_M are on the first side diagonal above ore below the diagonal. We can express these matrix elements in terms of the ladder operators

$$\begin{aligned} H_M^+ &= \frac{1}{2}\left(H_M^{(3)} + iH_M^{(1)}\right), \\ H_M^- &= \frac{1}{2}\left(H_M^{(3)} - iH_M^{(1)}\right). \end{aligned} \tag{3.16}$$

Using this substitution we can easily apply the transformation that diagonalizes $H_M^{(2)}$.

The matrix elements of H are

$$\begin{aligned} {}_{MZ}\langle n_a| H |m_a\rangle_{MZ} &= \delta_{m,n-1}\sqrt{Z+1-n}\sqrt{n(M-n+1)} \\ &\quad +\delta_{m,n+1}\sqrt{Z-n}\sqrt{(n+1)(M-n)} \\ &= \delta_{m,n-1}\sqrt{Z-n}\,\langle n| H_M^+ |m\rangle \\ &\quad +\delta_{m,n-1}\sqrt{Z-n}\,\langle n| H_M- |m\rangle \end{aligned} \tag{3.17}$$

so that H_M becomes

$$\begin{aligned} H_M = \frac{1}{2}\sqrt{Z+1-\frac{1}{2}(M-H_M^{(2)})}\left(H_M^{(3)} + iH_M^{(1)}\right) \\ + \frac{1}{2}\sqrt{Z-\tfrac{1}{2}(H_M^{(2)}+M)}\left(H_M^{(3)} - iH_M^{(1)}\right). \end{aligned} \tag{3.18}$$

This expression can easily be verified by taking its matrix elements with respect to the Fock-Dicke vectors. Please note that it is only meaningful if M is fixed, in order to obtain a corresponding expression for the unrestricted Hamilton operator H_o we had to replace M by an appropriate operator.

Using the unitary transformation U_{MZ} and inserting $U_{MZ}U_{MZ}^\dagger = 1$ where neces-

sary we obtain immediately an expression for the rotated Hamilton operator

$$\begin{aligned} U_{MZ}^{\dagger} H_M U_{MZ} &= \frac{1}{2}\sqrt{Z+1-\frac{1}{2}\left(M-H_M^{(3)}\right)}\left(H_M^{(2)}+iH_M^{(1)}\right) \\ &\quad +\frac{1}{2}\sqrt{Z-\frac{1}{2}\left(M-H_M^{(3)}\right)}\left(H_M^{(2)}-iH_M^{(1)}\right) \\ &= \frac{1}{2}\left(\sqrt{Z+1-\frac{1}{2}\left(M-H_M^{(3)}\right)}+\sqrt{Z-\frac{1}{2}(M-H_M^{(3)})}\right)H_M^{(2)} \\ &\quad +\frac{i}{2}\left(\sqrt{Z+1-\frac{1}{2}\left(M-H_M^{(3)}\right)}-\sqrt{Z-\frac{1}{2}(M-H_M^{(3)})}\right)H_M^{(1)}. \end{aligned} \tag{3.19}$$

Again we expand the square roots in a Taylor series (3.7) and treat the linear and quadratic terms as a perturbation of the leading term which is proportional to the diagonal operator $H_M^{(2)}$.

Inserting this approximation into (3.19) we obtain

$$\begin{aligned} U_{MZ}^{\dagger} H_M U_{MZ} \approx \frac{\hbar g}{2}\sqrt{Z}\Bigg(&\left(1-\frac{M-1}{4Z}+\frac{-M^2+2M-2}{32Z^2}\right)H_M^{(2)} \\ &+\frac{1}{4Z}\left(1+\frac{M-1}{4Z}\right)\left(H_M^{(3)}H_M^{(2)}+iH_M^{(1)}\right) \\ &-\frac{1}{32Z^2}\left(\left(H_M^{(3)}\right)^2 H_M^{(2)}+2iH_M^{(3)}H_M^{(1)}\right)\Bigg). \end{aligned} \tag{3.20}$$

The first term of the right-hand side is proportional to the diagonal operator $H_M^{(2)}$ and the proportionality factor contains only the constants Z and M. Therefore we can absorb it into the definition of the unperturbed operator. This means that we have obtained an expression which is correct to the first order of $\frac{M}{Z}$ and whose leading term is diagonal. The calculation of the matrix elements will show that this operator is hermitian.

We will determine the approximate eigenvalues of (3.20) by treating the second and third term as a perturbation of the first term. In order to do so we need their matrix elements with respect to the eigenstates of $H_M^{(2)}$

In order to find the matrix elements of (3.20) we have to calculate the matrix elements of the operators $H_M^{(3)}H_M^{(2)}+iH_M^{(1)}$ and $\left(H_M^{(3)}\right)^2 H_M^{(2)}+2iH_M^{(3)}H_M^{(1)}$ with respect to two Fock-Dicke vectors $|m\rangle_{MZ}$ and $|n\rangle_{MZ}$. These matrix elements are

nonzero only if $|n-m|=1$. The nonzero matrix elements are

$$\begin{aligned}{}_{MZ}\langle n|\, H_M^{(3)}H_M^{(2)}+iH_M^{(1)}\,|m\rangle_{MZ}\\ =\delta_{n,m-1}(2m-M-1)\sqrt{m(M-m+1)}\\ +\delta_{n,m+1}(2m-M+1)\sqrt{(m+1)(M-m)}\end{aligned}\quad(3.21)$$

and

$$\begin{aligned}\langle n|\left(H_M^{(3)}\right)^2H_M^{(2)}+2iH_M^{(3)}H_M^{(1)}\,|m\rangle\\ =\delta_{n,m}((2n(n-M)+M-2)(2n-M)\\ +\delta_{n,m-2}(2m-M-2)\sqrt{m(m-1)(M-m+1)(M-m+2)}\\ +\delta_{n,m+2}(2m-M+2)\sqrt{(m+1)(m+2)(M-m-1)(M-m)}.\end{aligned}\quad(3.22)$$

Inserting these results into (3.20) of the Hamilton operator $H_M$we obtain the matrix elements of H in the representation where $H_M^{(3)}$ is approximately diagonal. Since $H_M^{(3)}$ is an approximation to H this representation of H is approximately diagonal. For $Z\geq M$ the diagonal matrix elements are

$$\langle n|\, H\,|n\rangle=\sqrt{Z}(2n-M)\left(1-\frac{M-1}{4Z}-\frac{2n(M-n)+M(M-1)}{32Z^2}\right)\quad(3.23)$$

and the matrix elements on the first side diagonal are

$$\langle n|\, H\,|n+1\rangle=\left(\frac{1}{4\sqrt{Z}}+\frac{M-1}{16Z^{3/2}}\right)(2n+1-M)\sqrt{(n+1)(M-n)},\quad(3.24)$$

$$\langle n+1|\, H\,|n\rangle=\langle n|\, H\,|n+1\rangle\,.\quad(3.25)$$

There appear nonvanishing matrix elements on the second side diagonal which will be neglected in our approximation, $M\ll Z$, since they are of the order $\left(\frac{M-1}{Z}\right)^{5/2}$ and their contribution to the eigenvalues is of the order $\left(\frac{M-1}{Z}\right)^{7/2}$. For $Z<M$ we find similar expressions with Z and M interchanged.

The second term of (3.20) has only matrix elements on the first side diagonal. We obtain a correction $\Delta\lambda_n$ of the eigenvalues which is of second order in $\frac{M}{Z}$,

$$\Delta\lambda_n=\frac{\left|\langle n|\, H_M^{(3)}H_M^{(2)}+iH_M^{(1)}\,|n-1\rangle\right|^2-\left|\langle n|\, H_M^{(3)}H_M^{(2)}+iH_M^{(1)}\,|n+1\rangle\right|^2}{\left(1-\frac{M-1}{4Z}+\frac{-M^2+2M-2}{32Z^2}\right)},\quad(3.26)$$

where we have used the fact that the eigenvalues of $H^{(2)}$ are equidistant.

The matrix elements of the third term of (3.20) are on the diagonal and the second side diagonal. The matrix elements on the second side diagonal may be neglected as we have seen above and the matrix elements on the main diagonal are treated in first order perturbation theory.

Taking all together we obtain the eigenvalues in first order perturbation theory in the case $Z \gg M$:

$$\lambda_n = \frac{\hbar g}{2}\sqrt{Z}\Bigg((2n-M)\left(1-\frac{M-1}{4Z}+\frac{-M^2+2M-2}{32Z^2}\right) + \frac{\left(1+\frac{M-1}{4Z}\right)^2\left((2n-M)(1+(2n-M)^2-4n(M-n)-2M)\right)}{16Z^2\left(1-\frac{M-1}{4Z}+\frac{-M^2+2M-2}{32Z^2}\right)} - \frac{2n(M-n)+M-2}{32Z^{3/2}}\Bigg). \quad (3.27)$$

In the case $Z \ll M$ we can obtain the eigenvalues by exchanging Z and M as the comparison of (3.10) and (3.10) shows.

$$\lambda_n = \frac{\hbar g}{2}\sqrt{M}\Bigg((2n-Z)\left(1-\frac{M-1}{4Z}+\frac{-M^2+2M-2}{32Z^2}\right) + \frac{\left(1+\frac{M-1}{4Z}\right)^2\left((2n-M)(1+(2n-M)^2-4n(M-n)-2M)\right)}{16Z^2\left(1-\frac{M-1}{4Z}+\frac{-M^2+2M-2}{32Z^2}\right)} - \frac{2n(M-n)+M-2}{32Z^{3/2}}\Bigg), \quad (3.28)$$

in the same way since in this case we only have to exchange Z and M as the comparison of (3.10) and (3.11) shows.

We note that the scaling of the coupling is not possible in the regime $Z < M$. The dependency of the eigenvalues on the number of atoms is approximately linear. While in (3.27) for $Z > M$ the coupling constant g appears in a term of the form $g\sqrt{Z}$ this term has the form $g\sqrt{M}$ in (3.28) which holds for $Z < M$.

In the example $M = 4$ and $1 \leq Z \leq 100$ we will compare the approximate eigenvalues with the exact numerical solution.

Figure 3.4 shows the approximative and exact eigenvalues for $Z \approx M = 4$. The approximation gives good results for $Z \geq 8$ and surprisingly does not break down at $Z = M$. For $Z < M$ only eigenvalues with the largest absolute values are described well by the approximation.

Since in 3.4 the same value of g has been used for all atom numbers , the eigenvalues should be proportional to the square root of the number of atoms for

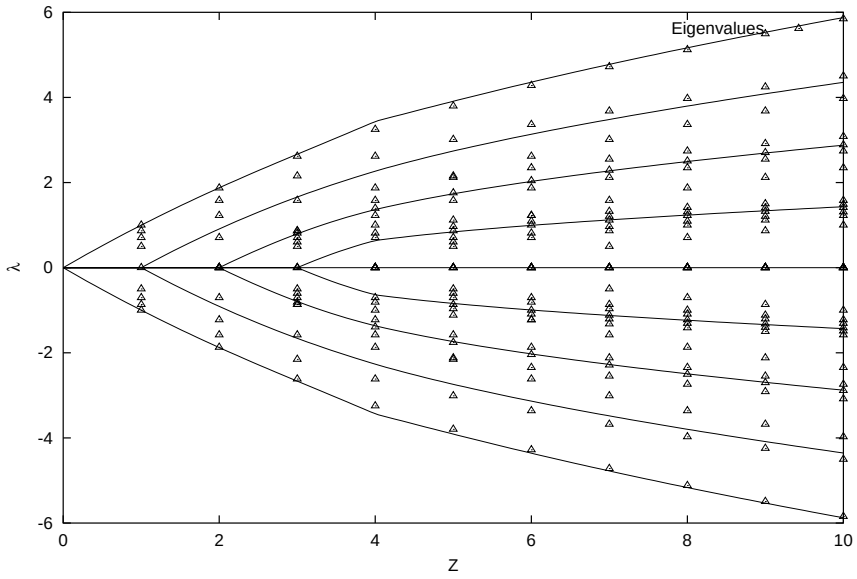

Figure 3.4: The exact eigenvalues (triangles) and the approximative eigenvalues from second order perturbation theory (lines) for $M = 4$, $1 \leq Z \leq 10$ and $l = \frac{Z}{2}$. At $Z = 4$ the two approximations $Z \ll M$ and $Z \gg M$ are no longer applicable. Nonetheless the approximative results are close to the exact results.

scaling behavior. This is not the case for $Z < M$ where the largest eigenvalues are approximately proportional to the number of atoms, as predicted by (3.28).

The exact eigenvalues and their second-order approximations for odd $Z \gg M$ are displayed in the figures 3.6 and 3.5. The eigenvalues corresponding to even and odd atom numbers lie on the same curves, but they have been plotted separately for graphical reasons. The approximation describes the eigenvalues very good. The eigenvalues are distributed almost equidistantly.

These results lead to the expectation that the largest deviation from the scaling behavior are found in the case $Z \approx M$ and in the case $Z \gg M$ scaling behavior dominates.

In the correction terms of (3.27) Z does not enter in the combination $g^2 Z$. We conclude that that the scaling of the coupling constant is only correct to lowest order of $\frac{M}{Z}$, and that higher orders of $\frac{M}{Z}$ are not described properly by the scaling of the coupling constant. This means that at $M \approx Z$ we do not expect that the scaling of g gives correct answers.

Finally, if $M > Z$ we expect to find a scaling in M and not in Z. This means that, except for very low energies it is in general not possible to solve a Z-atom problem by simply scaling the solution of a corresponding one-atom problem. We

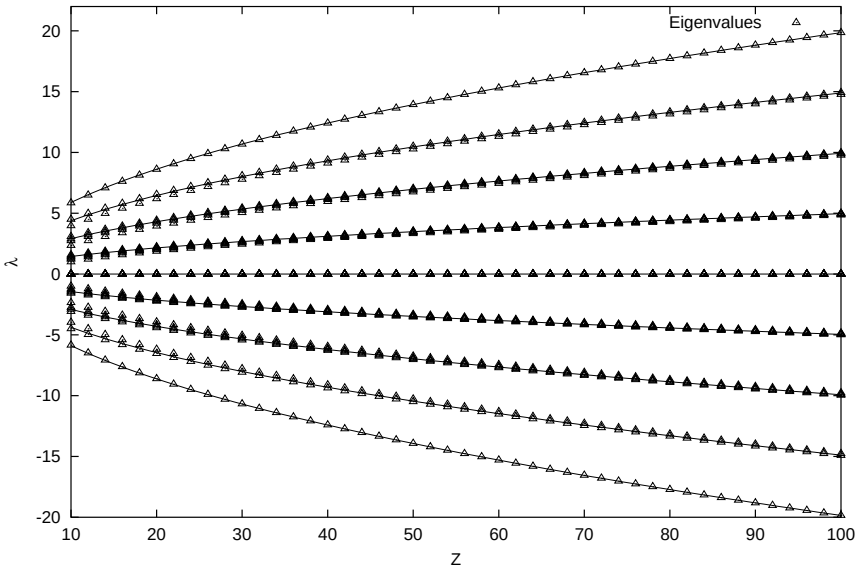

Figure 3.5: All eigenvalues corresponding to even numbers of atoms (triangles) and the approximative eigenvalues from second order perturbation theory (lines) for $M = 4$, $Z \geq 10$

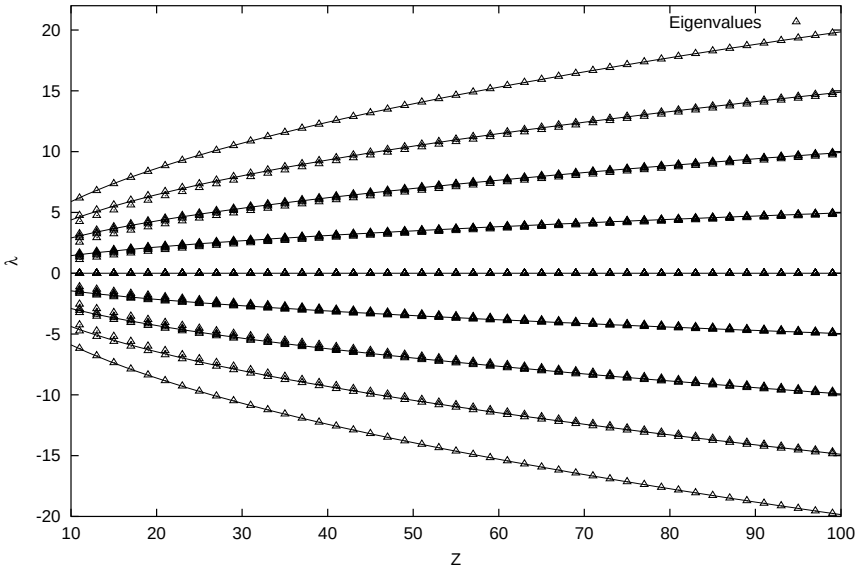

Figure 3.6: All eigenvalues corresponding to odd numbers of atoms (triangles) and the approximative eigenvalues from second order perturbation theory (lines) for $M = 4$, $Z \geq 10$

will illustrate this statement later with an application of the complete Z-atom solution.

Chapter 4

Symmetric Atomic Bases

In order to describe an experiment which measures only the state of the resonator mode and not the state of the atoms it is not necessary to know the state of the atoms involved in this experiment. This suggests that one could simplify the description by eliminating the atoms. Unfortunately the exact elimination of the atoms leads to to involved integro-differential equations [13].

The dimension of the state space of Z 2-level atoms is 4^Z, since each of these atoms is described by a $2-$by-2-dimensional density operator. This number increases very rapidly with increasing Z and makes it impossible to diagonalize the Liouville operator of a system with a large number of atoms. But there are two effects that reduce the number of dimensions: first, for low photon numbers not all atoms can be excited because there is not enough energy present to excite all atoms and, second, if one is only interested in the number of atoms found in a particular state, it is possible to symmetrise the atomic state space over all permutations of atoms.

We will use both of these effects in order to describe systems with many atoms. We assume that the density operator of the atoms is symmetric with respect to any permutation of the atoms. This is the case if the parameters describing the coupling of the atoms to the resonator mode are the same for all atoms and the atoms are prepared initially in a symmetric state. These symmetrized atomic states depend on collective variables, thus any information about individual atoms is lost and we keep only global information like the number of excited atoms.

This symmetrization procedure is possible if neither the initial state nor the equations of motion distinguish between individual atoms. The second condition is met since the Liouville operator commutes with the permutation operator.

This chapter will introduce three equivalent sets of basis operators, the atomic damping bases, which are a straightforward generalization of the atomic damping

bases introduced by H.J. Briegel in [4], the "spin flip" basis and the density operator generalization of the well-known Dicke vectors. All of these bases make use of the permutation symmetry of the atoms.

The purpose of introducing the atomic damping bases is to find the smallest atomic subspace which is closed with respect to the action of atomic dissipation and the interaction between the atoms and the resonator mode. This atomic subspace is symmetric with respect to arbitrary permutations of atoms. The dimension of this subspace is $\frac{1}{6}(Z+1)(Z+2)(Z+3)$ in contrast to 4^Z without symmetrization.

Unfortunately, the atomic damping bases are not very well suited for the description of systems where the interaction between the atoms and the resonator mode is the dominant effect. We will introduce a dissipative generalization of the Dicke vectors [11], the Dicke states[1]. Since the effect of the interaction Hamiltonian on the Dicke states is the same as the effect of the interaction Hamiltonian on the Dicke vectors the only remaining problem is the calculation of the effect of the atomic dissipation, for example the spontaneous emission of photons by excited atoms on the Dicke states.

In order to calculate these matrix element we we will need a third set of basis states which are variants of the eigenstates of the atomic dissipation. Using these states we will derive a recurrence relation for the matrix elements of the atomic dissipation with respect to the basis of the Dicke states. This recurrence relation will be used in the next chapter to finally obtain the Dicke state matrix elements of the atomic Liouville Operator.

4.1 Damping Bases

The eigenoperators of the atomic dissipation at temperature $T = 0$ respectively without atomic pump processes may be easily defined in terms of one-atom operators. The $\hat{\sigma}_o = \frac{1}{2}(1-\hat{\sigma}_z), \hat{\sigma}_z, \hat{\sigma}_+, \hat{\sigma}_-$ are eigenoperators of the atomic Lindblad operator $\mathcal{L}_a$ with the eigenvalues $0, -B, -2B, -2B$ if $s = 0$. The last eigenvalue is degenerate. The parameter s describes an effective atomic pump process: If $s \neq 0$ the stationary state is $\hat{\sigma}_o = \frac{1}{2}(1+(2s-1)\hat{\sigma}_z)$ instead of ${\hat{\sigma}_o}^2$[2]. The eigenvalues are not affected by s.

From these one-atom eigenstates one can easily construct the Z-atom eigenstates. Since the atomic part of the Liouville operator is a sum of one-atom-operators

[1] Throughout this work, "Dicke states" denote density operators while "Dicke vectors" denotes bra or kets.

[2] This is impossible for a normal two-level atom. The parameter s describes an effective model where the pump levels have been eliminated somehow.

the direct product of these single-atom eigenstates is an eigenstate of the full Z-atom Liouville operator.

Since $\mathcal{L}_a$ is not hermitian it has different left and right eigenstates denoted by $\check{Q}$ and $\hat{Q}$ respectively.

In order to obtain eigenstates of $\mathcal{L}_a$ which are symmetric with respect to any permutation of the atoms we sum over all permutations of atoms.

The resulting symmetric eigenstates of the atomic dissipation are

$$\hat{Q}_{n_o,n_z,n_-,n_+} = \mathcal{S}\prod_{i=1}^{n_o}\hat{\sigma}_o^{(i)}\prod_{i=n_o+1}^{n_o+n_z}\hat{\sigma}_z^{(i)}\prod_{i=n_o+n_z+1}^{n_o+n_+}\hat{\sigma}_+^{(i)}\prod_{i=n_o+n_z+n_++1}^{Z}\hat{\sigma}_-^{(i)}, \quad (4.1)$$

$$\check{Q}_{n_o,n_z,n_-,n_+} = \frac{\hat{Q}_{n_o,n_z,n_+,n_-}}{N(Z,n_z,n_+,n_-)}, \quad (4.2)$$

$$N(Z,n_z,n_+,n_-) = \binom{Z}{n_z}\binom{Z-n_z}{n_+}\binom{Z-n_z-n_+}{n_-}, \quad (4.3)$$

where

$$\mathcal{S} = \frac{1}{Z!}\sum_{\text{Permutations}}$$

is the atomic symmetrization operator. The numbers n_o, n_z, n_+, n_- give the number of atoms in the corresponding states $\hat{\sigma}_o, \hat{\sigma}_z, \hat{\sigma}_+, \hat{\sigma}_-$ and $N(Z,n_z,n_+,n_-)$ is a normalization factor. The normalization factor counts the different possibilities to distribute the 4 atomic basis states into the Z positions. Since we assumed that the atoms are distinguishable by their positions, two states with the same numbers n_o, n_z, n_+, n_- but different distributions are orthogonal. The symmetrization was introduced because we want to drop the information about the state of an atom at a given position and keep only the information about the number of atoms in a given state. Any atomic state not contained in this set of basis state is unsymmetric with respect to at least one atomic permutation.

The symmetrized states are still biorthogonal:

$$\text{tr}\left(\check{Q}_{\bar{n}_o,\bar{n}_z,\bar{n}_-,\bar{n}_+}\hat{Q}_{n_o,n_z,n_-,n_+}\right) = \delta_{\bar{n}_o,n_o}\delta_{\bar{n}_z,n_z}\delta_{\bar{n}_+,n_+}\delta_{\bar{n}_-,n_-}. \quad (4.4)$$

The orthogonality of states with different indices is evident by definition of the $\check{Q}_{n_o,n_z,n_-,n_+}, \hat{Q}_{n_o,n_z,n_-,n_+}$ and the inner product of states carrying the same index is one because of the normalization factor $N(Z,n_z,n_+,n_-)$.

The dimension of the atomic state space under consideration in this manuscript is the number of atomic basis states remaining after the symmetrization procedure. We may find between 0 and Z atoms in the ground state. Having found n_o atoms

in the ground state, we may find between 0 and $Z-n_o$ atoms in the state $\hat{\sigma}_z$. Accordingly, we may find between 0 and $Z-n_o-n_z$ atoms in the state $\hat{\sigma}_+$. The number of atoms in the state $\hat{\sigma}_-$ is fixed once three other numbers are fixed. Therefore the eigenstates of atomic dissipation span a state of the dimension

$$\sum_{n_o=0}^{Z}\sum_{n_z=0}^{Z-n_o}\sum_{n_+=0}^{Z-n_o-n_z} 1 = \frac{1}{6}(Z+1)(Z+2)(Z+3). \tag{4.5}$$

Without symmetrization the space spanned by the direct products of the Z single-atom states is the 4^Z dimensional space of all atomic variables. For large atom numbers the dimension of the state space makes numerical calculations impossible. In contrast, the dimension of the symmetric state space increases only as Z^3.

Unfortunately, the matrix elements of the interaction Hamiltonian with respect to this basis set are very complicated. Therefore, they will not be used in practical calculations. The main purpose of their introduction is to obtain a simple picture of the state space under consideration: Since the atomic part of the interaction Hamiltonian can be constructed from $\hat{Q}_{0,0,Z,0}$ and $\hat{Q}_{0,0,0,Z}$ and the $\hat{Q}_{n_o,n_z,n_-,n_+}$ are closed with respect to commutation, it is clear that the $\hat{Q}$ span the state space which is invariant under the action of $\mathcal{L}$, i. e. form a basis of this state.

4.2 Dicke States

This set of basis states is named after R. H. Dicke who introduced these collective states in order to describe superradiant emission by a cloud of excited two-level systems [11].

A two-level system like an atom with two internal states may be formally described as a particle of spin $\frac{1}{2}$. Therefore, a system of Z two-level systems may be described collectively using the angular momentum obtained by coupling the individual spins together using the Clebsch-Gordan coefficients. The resulting state is an analog to an eigenstate of angular momentum with eigenvalue l.[3] The projection quantum number m gives the number of excited atoms The quantum number l gives the maximum and minimum values of m. It can be interpreted as the degree of symmetry of the collective atomic state.

Taking the sum over one-atom operators $\sigma_+^{(i)} = \frac{1}{2}(\sigma_x + \sigma_y)$ and $\sigma_-^{(i)} = \frac{1}{2i}(\sigma_x - \sigma_y)$

[3]The number l corresponds to the cooperativity number r in [11].

we obtain collective operators

$$S_- = \sum_i \sigma_-^{(i)},$$
$$S_+ = \sum_i \sigma_+^{(i)},$$
$$S_z = \frac{1}{2}\sum_i \sigma_z^{(i)}$$

which have the same properties as the well-known angular momentum operators.

The atomic part $\sum_i \sigma_\pm^{(i)}$ of the Hamilton operator acts on such an angular momentum eigenstate just like a ladder operator from the usual angular momentum theory. In particular, the Hamilton operator does not change the quantum number l. In other words, the ladder operators commute with the angular momentum operator

$$L^2 = \frac{Z}{2} + S_z^2 + \sum_{i\neq j} \sigma_+^{(i)}\sigma_-^{(j)}. \tag{4.6}$$

In the state with $m = -\frac{Z}{2}$ all atoms are in the ground state, while in a state with $m = \frac{Z}{2}$ all atoms are excited. The general relation between the projection quantum number m and the number n_a of excited atoms is

$$n_a = m + \frac{Z}{2} \tag{4.7}$$

States with $l < \frac{Z}{2}$ cannot consist of completely excited atoms or atoms that are all in the ground state. The most striking example is a state with $l = 0$ which can occur if Z is an even number. Here $\frac{Z}{2}$ atoms are excited and $\frac{Z}{2}$ are in the ground state. Such a state does not interact with the electro magnetic field and is therefore called a dark state.

The symmetric basis vectors of the atomic subspace with $l = \frac{Z}{2}$ are

$$\left| Z, \frac{Z}{2}, m \right\rangle := \frac{1}{\sqrt{\binom{Z}{n}}} \mathcal{S} | \underbrace{+\cdots+}_{n} \underbrace{-\cdots-}_{Z-n} \rangle$$

where $\mathcal{S}$ is the symmetrization operator. Alternatively, one could construct these states by applying a ladder operator to the ground state $|---\cdots-\rangle$. The most symmetric states are unique, in contrast to the less symmetric states.

Since the action of the ladder operators

$$S_- |l,m\rangle = \sqrt{l(l+1) - m(m-1)}\, |l, m-1\rangle\,,$$
$$S_+ |l,m\rangle = \sqrt{l(l+1) - m(m+1)}\, |l, m+1\rangle$$

which give the atomic part of the Hamiltonian depends on the quantum numbers l and m one expects that the coupling of these collective states $|Z, l, m\rangle$ to the electro magnetic field is very different from the one-atom theory of the usual Jaynes-Cummings model.

The space spanned by the states with $l = \frac{Z}{2}$ is much too small to investigate the effects of atomic spontaneous emission. This can be seen most easily by applying the atomic Lindblad operator $\mathcal{L}_a$ to the density operator

$$\left| Z, \frac{Z}{2}, m \right\rangle \left\langle Z, \frac{Z}{2}, m' \right|. \tag{4.8}$$

The resulting operator is no longer a left or right eigenstate of the angular momentum, but becomes a mixture of eigenstates of different angular momenta. Therefore a description that contains only the most symmetric states is incomplete. A complete description of the system suitable for calculating the effects of spontaneous emission must contain all values of l or at least an approximation where we can neglect some values of l.

In the previous section we have introduced the minimal state space sufficient to describe atomic spontaneous emission. In the next step we will construct a set of basis states of this space which consists of eigenoperators of L^2. We will see later that the unitary as well as the dissipative part of the Liouville operator have simple expressions in this basis.

A first attempt to obtain the basis states with $l < \frac{Z}{2}$ would be a straightforward application of the Clebsch-Gordan coefficients. These coefficients are well known from atomic spectral theory. This approach has two drawbacks: first, these Clebsch-Gordan Coefficients become increasingly involved when Z becomes large, and secondly, the states characterized by Z,l and m are not unique.

For example, there are two states with $Z = 3, l = \frac{1}{2}, m = \frac{1}{2}$:

$$\begin{aligned}
\left| 3, \frac{1}{2}, \frac{1}{2}, 1 \right\rangle &= \frac{1}{\sqrt{6}} \left(|++-\rangle + |+-+\rangle - 2\,|-++\rangle \right) \\
\left| 3, \frac{1}{2}, \frac{1}{2}, 2 \right\rangle &= \frac{1}{\sqrt{2}} \left(|++-\rangle - |+-+\rangle \right).
\end{aligned}$$

The states $|\pm\pm\pm\rangle$ on the right hand side are uncoupled three-atom-states.

Because of this ambiguity it is necessary to introduce a fourth index ,r, in order to label the different states $|Z, l, m, r\rangle$ with the same values of Z, l and m. The state vectors depend on r in a very complicated way.

There exists a hermitian operator that commutes with L^2 and L_z and such that states with the same value of Z, l and m are eigenstates with different eigenvalues. This operator may be constructed by projecting out some atoms and using

the angular momentum operator of the remaining atoms. In other words, this operator contains the details of the coupling procedure. Since we are only interested in collective properties of the atoms we do not need the explicit form of this operator which is given only for completeness' sake.

Every state is now uniquely characterized by Z, l, m and the quantum number r corresponding to the operator $\hat{r}$. The interpretation of r is that r contains the details of the coupling procedure.

With the definition

$$s_i := \begin{cases} 1, & i\text{-th atom symmetrically coupled} \\ 0, & i\text{-th atom antisymmetrically coupled} \end{cases} \tag{4.9}$$

the quantum number r may defined as:

$$r := \sum_i 2^{s_i}. \tag{4.10}$$

In order to construct the operator corresponding to the quantum number r one needs operators that act only onto a fraction of the atoms, therefore one has to label the atoms.

Let $\vec{L}^{(i,j)}$ act as the angular momentum on the atoms labelled $i, i+1, ..j$ and as the identity operator on the other atoms.

We may use these restricted operators to form a set of commuting nondegenerate observables whose eigenvalues can be used to label the Dicke vectors.

$$\left[\left(L^{(1,j)}\right)^2, \left(L^{(1,i)}\right)^2\right] = \left[\left(L^{(1,i)}\right)^2 + \left(L^{(i+1,y)}\right)^2, \left(L^{(1,i)}\right)^2\right] = 0, \tag{4.11}$$

for $i < j$. The first commutator vanishes because both operators are the same and the second commutator vanishes because the operators act on different atoms. By the same argument we obtain

$$\left[L_z^{(1,j)}, \left(L^{(1,i)}\right)^2\right] = \sum_{k=1}^{i} \left[L_z^{(k,k)}, \left(L^{(k,k)}\right)^2\right] = 0. \tag{4.12}$$

The operators $\left(L^{(1,i)}\right)^2, i = 1..Z$ and $L_z^{(1,i)}$ form a complete set of commuting observables on the space spanned by the Dicke vectors.

The operator $\hat{r}$ corresponding to the quantum number r may be expressed from the binary representation of $(s_1..s_z)$:

$$\hat{r} = \sum_i 2^{\left(L^{(1,i)}\right)^2 - \left(L^{(1,i-1)}\right)^2 + \frac{1}{2}}. \tag{4.13}$$

L^2, L_z and $\hat{r}$ also form a complete set of commuting observables.

Any operator that is symmetric with respect to permutations of atoms commutes with $\hat{r}$. This holds in particular for the Hamilton operator due to the symmetry of the ladder operators which are invariant under permutations of the atoms and do not depend on $\hat{r}$.

An Operator $\mathcal{O}$ that is symmetric under exchange of two atoms cannot mix the quantum numbers r and l:

$$\langle Z, l, m, r| \mathcal{O} |Z', l', m', r'\rangle = \delta_{Z,Z'}\delta_{l,l'}\delta_{r,r'} f_{\mathcal{O}}(Z, l, m, m'). \tag{4.14}$$

Dicke vectors with different values of r are orthogonal. This is because they are eigenstates of the hermitian operator $\hat{r}$ or, equivalently, because the Clebsch-Gordan coefficients have been constructed so that these vectors are orthogonal.

From the Dicke vectors we construct symmetric density operators by taking the sum over r:

$$\hat{\xi}_{Z,l,m,m'} = \sum_r |Z, l, m, r\rangle \langle Z, l, m', r| \tag{4.15}$$

$$\check{\xi}_{Z,l,m,m'} = \frac{1}{g(Z,l)} \sum_r |Z, l, m', r\rangle \langle Z, l, m, r| . \tag{4.16}$$

The number $g(Z, l)$ is a normalization factor ensuring the normalization condition $\mathrm{tr}\left(\hat{\xi}_{Z,l,m,m'}\check{\xi}_{Z,l,m,m'}\right) = 1$. Note that m and m' have been exchanged in the definition of the dual basis states in order to ensure the biorthogonality of $\hat{\xi}_{Z,l,m,m'}$ and $\check{\xi}_{Z,l,m,m'}$. Note that this definition does not depend on properties of $\hat{r}$.

The properties of these operators will be examined in depth later. The density operators $\hat{\xi}$ are the basis operators of the operator space under consideration, the operators $\check{\xi}$ are the dual basis operators. Since $\mathcal{L}$ is not hermitian, one has to distinguish between basis and dual eigenoperators.

The summation over r is in in fact a symmetrization procedure. The most general simultaneous right and left eigenstate of L^2 with eigenvalue $l(l+1)$ is a linear combination of the dyadic products $|Z, l, m, r\rangle \langle Z, l, m', r'|$, but because of the permutation symmetry we need only a subset of these operators, namely those defined in (4.16).

Since the ladder operators commute with L^2 matrix elements between basis states with $m \neq m'$ can be expressed by matrix elements with $m = m'$. Hence it is sufficient to regard only the special case $m = m'$.

The states with $r \neq r'$ cancel out when the symmetrization over atomic exchange is performed and the sum contains only contributions with $r = r'$.

The example $\hat{\xi}_{3,\frac{1}{2},\frac{1}{2},\frac{1}{2}}$ shall illustrate the symmetrization:

$$\begin{aligned}\hat{\xi}_{3,\frac{1}{2},\frac{1}{2},\frac{1}{2}} &= \frac{2}{3}\left(|++-\rangle\langle++-| + |+-+\rangle\langle+-+| + |-++\rangle\langle-++|\right) \\ &\quad -\frac{1}{3}\left(|++-\rangle\langle+-+| + |++-\rangle\langle-++| + |+-+\rangle\langle++-|\right. \\ &\quad \left. + |+-+\rangle\langle-++| + |-++\rangle\langle++-| + |-++\rangle\langle+-+|\right)\end{aligned}$$

If an arbitrary atomic permutation is applied simultaneously to the bras and the kets of this example, the operator is reproduced. Therefore the operator of this example is invariant under atomic permutations.

The states with $l < \frac{Z}{2}$ are

$$\begin{aligned}g(Z,l) &= \binom{Z-1}{\frac{Z}{2}-l} - \binom{Z-1}{\frac{Z}{2}-l-2} \\ &= \binom{Z-1}{\frac{Z}{2}-l}\frac{Z(2l+1)}{(\frac{Z}{2}+l+1)(\frac{Z}{2}+l)} \\ &= \frac{Z!(2l+1)}{(\frac{Z}{2}+l+1)!(\frac{Z}{2}-l)!}\end{aligned} \tag{4.17}$$

-fold degenerate, as can be seen as follows: A state with Z atoms and angular momentum l may either be obtained by coupling a state with $Z-1$ atoms and angular momentum $l-1/2$ to an additional atom symmetrically or by coupling a state with $Z-1$ atoms and angular momentum $l+1/2$ to an additional atom antisymmetrically. The number of possible combinations to do so is the number of states with $Z-1$ atoms and angular momentum $l-1/2$ respectively with angular momentum $l+1/2$ in the second case. This leads to a recurrence relation for the number $g(Z,l)$ of possible combinations:

$$g(Z,l) = g(Z-1,l+1/2) + g(Z-1,l-1/2). \tag{4.18}$$

with the initial conditions

$$g(1,1/2) = 1, \tag{4.19}$$

$$g(Z,-1/2) = 0. \tag{4.20}$$

The recurrence (4.18) reminds one of the calculation of the binomial coefficients using Pascal's Triangle. Indeed, the recurrence relation for $g(Z,m)$ can be solved

by subtracting two Pascal's Triangles:

$Z \diagdown l$	2	$\frac{3}{2}$	1	$\frac{1}{2}$	0	$(-\frac{1}{2})$							
0					1		–1						
1				1		1−1		–1					
2			1		2−1		1−2		–1				
3		1		3−1		3−3		1−3		–1			
4	1		4−1		6−4		4−6		1−4		–1		
⋮						⋮							

(4.21)

The left half of this diagram contains the $g(Z,l)$, since the entries in the scheme above solve the recurrence relation (4.18) with the start conditions (4.19,4.20) if the line number counted from the top is taken as Z and the row number, counted from the middle, as l. [4]

In a system without atomic spontaneous emission this degeneracy has no consequences, even if unsymmetric states like dark states are considered. But the degeneracy enters explicitly into the calculation of the matrix elements of the atomic Liouville operator, since this operator couples states with different values of l.

The basis operators do not have trace one:

$$\mathrm{tr}\left(\hat{\xi}_{Z,l,m,m'}\right) = g(Z,l), \tag{4.22}$$

$$\mathrm{tr}\left(\check{\xi}_{Z,l,m,m'}\right) = 1. \tag{4.23}$$

These definitions have been chosen because they simplify the calculation of the matrix elements of the atomic dissipation.

The normalization condition is

$$\mathrm{tr}\left(\check{\xi}_{Z,l,m,m'}\hat{\xi}_{Z,\bar{l},\bar{m},\bar{m}'}\right) = \delta_{l,\bar{l}}\delta_{m,\bar{m}}\delta_{m',\bar{m}'}. \tag{4.24}$$

The trace product of a Dicke basis state and its dual state contains two symmetrization sums, but one of them collapses because of the biorthogonality of the

[4] The result (4.17) can be found in [11], but no derivation is given there.

Dicke vectors:

$$\begin{aligned}
&\mathrm{tr}\left(\check{\xi}_{Z,l,m,m'}\hat{\xi}_{Z,\bar{l},\bar{m},\bar{m}'}\right)\\
&=\frac{1}{g(Z,l)}\mathrm{tr}\left(\sum_{r,r'}|Z,l,m,m',r\rangle\langle Z,l,m,m',r|\,|Z,l,m,m',r'\rangle\langle Z,l,m,m',r'|\right)\\
&=\frac{1}{g(Z,l)}\mathrm{tr}\left(\sum_{r}|Z,l,m,m',r\rangle\langle Z,l,m,m',r|\,|Z,l,m,m',r\rangle\langle Z,l,m,m',r|\right)\\
&=\frac{1}{g(Z,l)}\mathrm{tr}\left(\sum_{r}|Z,l,m,m',r\rangle\langle Z,l,m,m',r|\right)=1. \quad (4.25)
\end{aligned}$$

One might think that there was another equivalent definition

$$\tilde{\xi}^{(Z,l,m,m')}=\sum_{r,r'}|Z,l,m,r\rangle\langle Z,l,m',r'|\,, \quad (4.26)$$

but this definition does not satisfy the symmetrization requirement (4.30), since $\mathcal{S}\,|Z,l,m,r\rangle\langle Z,l,m',r'|=0$ for $r\neq r'$.

The space spanned by the Dicke states is identical to the space spanned by the eigenstates of the atomic dissipation. To prove this claim we note that all Dicke states are by construction symmetric with respect to exchange of atoms and therefore the state spanned by the Dicke states is contained in the state spanned by the eigenoperators of atomic dissipation. In order to complete the proof we give the dimension of the state spanned by the Dicke states.

If Z is even, the Dicke states span a space of the dimension

$$\sum_{l=0}^{Z/2}\sum_{m=-l}^{l}\sum_{m=-l}^{l}1=\frac{1}{6}(Z+1)(Z+2)(Z+3); \quad (4.27)$$

and if Z is odd, the functional dependency of the dimension on Z is the same:

$$\sum_{l=1/2}^{Z/2}\sum_{m=-l}^{l}\sum_{m_{=}-l}^{l}1=\frac{1}{6}(Z+1)(Z+2)(Z+3). \quad (4.28)$$

This is exactly the dimension of the space spanned by the eigenstates of atomic dissipation.

We conclude that the space spanned by the Dicke states is the symmetric atomic space.

Density operators of the form $|Z,l,m,r\rangle\langle Z,l',m',r'|, l \neq l'$ or any linear combination of density operators of this type are not contained in the symmetric subspace. These operators are orthogonal to all Dicke states and therefore linearly independent from the Dicke states. If they were contained in the symmetric subspace the space spanned by the Dicke states could not have the same dimension as the symmetric space.

In particular, the image of a state from the symmetric space under the action of the Liouville operator $\mathcal{L}$ is contained in the symmetric space. Therefore the expansion

$$\mathcal{L}_a\hat{\xi}_{Z,l,m,m'} = \sum_{\bar{Z},\bar{l},\bar{m},\bar{m}'} c_{Z,l,m,m';\bar{Z},\bar{l},\bar{m},\bar{m}'}\hat{\xi}_{\bar{Z},\bar{l},\bar{m},\bar{m}'} \tag{4.29}$$

is possible.

Only very few of the coefficients $c_{Z,l,m,m';\bar{Z},\bar{l},\bar{m},\bar{m}'}$ are nonzero. The selection rules for these coefficients and their values will be derived in the chapter 5.

Alternatively one could introduce the Dicke states as simultaneous left and right eigenoperators of the angular momentum:

$$\begin{aligned}
L^2\hat{\xi}_{Z,l,m,m'} &= l(l+1)\hat{\xi}_{Z,l,m,m'},\\
\hat{\xi}_{Z,l,m,m'}L^2 &= l(l+1)\hat{\xi}_{Z,l,m,m'},\\
L_z\hat{\xi}_{Z,l,m,m'} &= m\hat{\xi}_{Z,l,m,m'},\\
\hat{\xi}_{Z,l,m,m'}L_z &= m'\hat{\xi}_{Z,l,m,m'},\\
\mathcal{S}\hat{\xi}_{Z,l,m,m'} &= \hat{\xi}_{Z,l,m,m'},\\
\mathrm{tr}\left(\check{\xi}_{Z,l,m,m'}\xi_{Z,\bar{l},\bar{m},\bar{m}'}\right) &= \delta_{l,\bar{l}}\delta_{m,\bar{m}}\delta_{m',\bar{m}'}.
\end{aligned} \tag{4.30}$$

The operator $\mathcal{S}$ is the symmetrization operator. Since the Dicke states are symmetric with respect to any atomic permutation operation, they are eigenstates of $\mathcal{S}$ with eigenvalue 1. $\mathcal{S}$ acts on its argument from the right and left side simultaneously like the Liouville operator.

Because of the commutation relations (4.11,4.12) it is clear that such states exist. Hence, the equations (4.30) are consistent. However, these states are only useful in combination with the explicit expression (4.17) for the degeneracy $g(Z,l)$ if atomic dissipation is considered. The simple requirement that that basis states should be biorthogonal is not sufficient since $g(Z,l)$ will enter explicitly into the calculation of the matrix elements of the atomic Liouville Operator.

4.3 Spin Flip Basis

The transformation between Dicke states and the dissipation eigenstates is complicated. The reason for this is that the damping eigenstates are not eigenstates of L_z. In order to calculate these matrix elements we introduce a third set of basis vectors which will be called spin flip basis. This basis set is very similar to the damping basis, but it consists of eigenstates of L_z.

The only difference between this third basis and the atomic damping basis is that the operators σ_o and σ_z have been replaced by projectors on the spin-up and spin-down states. Since this has some important consequences we nevertheless examine this new basis set in detail.

We start by grouping all states which can be constructed as the direct product of single-atom state of the form $|\pm\rangle\langle\pm|$ into groups which are invariant under exchange or permutations of atoms performed simultaneously on the ket and the bra of the state.

For example, for $Z = 3, m = -\frac{1}{2}$ such a group is

$$\begin{aligned} &|+--\rangle\langle-+-| \quad , \quad |+--\rangle\langle--+|, \\ &|-+-\rangle\langle+--| \quad , \quad |-+-\rangle\langle--+|, \\ &|--+\rangle\langle-+-| \quad , \quad |--+\rangle\langle--+|. \end{aligned}$$

In order to find this group one simply starts with the first state and then applies all possible permutations. The properties of the states which are invariant under permutations are the number of up and down states on each state and the number of atoms which are flipped up or down by the action of this operator.

The above may be formalized by introducing the operators

$$\hat{R}_{p_+,p_-,n_-,n_+} = \mathcal{S}\prod_{i=1}^{p_+}\pi_+^{(i)}\prod_{i=p_++1}^{p_++p_-}\pi_-^{(i)}\prod_{i=p_++p_-+1}^{p_++p_-+n_+}\sigma_+^{(i)}\prod_{i=p_++p_-+n_++1}^{Z}\sigma_-^{(i)}, \tag{4.31}$$

$$\check{R}_{p_+,p_-,n_-,n_+} = \frac{\hat{R}_{p_+,p_-,n_+,n_-}}{N(p_+,p_-,n_+,n_-)}. \tag{4.32}$$

The one-atom operators $\pi_+^{(i)}$ and $\pi_-^{(i)}$ are projection operators on the upper respectively lower state of the atom. The indices p_+ and p_- give the number of upper respectively lower projectors contained in the state R_{p_+,p_-,n_+,n_-} and n_+ gives the number of σ_+-operators found in the state.

The normalization factor

$$N(p_+,p_-,n_+,n_-) = \binom{p_+ + p_- + n_+ + n_-}{p_+}\binom{p_- + n_+ + n_-}{p_-}\binom{n_+ + n_-}{n_+} \tag{4.33}$$

counts the different possibilities to distribute the 4 atomic basis states into the Z positions. It is analogous to the normalization factor of the damping eigenstates.

Please note that in the dual basis states the meanings of n_- and n_+ have been swapped.The index i labels the different atoms. $\pi_\pm$ are the projectors on the upper respectively lower state of the atom labelled i.

The biorthogonality condition is

$$\mathrm{tr}\left(\check{R}_{\bar{p}_+,\bar{p}_-,\bar{n}_+,\bar{n}_-}\hat{R}_{p_+,p_-,n_+,n_-}\right) = \delta_{p_+\bar{p}_+}\delta_{p_-\bar{p}_-}\delta_{n_+\bar{n}_+}\delta_{n_-\bar{n}_-}. \tag{4.34}$$

The operators $\check{R}_{p_+,p_-,n_-,n_+}$ and $\hat{R}_{p_+,p_-,n_+,n_-}$ are by definition eigenoperators of the symmetrization operator $\mathcal{S}$. The dimension of the space spanned by these operators is the same as the dimension of the space spanned by the damping eigenbasis, since they differ from those only in the one-atom operators used in the construction. We conclude that they span the same space as the eigenoperators of the atomic dissipation.

The operators $\hat{R}_{p_+,p_-,n_-,n_+}$ are eigenoperators of the operator L_z which measures the number of excited atoms in a state vector:

$$L_z\hat{R}_{p_+,p_-,n_-,n_+} = \left(p_+ + n_+ + \frac{Z}{2}\right)\hat{R}_{p_+,p_-,n_-,n_+},$$
$$\hat{R}_{p_+,p_-,n_-,n_+}L_z = \left(p_+ + n_- + \frac{Z}{2}\right)\hat{R}_{p_+,p_-,n_-,n_+}.$$

The same holds for the adjoint operators. $\frac{Z}{2}$ has been added because of (4.7).

We introduce the operators $\mathcal{C}_\pm$ and $\mathcal{C} = \frac{1}{2}(\mathcal{C}_+ + \mathcal{C}_-)$ by

$$\mathcal{C}_+\hat{R}_{p_+,p_-,n_+,n_-} = n_+\hat{R}_{p_+,p_-,n_+,n_-}, \tag{4.35}$$
$$\mathcal{C}_-\hat{R}_{p_+,p_-,n_+,n_-} = n_-\hat{R}_{p_+,p_-,n_+,n_-}. \tag{4.36}$$

These operators count the number of spin flip operators in the basis state. In the picture of uncoupled atoms this means number of atoms which are in a different state on the right side and the left side of the basis operator.

In the example of section 4.2 one finds

$$\mathcal{C}_- \sum_{\text{Permutations}} |++-\rangle\langle++-| = \sum_{\text{Permutations}} |++-\rangle\langle++-|, \tag{4.37}$$
$$\mathcal{C}_+ \sum_{\text{Permutations}} |++-\rangle\langle++-| = 2\sum_{\text{Permutations}} |++-\rangle\langle++-|, \tag{4.38}$$
$$\mathcal{C}_- \sum_{\text{Permutations}} |++-\rangle\langle+-+| = 0 \tag{4.39}$$
$$\mathcal{C}_+ \sum_{\text{Permutations}} |++-\rangle\langle+-+| = \sum_{\text{Permutations}} |++-\rangle\langle++-|. \tag{4.40}$$

The action of the atomic Lindblad operator $\mathcal{L}_a$ on the spin flip basis states

$$\begin{aligned}\mathcal{L}_a\hat{R}_{p_+,p_-,n_+,n_-} &= -\frac{B}{2}(1-s)(p_+ + p_- + n_+)\hat{R}_{p_+,p_-,n_+,n_-} \\ &\quad -B(1-s)p_+\hat{R}_{p_+-1,p_-+1,n_+,n_-} \\ &\quad -\frac{B}{2}s(p_+ + p_- + n_-)\hat{R}_{p_+,p_-,n_+,n_-} \\ &\quad -Bsp_-\hat{R}_{p_++1,p_--1,n_+,n_-} \end{aligned} \tag{4.41}$$

is easily calculated using the fact that the nondiagonal parts of the atomic Lindblad operator vanish when acting on σ_+ or σ_-:

$$\sigma_-\sigma_-\sigma_+ = \sigma_-\sigma_+\sigma_+ = \sigma_-\pi_-\sigma_+ = \sigma_-\pi_+\sigma_+ = 0. \tag{4.42}$$

The atomic Liouville operator does not change the quantum numbers n_+ and n_-. The operators $\mathcal{C}_+$ and $\mathcal{C}_-$ do not change any of the quantum numbers p_+, p_-, n_+ and n_- and depend only on n_+ and n_-. Therefore $\mathcal{L}_a$ and $\mathcal{C}_\pm$ commute in the sense that

$$\mathcal{L}_a\mathcal{C}_\pm\rho = \mathcal{C}_\pm\mathcal{L}_a\rho \tag{4.43}$$

holds for any ρ from the symmetric space.

By the same reasoning $\mathcal{C}_-$ commutes with the atomic dissipation and with the part of the Liouville operator proportional to s.

In the following we will often use a simpler subset of the basis defined above. Since the atomic ladder operators may be used to shift the quantum numbers n_+ and n_- it is sufficient to treat the case $n_+ = n_-$. Therefore, one can reduce the bookkeeping by introducing for a fixed number Z of atoms a subset of the spin flip basis by

$$\hat{\chi}_{m,c} = \hat{R}_{\frac{Z}{2}+m-c,\frac{Z}{2}-m-c,c,c}, \tag{4.44}$$

$$\check{\chi}_{m,c} = \check{R}_{\frac{Z}{2}+m-c,\frac{Z}{2}-m-c,c,c}. \tag{4.45}$$

The index m has the same interpretation as the m quantum number of the Dicke states: in these states $\frac{Z}{2}+m$ atoms are excited.

The only nonzero matrix elements of the Lindblad operator between the $\hat{\chi}_{m,c}, \check{\chi}_{m,c}$ basis states are

$$\mathrm{tr}\left(\check{\chi}_{m-1,c}\mathcal{L}_{a,-}\hat{\chi}_{m,c}\right) = \frac{B}{2}\left(\frac{Z}{2} - (m-1) - c\right), \tag{4.46}$$

$$\mathrm{tr}\left(\check{\chi}_{m+1,c}\mathcal{L}_{a,+}\hat{\chi}_{m,c}\right) = \frac{B}{2}\left(\frac{Z}{2} + (m+1) - c\right), \tag{4.47}$$

$$\mathrm{tr}\left(\check{\chi}_{m,c}\mathcal{L}_{a,d}\hat{\chi}_{m,c}\right) = -B\left(\frac{Z}{2} + m\right). \tag{4.48}$$

These matrix elements are found easily by inserting the uncoupled representation of $\mathcal{L}_a$ and then counting the number of nonvanishing elements in the sum.

The dependence of these matrix elements on the spin flip index c can be understood easily, because the nondiagonal part of the Liouville operator gives zero when acting on the atomic states $|+\rangle\langle -|$ and $|-\rangle\langle +|$ and the index c counts the number of atoms found in one of these two states.

4.4 Recurrence Relation between Dicke and Spin Flip Basis States

In the following we will use the spin flip basis in an intermediate step of the calculation of the matrix elements of the atomic Liouville operator. But the explicit transformation between the two basis sets is very clumsy and involves the explicit calculation of the Dicke vectors using the Clebsch-Gordan-coefficients. Fortunately, we do not need to perform this calculation since a simple recurrence relation for the transformation matrix elements

$$x_{m,c}^{(Z,l,m)} = \mathrm{tr}\left(\hat{\xi}_{Z,l,m,m}\check{\chi}_{Z,m,c}\right) \tag{4.49}$$

is all we need.

Given these coefficients $x_{m,c}^{(Z,l,m)}$ we may express the Dicke state as a linear combination

$$\hat{\xi}_{Z,l,m,m} = \sum_{c=0}^{\frac{Z}{2}-|m|} x_{m,c}^{(Z,l,m)}\hat{\chi}_{Z,m,c} \tag{4.50}$$

of spin flip states.

The $\hat{\xi}_{Z,l,m,m}$ are eigenoperators of

$$L^2 = \frac{Z}{2} + S_z^2 + \sum_{i\neq j}\sigma_+^{(i)}\sigma_-^{(j)} \tag{4.51}$$

with eigenvalue $l(l+1)$.

We apply the single-atom expansion (4.51) of L^2 to the Dicke basis states and insert the completeness relation for the spin flip states

$$\hat{\xi}_{Z,l,m,m} = \sum_{c=0}^{\frac{Z}{2}-|m|} \hat{\chi}_{m,c}\mathrm{tr}\left(\check{\chi}_{m,c}\hat{\xi}_{Z,l,m,m}\right) \tag{4.52}$$

to obtain a first expression for the transformation coefficients:

$$\begin{aligned} L^2\hat{\xi}_{Z,l,m,m} &= \left(\frac{Z}{2}+m^2+\sum_{i\neq j}\sigma_+^{(i)}\sigma_-^{(j)}\right)\sum_{c,=0}^{\frac{Z}{2}-|m|} x_{m,c}^{(Z,l,m)}\hat{\chi}_{m,c} \\ &= \left(\frac{Z}{2}+m^2\right)\sum_{c=0}^{\frac{Z}{2}-|m|} x_{m,c}^{(Z,l,m)}\hat{\chi}_{m,c} \\ &\quad + \sum_{c,c'=0}^{\frac{Z}{2}-|m|} x_{m,c}^{(Z,l,m)}\hat{\chi}_{m,c'}\mathrm{tr}\left(\check{\chi}_{m,c'}\sum_{i\neq j}\sigma_+^{(i)}\sigma_-^{(j)}\hat{\chi}_{m,c}\right). \end{aligned} \tag{4.53}$$

In order to eliminate L^2 we need a second equation which we obtain from the eigenvalue relation together with the expansion (4.50) of the Dicke basis states:

$$\begin{aligned} L^2\hat{\xi}_{Z,l,m,m} &= l(l+1)\hat{\xi}_{Z,l,m,m} \\ &= \left(l(l+1))\sum_{c=0}^{\frac{Z}{2}-|m|} x_{m,c}^{(Z,l,m)}\hat{\chi}_{m,c}\right). \end{aligned} \tag{4.54}$$

We project the two expressions for $L^2\hat{\xi}_{Z,l,m,m}$ onto $\hat{\chi}_{m,c}$ to obtain the relation

$$\begin{aligned} \left(\frac{Z}{2}+m^2\right)x_{m,c}^{(Z,l,m)}\hat{\chi}_{m,c} + \sum_{c'=0}^{\frac{Z}{2}-|m|} x_{m,c}^{(Z,l,m)}\hat{\chi}_{m,c'}\mathrm{tr}\left(\check{\chi}_{m,c'}\sum_{i\neq j}\sigma_+^{(i)}\sigma_-^{(j)}\hat{\chi}_{m,c}\right) \\ = \left(l(l+1))x_{m,c}^{(Z,l,m)}\hat{\chi}_{m,c}\right) \end{aligned} \tag{4.55}$$

for the transformation coefficients $x_{m,c}^{(Z,l,m)}$.

The matrix elements $\mathrm{tr}\left(\check{\chi}_{m,\bar{c}}\sum_{i\neq j}\sigma_+^{(i)}\sigma_-^{(j)}\hat{\chi}_{m,c}\right)$ vanish if $|\bar{c}-c|>1$ because the operator exchanges at most two atoms[5]. In order to evaluate these matrix elements, we simply have to count [6] the number of atomic indices i,j such that $\mathrm{tr}\left(\check{\chi}_{m,\bar{c}}\sigma_+^{(i)}\sigma_-^{(j)}\hat{\chi}_{m,c}\right)=1$. From the definition (4.32,4.44) of the $\check{\chi}_{m,\bar{c}}$ it is clear that these matrix elements can only assume the values 0 or 1.

[5] By definition of $\mathcal{C}_\pm$ c changes by one, even though two atoms are involved.

[6] In order to perform this count, it is helpful to note that all three operators are symmetric with respect to permutations of atoms. Therefore, we may drop one permutation and compensate for that by dropping the normalization factor in $\check{\chi}_{m,c}$.

Thus we obtain the matrix elements

$$\operatorname{tr}\left(\check{\chi}_{Z,m,\bar{c}}\sum_{i\neq j}\sigma_+^{(i)}\sigma_-^{(j)}\check{\chi}_{Z,m,c}\right)=\begin{cases}\bar{c}^2, & c=\bar{c}-1\\ Z\bar{c}-2\bar{c}^2, & c=\bar{c}\\ \left(\frac{Z}{2}+m-\bar{c}\right)\left(\frac{Z}{2}-m-\bar{c}\right), & c=\bar{c}+1\\ 0 & \text{else.}\end{cases} \tag{4.56}$$

We need only the special case $m = m'$ because we will see that arbitrary matrix elements can be reduced to this special case.

By comparing the coefficients of the expansion of the matrix elements of L^2 one obtains the following recurrence relation:

$$\begin{aligned}x_{m,c+1}^{(Z,l,m,m)}\left(\frac{Z}{2}+m-c\right)\left(\frac{Z}{2}-m-c\right)=\\ -\left(\frac{Z}{2}+m^2+Zc-2c^2-l(l+1)\right)x_{m,c}^{(Z,l,m,m)}+c^2x_{m,c-1}^{(Z,l,m,m)}.\end{aligned} \tag{4.57}$$

This still holds for $c = 0$, where (4.57) becomes

$$x_{m,1}^{(Z,l,m,m)}\left(\frac{Z}{2}+m\right)\left(\frac{Z}{2}-m\right)=-\left(\frac{Z}{2}+m^2-l(l+1)\right)x_{m,0}^{(Z,l,m,m)}. \tag{4.58}$$

The value of $x_{m,0}^{(Z,l,m)}$ may be fixed so that

$$\operatorname{tr}\left(\hat{\xi}_{Z,l,m,m}\right)=\operatorname{tr}\left(\sum_{c=0}^{\frac{Z}{2}-|m|}x_{m,c,c}^{(Z,l,m,m)}\hat{\chi}_{m,c,c}\right) \tag{4.59}$$

holds. Since $\operatorname{tr}(\hat{\chi}_{m,c,c}) = 0$ for $c > 0$ this condition simplifies to

$$x_{m,0,0}^{(Z,l,m,m)}=\operatorname{tr}\left(\hat{\xi}_{Z,l,m,m}\right)=g(Z,l). \tag{4.60}$$

In principle one could solve the recurrence relation (4.57), thus obtaining all the coefficients $x_{m,c}^{(Z,l,m)}$.

Since the calculation of the matrix elements of the atomic Liouville operator with respect to the spin flip states is easy, this would yield the desired matrix elements. But in chapter 5 we will see that we can obtain those matrix elements even without solving the recurrence relation directly.

4.5 Basis States of the Atoms and the Resonator Mode

In order to describe the interaction between the atoms and the resonator mode we need a basis of the product space of the atoms and the resonator mode. In exact resonance the total energy

$$M = \frac{1}{2}(Z + m + n + m' + n') \tag{4.61}$$

contained in photons and excited atoms is invariant under the action of the interaction Hamiltonian. Furthermore, the off-diagonality

$$K = (m + n - m' - n') \tag{4.62}$$

is also invariant under the action of the interaction Hamiltonian. Therefore we will use the indices M, K, m, m' instead of m, m', n, n'. The new basis states are

$$\hat{\xi}^{(M,K)}_{Z,l,m,m'} = \left| M - m + \frac{1}{2}(K - Z) \right\rangle \left\langle M - m' + \frac{1}{2}(-K - Z) \right| \hat{\xi}_{Z,l,m,m'} \tag{4.63}$$

$$\check{\xi}^{(M,K)}_{Z,l,m,m'} = \left| M - m' + \frac{1}{2}(-K - Z) \right\rangle \left\langle M - m + \frac{1}{2}(K - Z) \right| \check{\xi}_{Z,l,m,m'} \tag{4.64}$$

The bras and kets here denote Fock states.

The biorthogonality relation

$$\mathrm{tr}\left(\check{\xi}^{(\bar{M},\bar{K})}_{Z,\bar{l},\bar{m},\bar{m}'} \hat{\xi}^{(M,K)}_{Z,l,m,m'} \right) = \delta_{M,\bar{M}} \delta_{K,\bar{K}} \delta_{l,\bar{l}} \delta_{m,\bar{m}} \delta_{m'\bar{m}'} \tag{4.65}$$

requires that we reverse the sign of K and the order of m and m' in the dual states.

The indices m and m' run from $-l$ to $\min(l, M - \frac{Z}{2})$. The second upper limit on m and m' expresses that at most M excited atoms are possible. For $l < \frac{Z}{2}$ the atomic excitation is confined between $\frac{Z}{2} - l$ and $\frac{Z}{2} + l$. This fact may be used to reduce the dimension of the state space significantly.

Chapter 5

Matrix Elements of the Liouville Operator

With the help of the spin flip basis (4.31) introduced in chapter 4 it is now possible to calculate the matrix elements

$$\mathrm{tr}\left(\check{\xi}_{Z,\bar{l},\bar{m},\bar{m}'}\mathcal{L}\hat{\xi}_{Z,l,m,m'}\right). \tag{5.1}$$

of the atomic spontaneous emission with respect to the basis of Dicke states (4.16).

As we will see, there are compact analytical expressions for these matrix elements. Using this result we obtain a basis that is equally well suited to the description of the dissipation as well as to the interaction between the atoms and the resonator mode.

As a first step we will introduce selection rules for the matrix elements (5.1). These selection rules remind one of the selection rules associated with the emission of photons by atoms, but they are of completely different origin.

In the next step we will use the spin flip basis to derive a recurrence relation for the matrix elements. The solution of this recurrence relation for its first three elements is sufficient obtain the desired matrix elements.

In this chapter we also give the matrix elements of the Hamiltonian.

5.1 The Selection Rules

In quantum mechanics the matrix elements of operators may be restricted by symmetry considerations. If an operator commutes with another operator the

matrix elements between states corresponding to different eigenvalues of the other operator must be zero.

The atomic Liouville operator $\mathcal{L}_a$ does not commute with the angular momentum operator L^2. But since the Liouville operator is a sum of single-atom operators and each single-atom operator can change the angular momentum at most by one we obtain an analog to the common selection rules from quantum electrodynamics: Matrix elements of the atomic Liouville operator between Dicke states that differ by more than 1 in their angular momentum quantum number l must be zero.

Since the Hamilton operator commutes with L^2 this holds also for the complete Liouville operator.

This is the angular momentum selection rule: for the matrix element (5.1) to be nonzero the condition

$$l - \bar{l} \in \{-1, 01\} \tag{5.2}$$

must be met.

In the picture of uncoupled atoms the proof of this selection goes as follows: We start with an cluster of atoms coupled to a Dicke state with angular momentum l If a spontaneous emission or an absorption of a photon from the bath or the pump source occurs, the atom affected by that process drops out of the Dicke vector used in the construction of the Dicke states. The remaining atoms are a linear combination of states with angular momentum l' where $|l - l'| = \frac{1}{2}$. Upon recombining the atom with the other atoms we obtain a linear combination of states with angular momentum $\bar{l}$ where $|l' - \bar{l}| = \frac{1}{2}$. Then the triangle inequality gives the desired bound on $\bar{l}$:

$$|l - \bar{l}| = |l - l' + l' - \bar{l}| \leq |l - l'| + |l' - \bar{l}| = 1. \tag{5.3}$$

The difference $l - \bar{l}$ must have integer values since the angular momenta are half-integers if the number of atoms is odd and integers if the number of atoms is even.

The arguments presented here do not establish that the action of the atomic Liouville operator on a Dicke state returns a Dicke state. But this has been shown in section 4.2.

This angular momentum selection rule is the crucial point for the calculation of the matrix elements we are going to present here.

The Lindblad operator is a superoperator which acts in the same way from the left side and the right side of a density operator. Therefore the off-diagonality

$m - m'$ of a Dicke state $\xi_{Z,l,m,m'}$ is not altered by the dissipative dynamics. This is the off-diagonality selection rule

$$m - m' = \bar{m} - \bar{m}'. \tag{5.4}$$

The processes under consideration here will not alter the number of photons absorbed in the system by more than one. This is the energy selection rule:

$$m + m' - (\bar{m} + \bar{m}') = \begin{cases} 1 & \text{loss part} \\ 0 & \text{diagonal part,} \\ -1 & \text{gain part.} \end{cases} \tag{5.5}$$

For the combined Fock-Dicke states the last two rules map onto rules for the off-diagonality index K defined in (4.62) and the total energy M (4.61). The off-diagonality selection rule becomes:

$$K = \bar{K}, \tag{5.6}$$

and the energy selection rule becomes:

$$M - \bar{M} = \begin{cases} 1 & \text{loss part,} \\ 0 & \text{diagonal part, .} \\ -1 & \text{gain part.} \end{cases} \tag{5.7}$$

5.2 The Hamilton Operator

In chapter 3 the matrix elements of the Hamilton operator with respect to the Dicke states have been calculated. The atomic ladder operators $S_+ = \sum_i \sigma_+^{(i)}$, $S_- = \sum_i \sigma_-^{(i)}$ which represent the atomic part of the interaction Hamiltonian act on the Dicke states $|Z, l, m, r\rangle$ like ordinary angular momentum operators. Therefore the matrix elements are

$$\begin{aligned} \mathrm{tr}\left(\check{\xi}_{Z,l,\bar{m},\bar{m}'} S_+ \hat{\xi}_{Z,l',m,m'}\right) &= \\ &\sqrt{(l - \bar{m}')(l + \bar{m}' + 1)}\delta_{l,l'}\delta_{\bar{m}'+1,m}\delta_{\bar{m},m}, \end{aligned} \tag{5.8}$$

$$\begin{aligned} \mathrm{tr}\left(\check{\xi}_{Z,l,\bar{m},\bar{m}'} S_- \hat{\xi}_{Z,l',m,m'}\right) &= \\ &\sqrt{(l - \bar{m}' + 1)(l + \bar{m}')}\delta_{l,l'}\delta_{\bar{m}'-1,m}\delta_{\bar{m},m}. \end{aligned} \tag{5.9}$$

5.3 The Mode Dissipation

Since the basis used for resonator mode are Fock states the matrix elements of the resonator mode are easily calculated. At a Temperature corresponding to n_{th} thermal photons the nonzero matrix elements of the mode dissipation Liouville operator between the outer products of the Fock states $|n\rangle |n'\rangle$ are:

$$\begin{aligned} \mathrm{tr}\left(|n\rangle \langle n'| \mathcal{L}_f |n\rangle \langle n'|\right) &= A(n+n'+2n_{th}(n+m+1)), \\ \mathrm{tr}\left(|n-1\rangle \langle n'-1| \mathcal{L}_f |n\rangle \langle n'|\right) &= 2A(1+n_{th})\sqrt{nn'}, \\ \mathrm{tr}\left(|n+1\rangle \langle n'+1| \mathcal{L}_f |n\rangle \langle n'|\right) &= 2An_{th}\sqrt{(n+1)(n'+1)}. \end{aligned} \tag{5.10}$$

5.4 Diagonal Part of the Atomic Dissipation

The atomic Liouville can be decomposed into two parts. The first is the anticommutator with $\sum_i \sigma_+^{(i)}\sigma_-^{(i)}$ for the loss part and $\sum_i \sigma_-^{(i)}\sigma_+^{(i)}$ for the gain part. Both of these operators are diagonal in any of the three bases introduced in chapter 4. Since we did not require the atomic states to be diagonal with respect to the number of excited atoms, each basis operator depends on two numbers of excited atoms. The anticommutator with $\sum_i \sigma_+^{(i)}\sigma_-^{(i)}$ is the sum of the number of excited atoms from the row index and from the column index.

The matrix elements of this anticommutator are:

$$\mathrm{tr}\left(\check{\xi}^{(Z,\bar{l},\bar{m},\bar{m}')}\left\{\sum_i \sigma_+^{(i)}\sigma_-^{(i)}, \hat{\xi}_{Z,l,m,m'}\right\}\right) = (Z+m+m')\delta_{l,\bar{l}}\delta_{m,\bar{m}}\delta_{m',\bar{m}'} \tag{5.11}$$

This part of the Lindblad operator will be denoted occasionally as $\mathcal{L}_{a,d}$.

5.5 Gain and Loss Part of the Atomic Dissipation

The second part of the atomic Liouville operator is

$$\mathcal{L}_{a,l}\rho = B\sum_i \sigma_+^{(i)}\rho_a\sigma_-^{(i)} \tag{5.12}$$

in case of the loss part and

$$\mathcal{L}_{a,g}\rho = B\sum_i \sigma_-^{(i)}\rho_a\sigma_+^{(i)} \tag{5.13}$$

in case of the gain part.

These are the parts of the atomic Liouville operator that do not commute with the angular momentum. The calculation of its matrix elements will be performed in the following steps: First, we will express the matrix elements of the gain part through matrix elements of the loss part with the help of a symmetry operation. Second, we will show that there are three representative matrix element, corresponding to $|l - \bar{l}| = -1, 0$ or 1 from which all other matrix elements can be calculated with the help of ladder operators. Third, we will use the angular momentum selection rule (5.2) to establish that these representative matrix element may be obtained from a set of three linearly independent equations. Fourth, we will use the recurrence relation (4.57) to find these three equations.

The matrix elements of the loss part of the Lindblad operator will be denoted as

$$\begin{aligned}
\lambda_-(Z,l,m,m') &= \mathrm{tr}\left(\check{\xi}^{(Z,l,m,m')}\mathcal{L}_{a,l}\hat{\xi}^{(Z,l+1,m+1,m'+1)}\right), \\
\lambda_o(Z,l,m,m') &= \mathrm{tr}\left(\check{\xi}_{Z,l,m,m'}\mathcal{L}_{a,l}\hat{\xi}^{(Z,l,m+1,m'+1)}\right), \\
\lambda_+(Z,l,m,m') &= \mathrm{tr}\left(\check{\xi}_{Z,l,m,m'}\mathcal{L}_{a,l}\hat{\xi}^{(Z,l-1,m+1,m'+1)}\right). \qquad (5.14)
\end{aligned}$$

The index refers to the change in the angular momentum due to the action of $L_{a,l}$. The angular momentum cannot change by more than one. This selection rule looks completely analogous to the selection rule known from the interaction of a single atom with an electromagnetic field, but it is of completely different origin.

Analogous matrix elements are defined for the gain part:

$$\begin{aligned}
\lambda'_-(Z,l,m,m') &= \mathrm{tr}\left(\check{\xi}^{(Z,l,m,m')}\mathcal{L}_{a,g}\hat{\xi}^{(Z,l+1,m+1,m'+1)}\right), \\
\lambda'_o(Z,l,m,m') &= \mathrm{tr}\left(\check{\xi}^{(Z,l,m,m')}\mathcal{L}_{a,g}\hat{\xi}^{(Z,l,m+1,m'+1)}\right), \\
\lambda'_+(Z,l,m,m') &= \mathrm{tr}\left(\check{\xi}^{(Z,l,m,m')}\mathcal{L}_{a,g}\hat{\xi}^{(Z,l-1,m+1,m'+1)}\right). \qquad (5.15)
\end{aligned}$$

5.5.1 The Relation between the Gain and the Loss Part

The matrix elements λ of the loss part of the atomic Lindblad operator can be expressed by the matrix elements λ' of the gain part and vice versa. With the help of this relation only half of the matrix elements actually have to be calculated.

We will establish this relation between the gain part and the loss part using a simple symmetry relation. Let $\mathcal{O}(\{\sigma_+^{(i)}\}, \{\sigma_-^{(i)}\}, \{\sigma_z^{(i)}\})$ be some function of

one-atom-operators. Then

$$\begin{aligned}\mathrm{tr}\left(\hat{\xi}_{Z,l,m,m'}\mathcal{O}(\{\sigma_+^{(i)}\},\{\sigma_-^{(i)}\},\{\sigma_z^{(i)}\})\check{\xi}_{Z,l,\bar{m},\bar{m}'}\right)\\ = \mathrm{tr}\left(\hat{\xi}_{Z,l,-m,-m'}\mathcal{O}(\{\sigma_-^{(i)}\},\{\sigma_+^{(i)}\},\{-\sigma_z^{(i)}\})\check{\xi}_{Z,l,-\bar{m},-\bar{m}'}\right) \quad (5.16)\end{aligned}$$

holds. In order to prove this we first have to introduce the symmetry operator T by the following five relations:

$$\begin{aligned} T\,|Z,l,m,r\rangle &= |Z,l,-m,r\rangle\,,\\ T^2 &= \mathbf{1},\\ T^\dagger &= T,\\ T\sigma_+^i T &= \sigma_-^{(i)}, \quad i=1\cdots Z,\\ T\sigma_-^i T &= \sigma_+^{(i)}, \quad i=1\cdots Z,\\ T\sigma_z^i T &= -\sigma_z^{(i)}, \quad i=1\cdots Z. \end{aligned} \quad (5.17)$$

The operator T simply flips all atomic spins.

Because of (5.17) the operator T maps any eigenvector of L_z with eigenvalue m onto an eigenvector of L_z with eigenvalue $-m$. Furthermore, T does not act on the index r from the Dicke vectors, as can be seen from the Clebsch-Gordan-coefficients or the definition of the operator $\hat{r}$ in (4.13). This establishes the action of the symmetry operator T on the Dicke states

$$\begin{aligned} T\check{\xi}_{Z,l,m,m'}T &= \check{\xi}_{Z,l,-m,-m'},\\ T\hat{\xi}_{Z,l,m,m'}T &= \hat{\xi}_{Z,l,-m,-m'}. \end{aligned} \quad (5.18)$$

Using this transformation property of the Dicke states we establish equation (5.16) by repeated insertion of the unit operator (5.17) into the trace in the right hand side of (5.16) and using the cyclic property of the trace:

$$\begin{aligned}&\mathrm{tr}\left(\hat{\xi}_{Z,l,-m,-m'}\mathcal{O}(\{\sigma_-^{(i)}\},\{\sigma_+^{(i)}\},\{-\sigma_z^{(i)}\})\check{\xi}_{Z,\bar{l},-\bar{m},-\bar{m}'}\right)\\ &\quad= \mathrm{tr}\left(\hat{\xi}_{Z,l,-m,-m'}\mathcal{O}(\{T\sigma_+^{(i)}T\},\{T\sigma_-^{(i)}T\},\{T\sigma_z^{(i)}T\})\check{\xi}_{Z,\bar{l},-\bar{m},-\bar{m}'}\right)\\ &\quad= \mathrm{tr}\left(T\hat{\xi}_{Z,l,-m,-m'}T\mathcal{O}(\{\sigma_+^{(i)}\},\{\sigma_-^{(i)}\},\{\sigma_z^{(i)}\})T\check{\xi}_{Z,\bar{l},-\bar{m},-\bar{m}'}T\right)\\ &\quad= \mathrm{tr}\left(\hat{\xi}_{Z,l,m,m'}\mathcal{O}(\{\sigma_+^{(i)}\},\{\sigma_-^{(i)}\},\{\sigma_z^{(i)}\})\check{\xi}_{Z,\bar{l},\bar{m},\bar{m}'}\right). \quad (5.19)\end{aligned}$$

In particular, the atomic parts of the Lindblad operator $\mathcal{L}_a$ is of the form $\mathcal{O}$ and one can see immediately that $T\mathcal{L}_{a,l}T = \mathcal{L}_{a,g}$ holds, so that T maps the gain part of the atomic Liouville operator onto its loss part and vice versa.

Therefore, the desired relation between the matrix elements of the gain part and the loss part of the atomic Liouville operator is a special case of (5.16) and we obtain:

$$\mathrm{tr}\left(\hat{\xi}_{Z,\bar{l},\bar{m},\bar{m}'}\mathcal{L}_{a,g}\check{\xi}_{Z,l,m,m'}\right) = \mathrm{tr}\left(\hat{\xi}_{Z,l,-\bar{m},-\bar{m}'}\mathcal{L}_{a,l}\check{\xi}_{Z,\bar{l},-m,-m'}\right). \tag{5.20}$$

The matrix element of the loss part are zero if $\bar{m} \neq m$ or $\bar{m}' \neq m'$

5.5.2 The Three Representative Matrix Elements

The calculation of the matrix elements of the loss part can be reduced to the calculation of three representative matrix elements. This reduction is performed using the ladder operators $L_- = \sum_i \sigma_-^{(i)}$.

The ladder operator L_- commutes with the loss part of $\mathcal{L}_{a,l}$ of the dissipation, since the relation

$$\mathcal{L}_{a,l}\left(L_-^{(\nu)}\rho L_+^{(\mu)}\right) = L_-^{(\nu)}\mathcal{L}_{a,l}\left(\rho\right)L_+^{(\mu)} \tag{5.21}$$

holds for any atomic density operator ρ.

Using these relations, we can connect matrix elements with different values of $m, m', \bar{m}$ and $\bar{m}'$ by expressing the Dicke basis states by other Dicke states multiplied by ladder operators. Then we exchange these ladder operators with the Liouville operator and finally apply them to the Dicke basis states of the matrix element.

Now we have to consider the three cases $\bar{l} = l-1$, $\bar{l} = l-1$, $\bar{l} = l+1$. In the case $\bar{l} = l-1$, the maximal possible value of $\bar{m}$ or $\bar{m}'$ is $\bar{l}$. But in the case $\bar{l} = l$, the maximal possible value of $\bar{m}$ or $\bar{m}'$ is $\bar{l}-1$ since the maximal possible value of m respectively m' is l and the atomic Liouville operator reduces the number of excited atoms by 1. By the same argument, in the case $\bar{l} = l+1$ the maximally possible value of $\bar{m}$ $\bar{m}'$ is $\bar{l}-2$. In each of these three case we express arbitrary matrix elements by the one corresponding to the maximal value of $\bar{m}$ and $\bar{m}'$.

$$\begin{aligned}
\lambda_-(Z,l,m,m') &= \frac{\sqrt{(l+m)(l+m-1)(l+m')(l+m'-1)}}{2l(2l-1)}\lambda_-(Z,l,l,l),\\
\lambda_o(Z,l,m,m') &= \frac{\sqrt{(l-m+1)(l+m)(l-m'+1)(l+m')}}{2l}\lambda_o(Z,l,l-1,l-1),\\
\lambda_+(Z,l,m,m') &= \frac{\sqrt{(l-m)(l-m-1)(l-m')(l-m'-1)}}{2}\lambda_+(Z,l,l-2,l-2).
\end{aligned} \tag{5.22}$$

The square roots are the remainders of the canceled ladder operators.

These three matrix elements remain to be calculated. To proceed we note that because of the angular momentum selection rule (5.2) and the fact that the atomic Liouville Operator is a linear operator on the space spanned by the Dicke states it follows that there are $\lambda_-, \lambda_o, \lambda_+$ such that

$$\begin{aligned}\mathcal{L}_{a,l}\hat{\xi}^{(Z,l,m,m)} &= \lambda_+^{(Z,l+1,m-1,m-1)}\hat{\xi}^{(Z,l+1,m-1,m-1)} \\ &\quad +\lambda_o^{(Z,l,m-1,m-1)}\hat{\xi}^{(Z,l,m-1,m-1)} \\ &\quad +\lambda_-^{(Z,l-1,m-1,m-1)}\hat{\xi}^{(Z,l-1,m-1,m-1)}.\end{aligned} \tag{5.23}$$

The difference between the angular momentum of the states on the right side of equation (5.24) and the state on the left side cannot exceed one because of the angular momentum selection rule. Other values of m on the right side are impossible because the spontaneous emission emission of one photon reduces m by one.

From this equation we obtain three linearly independent equations for the matrix elements λ_-, λ_+ and λ_o if we project the equation on different spin flip basis states using the expansion (4.44) of the Dicke states with respect to the spin flip states[1].

The projected equation

$$\begin{aligned}x_{m,c}^{Z,l,m}\mathrm{tr}\left(\check{\chi}_{m,c}\mathcal{L}_{a,l}\hat{\chi}_{m,c}\right) &= \lambda_+^{(Z,l+1,m-1,m-1)}x_{m-1,c}^{(Z,l+1,m-1)} \\ &\quad +\lambda_o^{(Z,l,m-1,m-1)}x_{m-1,c}^{(Z,l,m-1)} \\ &\quad +\lambda_-^{(Z,l-1,m-1,m-1)}x_{m-1,c}^{(Z,l-1,m-1)}\end{aligned} \tag{5.24}$$

is now taken for the three different values of $c = 0, 1, 2$. Thus we obtain the three different equations for the matrix elements.

We write the equations (5.24) in compact matrix notation. With

$$\lambda = \begin{pmatrix} \lambda_+^{(Z,l+1,m-1,m-1)} \\ \lambda_o^{(Z,l,m-1,m-1)} \\ \lambda_-^{(Z,l-1,m-1,m-1)} \end{pmatrix}, \tag{5.25}$$

$$\lambda' = \begin{pmatrix} x_{m,0}^{Z,l,m}\mathrm{tr}\left(\check{\chi}_{m,0}\mathcal{L}_{a,l}\hat{\chi}_{m,0}\right) \\ x_{m,1}^{Z,l,m}\mathrm{tr}\left(\check{\chi}_{m,0}\mathcal{L}_{a,l}\hat{\chi}_{m,0}\right) \\ x_{m,2}^{Z,l,m}\mathrm{tr}\left(\check{\chi}_{m,0}\mathcal{L}_{a,l}\hat{\chi}_{m,0}\right) \end{pmatrix}, \tag{5.26}$$

[1]This is the step that made the introduction of the spin flip states necessary. Since the atomic damping bases are not eigenstates of L_z we cannot use them here. The sum over c collapses because of the definition of the spin flip states.

and

$$\mathbf{X} = \begin{pmatrix} x_{l-2,0}^{(Z,l-1,l-2)} & x_{l-2,1}^{(Z,l-1,l-2)} & x_{l-2,2}^{(Z,l-1,l-2)} \\ x_{l-2,0}^{(Z,l,l-2)} & x_{l-2,1}^{(Z,l,l-2)} & x_{l-2,2}^{(Z,l,l-2)} \\ x_{l-2,0}^{(Z,l+1,l-2)} & x_{l-2,1}^{(Z,l+1,l-2)} & x_{l-2,2}^{(Z,l+1,l-2)} \end{pmatrix} \tag{5.27}$$

the equation 5.24 becomes $\lambda' = \mathbf{X}\lambda$ and the matrix element $\lambda_+(Z, l, l-2, l-2)$ is finally found as the first element of the vector λ.

The matrix elements of $\mathbf{X}$ have been calculated in section 4.4. For $c = 0$ they are given by $g(Z, l)$, for $c \geq 1$ they are calculated by solving the recurrence relations (4.57) respectively (4.58).

The matrix $\mathbf{X}$ can be easily inverted using some computer algebra program. But before doing so we well split it into a product of diagonal matrices and Hessenberg matrices.

From the start condition (4.60) of the recurrence relation(4.57) and the explicit form (4.17) of the $g(Z, l)$ we note that

$$\frac{x_{m,c}^{(Z,l+1,m)}}{x_{m,c}^{(Z,l,m)}} = \frac{(Z/2-l)\,(2l+2)}{(Z/2+l+1)\,(Z/2+l+2)}. \tag{5.28}$$

Furthermore, the $x_{m,c}^{(Z,l,m)}, c = 1, 2$ are multiples of $x_{m,o}^{(Z,l,m)}$. These relations may be used to split off diagonal matrices from $\mathbf{X}$. Splitting the remaining matrix in a upper and a lower Hessenberg form, we obtain the product

$$\begin{aligned} \mathbf{X} = &\begin{bmatrix} \frac{1}{2} & 0 & 0 \\ 0 & -\frac{Z-2l-2\delta+2}{4} & 0 \\ 0 & 0 & \frac{(Z+2l+2\delta-4)(Z+2l+2\delta-2)}{16} \end{bmatrix} \begin{bmatrix} 1 & 0 & 0 \\ -1 & 1 & 0 \\ 1 & -2 & 1 \end{bmatrix} \\ &\begin{bmatrix} 1 & 0 & 0 \\ 0 & \frac{-1}{4(l+\delta)} & 0 \\ 0 & 0 & \frac{Z-2\,l-2\,\delta}{8(l+\delta+1)(2\,l+2\,\delta+1)} \end{bmatrix} \begin{bmatrix} 1 & -Z+2\,l+2\,\delta-2 & \frac{(l+\delta+1)(Z-2\,l-2\,\delta+2)}{l+\delta} \\ 0 & 1 & -\frac{2\,l+2\,\delta+1}{l+\delta} \\ 0 & 0 & 1 \end{bmatrix} \\ &\begin{bmatrix} \frac{Z+2\,l+2\,\delta}{2\,l+2\,\delta-1} & 0 & 0 \\ 0 & \frac{(Z+2\,l+2\,\delta)(Z+2\,l+2\,\delta+2)}{2\,l+2\,\delta+1} & 0 \\ 0 & 0 & \frac{(Z+2\,l+2\,\delta+4)(Z+2\,l+2\,\delta+2)(Z+2\,l+2\,\delta)}{(2\,l+2\,\delta+3)(Z-2\,l-2\,\delta)} \end{bmatrix}, \end{aligned} \tag{5.29}$$

which is inverted easily.

In the same way the matrix elements of $\lambda_o^{(Z,l+1,l-1,l-1)}$ and $\lambda_-^{(Z,l+1,l,l)}$ are obtained. The inversion procedure above must be repeated, because different values of m are used in (5.24) and (5.24).

Thus, we obtain the desired matrix elements

$$\begin{aligned}
\lambda_-(Z,l,l,l) &= \frac{Z}{2}-l,\\
\lambda_o(Z,l,l-1,l-1) &= \frac{Z+2}{2(l+1)},\\
\lambda_+(Z,l,l-2,l-2) &= \frac{\frac{Z}{2}+l+1}{l(2l+1)}.
\end{aligned} \tag{5.30}$$

5.5.3 Matrix Elements of the Atomic Liouville Operator

Inserting (5.30) into equation (5.22) which expresses arbitrary matrix elements of the loss part of the atomic Liouville operator in terms of the three representative matrix elements we obtain all other matrix elements:

$$\begin{aligned}
\mathrm{tr}\left(\check{\xi}^{(Zlmm')}\mathcal{L}_{a,l}\hat{\xi}^{(Z,l+1,m+1,m'+1)}\right) &= \\
&\frac{\sqrt{(l+m)(l+m-1)(l+m')(l+m'-1)}}{2l(2l-1)}\frac{Z-2l}{2},\\
\mathrm{tr}\left(\check{\xi}_{Z,l,m,m'}\mathcal{L}_{a,l}\hat{\xi}^{(Z,l,m+1,m'+1)}\right) &= \\
&\frac{\sqrt{(l-m+1)(l+m)(l-m'+1)(l+m')}}{2l}\frac{Z+2}{2(l+1)},\\
\mathrm{tr}\left(\check{\xi}_{Z,l,m,m'}\mathcal{L}_{a,l}\hat{\xi}^{(Z,l-1,m+1,m'+1)}\right) &= \\
&\frac{\sqrt{(l-m)(l-m-1)(l-m')(l-m'-1)}}{2}\frac{\frac{Z}{2}+l+1}{l(2l+1)}.
\end{aligned} \tag{5.31}$$

From these matrix elements we obtain immediately the matrix elements of the gain part using the relation (5.20) which relates the matrix elements of the gain and the loss part:

$$\begin{aligned}
\mathrm{tr}\left(\check{\xi}^{(Z,l,m,m')}\mathcal{L}_{a,g}\hat{\xi}^{(Z,l+1,m+1,m'+1)}\right) &= \\
&\mathrm{tr}\left(\check{\xi}^{(Z,l,-m,-m')}\mathcal{L}_{a,l}\hat{\xi}^{(Z,l+1,-m-1,-m'-1)}\right),\\
\mathrm{tr}\left(\check{\xi}_{Z,l,m,m'}\mathcal{L}_{a,g}\hat{\xi}^{(Z,l,m+1,m'+1)}\right) &= \\
&\mathrm{tr}\left(\check{\xi}_{Z,l,-m,-m'}\mathcal{L}_{a,l}\hat{\xi}^{(Z,l,-m-1,-m'-1)}\right),\\
\mathrm{tr}\left(\check{\xi}_{Z,l,m,m'}\mathcal{L}_{a,g}\hat{\xi}^{(Z,l-1,m+1,m'+1)}\right) &= \\
&\mathrm{tr}\left(\check{\xi}_{Z,l,-m,-m'}\mathcal{L}_{a,l}\hat{\xi}^{(Z,l-1,-m-1,-m'-1)}\right).
\end{aligned} \tag{5.32}$$

This completes the calculation of the matrix elements.

The Dicke representation of the master equation is not in Lindblad form. Nevertheless, using (4.17) one can still show that the trace of the contribution of $\mathcal{L}_a$ to $\mathcal{L}_a\xi_{Z,l,m,m}$ is zero:

$$\mathrm{tr}\left(\mathcal{L}\xi_{Z,l,m,m}\right) = 0. \tag{5.33}$$

If this condition was violated, the time evolution would not conserve the trace of the density operator. Since the original Liouville operator is in Lindblad form, this result is expected and rather a control of the calculations presented here than a test of the underlying model.

The trace above contains the degeneracy factors $g(Z,l-1)$, $g(Z,l)$ and $g(Z,l+1)$ because they do not contain the dual basis operator. In order to simplify it to zero, the explicit form (4.17) of the $g(Z,l)$ is used:

$$\begin{aligned}
&\mathrm{tr}\left(\mathcal{L}\xi_{Z,l,m,m}\right)\\
&\quad= \lambda_+(Z,l+1,m-1,m-1)g(Z,l+1)\\
&\qquad+\lambda_o(Z,l,m-1,m-1)g(Z,l)\\
&\qquad+\lambda_-(Z,l-1,m-1,m-1)g(Z,l-1)\\
&\qquad-\left(\frac{Z}{2}+m\right)g(Z,l)\\
&\quad= g(Z,l)\Bigg(\lambda_+(Z,l+1,m-1,m-1)\frac{g(Z,l+1)}{g(Z,l)}\\
&\qquad\qquad+\lambda_o(Z,l,m-1,m-1)\\
&\qquad\qquad+\lambda_-(Z,l-1,m-1,m-1)\frac{g(Z,l-1)}{g(Z,l)}\\
&\qquad\qquad-\left(\frac{Z}{2}+m\right)\Bigg)\\
&\quad= g(Z,l)\Bigg(\frac{(l-2-m)(-l+m-1)(Z-2l)}{4(l+1)(2l+1)}\\
&\qquad\qquad+\frac{(l+m)(l+m-1)(Z-2l)}{(l+1)(2l+1)}\\
&\qquad\qquad+\frac{(l-1+m)(l+m)(Z+2l+2)}{l(2l+1)}\\
&\qquad\qquad-\left(\frac{Z}{2}+m\right)\Bigg)\\
&\quad= 0.
\end{aligned}$$

5.6 Matrix Elements of the Complete Liouville Operator

We combine the matrix elements of the atomic Liouville operator (5.30, 5.22), the mode Liouville operator (5.10) and the matrix elements of the commutator with the Hamilton operator and 5.20) to obtain the matrix elements of

$$
\begin{aligned}
&\mathrm{tr}\left(\check{\xi}^{(Z,\bar{M},K)}_{\bar{l},\bar{m},\bar{m}'}\mathcal{L}\hat{\xi}^{(Z,M,K)}_{l,m,m'}\right)\\
&= -\tfrac{ig}{2}\sqrt{(\bar{l}-\bar{m})(\bar{l}+\bar{m}+1)(\bar{M}-K-\bar{m})}\delta_{l,\bar{l}}\delta_{m-1,\bar{m}}\delta_{m',\bar{m}'}\delta_{M',\bar{M}'}\\
&\quad -\tfrac{ig}{2}\sqrt{(\bar{l}-\bar{m}+1)(\bar{l}+\bar{m})(\bar{M}-K-\bar{m}+1)}\delta_{l,\bar{l}}\delta_{m+1,\bar{m}}\delta_{m',\bar{m}'}\delta_{M',\bar{M}'}\\
&\quad +\tfrac{ig}{2}\sqrt{(\bar{l}-\bar{m}')(\bar{l}+\bar{m}'+1)(\bar{M}-K-\bar{m}')}\delta_{l,\bar{l}}\delta_{m'-1,\bar{m}'}\delta_{m,\bar{m}}\delta_{M',\bar{M}'}\\
&\quad +\tfrac{ig}{2}\sqrt{(\bar{l}-\bar{m}'+1)(\bar{l}+\bar{m}')(\bar{M}-K-\bar{m}'+1)}\delta_{l,\bar{l}}\delta_{m'+1,\bar{m}'}\delta_{m,\bar{m}}\delta_{M',\bar{M}'}\\
&\quad -\tfrac{B}{8}(Z+m_i+m_j+2s)\delta_{l,\bar{l}}\delta_{m,\bar{m}}\delta_{m',\bar{m}'}\delta_{M,\bar{M}}\\
&\quad +\tfrac{B}{4}(1-s)\tfrac{\sqrt{(\bar{l}+\bar{m}+1)(\bar{l}+\bar{m}+2)(\bar{l}+\bar{m}'+1)(\bar{l}+\bar{m}'+2)}}{2(2\bar{l}+1)(\bar{l}+1)}\left(\tfrac{Z}{2}-\bar{l}\right)\delta_{l-1,\bar{l}}\delta_{m-1,\bar{m}}\delta_{m'-1,\bar{m}'}\delta_{M-1,\bar{M}}\\
&\quad +\tfrac{B}{4}(1-s)\tfrac{\sqrt{(\bar{l}+\bar{m}+1)(\bar{l}-\bar{m})(\bar{l}+\bar{m}'+1)(\bar{l}-\bar{m}')}}{2\,\bar{l}(\bar{l}+1)}\left(\tfrac{Z}{2}+1\right)\delta_{l,\bar{l}}\delta_{m-1,\bar{m}}\delta_{m'-1,\bar{m}'}\delta_{M-1,\bar{M}}\\
&\quad +\tfrac{B}{4}(1-s)\tfrac{\sqrt{(\bar{l}-\bar{m})(\bar{l}-\bar{m}-1)(\bar{l}-\bar{m}')(\bar{l}-\bar{m}'-\bar{1})}}{2\,l(2\,l+1)}\left(\tfrac{Z}{2}+\bar{l}+1\right)\delta_{l+1,\bar{l}}\delta_{m+1,\bar{m}}\delta_{m'+1,\bar{m}'}\delta_{M+1,\bar{M}}\\
&\quad +\tfrac{B}{4}s\tfrac{\sqrt{(\bar{l}-\bar{m})(\bar{l}-\bar{m}-1)(\bar{l}-\bar{m}')(\bar{l}-\bar{m}'-1)}}{4l(2l-1)}(Z-2\bar{l}+2)\delta_{l-1,\bar{l}}\delta_{m+1,\bar{m}}\delta_{m'+1,\bar{m}'}\delta_{M+1,\bar{M}}\\
&\quad +\tfrac{B}{4}s\tfrac{\sqrt{(\bar{l}-\bar{m}+1)(\bar{l}+\bar{m})(\bar{l}-\bar{m}+1')(\bar{l}+\bar{m}')}}{4\bar{l}(l+1)}(Z+2)\delta_{l,\bar{l}}\delta_{m+1,\bar{m}}\delta_{m'+1,\bar{m}'}\delta_{M+1,\bar{M}}\\
&\quad +\tfrac{B}{4}s\tfrac{\sqrt{(\bar{l}+\bar{m}+1)(\bar{l}+\bar{m}+2)(\bar{l}+\bar{m}'+1)(\bar{l}+m'+2)}}{4\bar{l}(2\bar{l}+1)}(Z+2\bar{l}+2)\delta_{l+1,\bar{l}}\delta_{m+1,\bar{m}}\delta_{m'+1,\bar{m}'}\delta_{M+1,\bar{M}}\\
&\quad -\tfrac{A}{2}(1+\nu)(2M+2K-m-m')\delta_{l,\bar{l}}\delta_{m,\bar{m}}\delta_{m',\bar{m}'}\delta_{M,\bar{M}}\\
&\quad +A\nu\sqrt{(M+K-m)(M+K-m')}\delta_{l,\bar{l}}\delta_{m,\bar{m}}\delta_{m',\bar{m}'}\delta_{M+1,\bar{M}}\\
&\quad +A\sqrt{(M+K-m+1)(M+K-m'+1)}\delta_{l,\bar{l}}\delta_{m,\bar{m}}\delta_{m',\bar{m}'}\delta_{M-1,\bar{M}}. \qquad (5.34)
\end{aligned}
$$

Chapter 6

Eigenvalues and Eigenvectors

6.1 The Matrix Recurrence Relation

I section 4.5 we introduced the combined indices M and K which depend the numbers of photons of the resonator mode plus the number of photons absorbed into an atomic excitation. M is half the sum of the row and column index and K is the difference so that K gives the total distance of the index from the diagonal which is invariant under the dissipation processes studies here and the Jaynes-Cummings model.

The Liouville operator is diagonal in Z and K. At zero temperature $n_{th} = 0$ and without atomic pumping $s = 0$ the matrix elements $\check{\rho}_{Z,\bar{M},\bar{K},\bar{l},\bar{m},\bar{m}'}\mathcal{L}\hat{\rho}_{Z,M,K,l,m,m'}$ are zero if $\bar{M} > M$. Furthermore, the matrix elements are zero for $\bar{M} - M > 1$.

In order to simplify the notation one may combine all basis states with given values of Z, M and K in a basis states $\hat{\Xi}^{Z,M,K}$ and a corresponding dual basis states $\check{\Xi}^{Z,M,K}$. The Hamiltonian part of the Liouville operator and the diagonal part of the atomic Lindblad operator have nonvanishing matrix elements only between vectors having the same Z, M and K, while the gain part increases M by 1 and the loss part reduces M by 1:

$$\mathrm{tr}\left(\check{\Xi}^{\bar{Z},\bar{M},\bar{K}}\mathcal{L}_{a,l}\hat{\Xi}^{Z,M,K}\right) = 0, \bar{M} \neq M - 1, \tag{6.1}$$

$$\mathrm{tr}\left(\check{\Xi}^{\bar{Z},\bar{M},\bar{K}}\mathcal{L}_{a,g}\hat{\Xi}^{Z,M,K}\right) = 0, \bar{M} \neq M + 1. \tag{6.2}$$

This is a straightforward generalisation of a well known result for $Z = 1$.

Now one may write the master equation

$$\mathcal{L}\hat{\rho} = \Lambda\hat{\rho} \tag{6.3}$$

in the form of a linear equation system:

$$\begin{aligned}\Lambda\hat{\Xi}_{\Lambda}^{(Z,M,K)} &= \mathcal{M}^{(Z,M,K)}\hat{\Xi}_{\Lambda}^{(Z,M,K)} \\ &\quad +\mathcal{F}^{(Z,M+1,K)}\hat{\Xi}_{\Lambda}^{(Z,M+1,K)} \\ &\quad +\mathcal{G}^{(Z,M-1,K)}\hat{\Xi}_{\Lambda}^{(Z,M-1,K)},\end{aligned} \tag{6.4}$$

where the operators $\mathcal{M}, \mathcal{F}$ and $\mathcal{G}$ may be read off (5.34).

In particular, we find $\mathcal{G} = 0$ if the thermal photon number n_{th} and the atomic pump parameter s are zero. In this case the recurrence relation reads

$$\mathcal{M}_{(\mathcal{Z},\mathcal{M},\mathcal{K})}\Xi^{(Z,M,K)} = \Lambda_{(Z,M,K)}\Xi^{(Z,M,K)}, \tag{6.5}$$

$$\left(\Lambda_{(Z,M,K)} - \mathcal{M}_{(\mathcal{Z},\mathcal{M}',\mathcal{K})}\right)\Xi^{(Z,M,K)} = \mathcal{F}_{(Z,M'+1,K)}\Xi^{(Z,M'+1,K)} \tag{6.6}$$

for $M' < M$.

In this case the eigenvalues may be obtained as the eigenvalues of $\mathcal{M}^{(Z,M,K)}$ and the eigenstates from the eigenvectors. Because all eigenvalues are different, the operator

$$\left(\Lambda_{(Z,M,K)} - \mathcal{M}_{(\mathcal{Z},\mathcal{M}',\mathcal{K})}\right)\mathcal{F}_{(Z,M'+1,K)} \tag{6.7}$$

exists if $M' < M$ and the eigenstates may be obtained by an iterative application of (6.6)

The matrix elements of $\mathcal{M}^{(Z,M,K)}$ between generalised Dicke states with different angular momentum l vanish because different values of l are coupled only by the gain and loss part of the Liouville operator. The remaining matrix has the dimension $(l+1)^2$, if $M > 2l+1$ and M^2 otherwise. In any case, there are four indices, two for each generalised Dicke state. The matrix elements are

$$\mathcal{M}_{m,m';\bar{m},\bar{m}'} = \begin{cases} \langle Z,l,m'|\, H + \mathcal{L}_{a,d}\,|Z,l,\bar{m}'\rangle\,, & \text{if} \quad m = \bar{m}, \\ \langle Z,l,m|\, -H + \mathcal{L}_{a,d}\,|Z,l,\bar{m}\rangle\,, & \text{if} \quad m' = \bar{m}', \\ 0, & \text{else.} \end{cases} \tag{6.8}$$

6.2 The Degeneracy of the Eigenvalue Matrix

The eigenvalue matrix $\mathcal{M}$ shows a degeneracy which results from its construction from the commutator with the Hamiltonian, $\mathcal{H}$, and the anticommutator with the diagonal part of the dissipation. $\mathcal{H}$ is the operator that maps any density operator on its commutator with the Hamiltonian.

In the generalised Dicke basis the symmetry operator $\mathcal{S}^{(\mathcal{M})}$ of the degeneracy of $\mathcal{M}$ has the matrix elements

$$\mathcal{S}^{(\mathcal{M})}_{m,m';\bar{m},\bar{m}'} = \begin{cases} (-1)^{m-m'}, & \text{if} \quad m = \bar{m}, \\ 0, & \text{else.} \end{cases} \tag{6.9}$$

Using the fact that H is symmetric and that the number state representation of H has nonvanishing matrix elements only on the first off-diagonal and $\mathcal{L}_{a,d}$ has no nonzero off-diagonal matrix elements, it can be shown easily that

$$\left[\mathcal{S}^{(\mathcal{M})}, \mathcal{M}\right] = 0. \tag{6.10}$$

The Dicke state representation of the eigenvectors $|\lambda\rangle$ of H may be chosen so that

$$\langle\lambda|Z, M, K, l, m\rangle = (-1)^{m-1} \langle -\lambda|Z, M, K, l, m\rangle \,, \tag{6.11}$$

as can be seen immediately from the matrix representation of the eigenvalue equation.

Using these results we construct a new operator basis which consists of simultaneous eigenvectors of $\mathcal{H}$ and $\mathcal{S}$.

The index m runs from $-l$ which means that the amount energy that is not absorbed by dark states of the cluster or atoms is contained in the resonator mode, to $d = \min(l, M - \frac{Z}{2})$ which means that the atomic cluster contains as much energy as consistent with its angular momentum all atoms are excited and the remaining energy is contained in the resonator mode. There are $\frac{1}{2}(d + l + 1)(d + l + 2)$ eigenoperators of of $\mathcal{S}$ with eigenvalue 1. Their Dicke state representation is

$$\rho_{+,m} = |Z, M, K, l, m\rangle \langle Z, M, K, l, d + l + 2 - m| \,, \tag{6.12}$$

$$\begin{aligned} \rho_{+,m,m'} = \frac{1}{\sqrt{2}}\big(&|Z, M, K, l, m\rangle \langle Z, M, K, l, m'| \\ &+ |Z, M, K, l, d + 2 - m\rangle \langle Z, M, K, l, d + l + 2 - m'|\big) \end{aligned} \tag{6.13}$$

with the auxiliary condition

$$m + (l + d + 1)(m' - 1) < d + l + 2 - m + (l + d + 1)(d + l + 2 - m' - 1)$$

that guarantees the uniqueness of the eigenvectors. The Dicke state representation of the $\frac{1}{2}(d + l + 1)(d + l)$ eigenoperators of of $\mathcal{S}$ with eigenvalue -1 is

$$\begin{aligned} \rho_{-,m,m'} = \frac{1}{\sqrt{2}}\big(&|Z, M, K, l, m\rangle \langle Z, M, K, l, m'| \\ &- |Z, M, K, l, d + 2 - m\rangle \langle Z, M, K, l, d + l + 2 - m'|\big). \end{aligned} \tag{6.14}$$

The calculation of the eigenvectors may be significantly simplified with the help of this symmetry, since the eigenvectors of a non-hermitian complex matrix are not necessarily orthogonal, and therefore it is difficult to find a complete set of eigenvectors of a degenerate nonsymmetric matrix.

6.3 The Stroboscopic Mode Propagator

By specifying the state in which the atoms enter the cavity and the procedure applied to the atoms after they leave the resonator, on can trace out atomic degrees of freedom.

If one chooses to measure the atoms after they leave the resonator, the atom will be projected onto the corresponding eigenstate after it leaves the resonator. Since the atom and the resonator mode are entangled at this moment, the resonator will be projected on the corresponding state.

Using the eigenstates and eigenvalues of the coupled system of atoms one obtains the map describing the time propagation from the moment when the cluster enters the cavity to the moment when the cluster leaves the cavity. Shortly before the cluster enters the cavity the atoms are described by an atomic density operator $\hat{\rho}_{atom,in}$. The procedure applied to the atoms after they leave the resonator, for example a measurement of the atomic states, may be described by a multiplication by dual atomic density operator describing this procedure $\check{\rho}_{atom,out}$ followed by tracing out the atoms, thus obtaining an operator containing mode variables only.

After the interaction of duration τ with the atoms a period of pure dissipation follows.

Putting all together, one obtains

$$\begin{aligned} \rho(t+\tau) &= \sum_i \mathrm{tr}\left(\check{\rho}\hat{\Xi}_i\right) \mathrm{e}^{\lambda_i \tau} \mathrm{tr}\left(\check{\Xi}_i \rho(t) \hat{\rho}_{atom,in}\right), \\ \rho(t+T) &= \sum_j \check{\Xi}_j \mathrm{e}^{\lambda_j (T-\tau)} \mathrm{tr}\left(\check{\Xi}_j \rho(t+\tau)\right), \end{aligned} \tag{6.15}$$

where T is the cycle duration of the pump mechanism and $\hat{\Xi}_i \check{X} i_i$ are the left and right eigenstates of the coupled system corresponding to the eigenvalue λ_i and $\hat{\Xi}_j^{(o)}, \check{X} i_j^{(o)}, \lambda_j^{(o)}$ are the eigenstates and eigenvalues of pure mode dissipation.

Since $\rho(t+T)$ depends linearly on $\rho(t)$ (6.15) may be read as the definition of a map $\mathcal{M}$ with

$$\rho(t+T) = \mathcal{M}\rho(t). \tag{6.16}$$

6.3.1 The Eigenstate Dual to the Stationary State

The dual eigenstate corresponding to the eigenvalue 0 has the form $\mathrm{tr}\left(\check{\xi}_{Z,l,m,m'}\right) = g(Z,l)$ since any eigenstate $\rho = \sum_i c_i \hat{\xi}_{Z,l_i,m_i,m_i'}$ corresponding to a nonzero eigenvalue is traceless and orthogonal to the stationary state $\hat{\rho}_o = \sum_i d_i \check{\xi}_{Z,l_i,m_i,m_i'}$. Therefore

$$\begin{aligned} \mathrm{tr}\,(\rho) &= \sum_i c_i g(Z,l_i) = 0, \\ \mathrm{tr}\,(\check{\rho}_o \rho) &= \sum_i c_i d_i = 0 \end{aligned}$$

hold. Since the c_i are arbitrary otherwise, the second condition can only be fulfilled if

$$d_i = g(Z,l_i). \tag{6.17}$$

This result may be used to control numerical calculations of eigenstates: In the calculations presented here the only normalization condition imposed artificially is that $\mathrm{tr}\,(\hat{\rho}_o) = 1$. The dual eigenstate corresponding to the eigenvalue 0 can then be tested against (6.17).

6.4 Coherent Driving Field

If the cavity is driven by an external resonant coherent field the interaction picture Hamiltonian contains the additional term

$$H_c = \epsilon(a^\dagger + a) \tag{6.18}$$

that describes the interaction of the field mode with the Hamiltonian.

In contrast to the atomic pump mechanism this mechanism connects different values of K and any eigenstate of the Liouville operator contains all values of M and K. Therefore, one has to diagonalize the full Liouville operator in one step. In order to obtain a finite-dimensional Liouville operator the energy M has to be cut off somewhere.

Not all eigenstates resulting from this procedure are physically correct. Only those eigenstates with a negligible occupation probability at the cutoff may be used in further calculations. In practice this is not a problem, since these states are orthogonal to all relevant states if the cutoff has been chosen large enough.

In this case, the diagonalization of the Lindblad operator has to be performed by one single diagonalization of a large nonsymmetric matrix.

Chapter 7

Masers with many Atoms

A maser is a resonator cavity with a very long photon lifetime. The resonator mode of this cavity is pumped by excited atoms crossing the cavity in an atomic beam. The atoms emit and absorb photons during their flight through the resonator. The state in which the atoms leave the maser depends sensitively on the number of atoms in the maser, the time the atoms need to traverse the maser [29] and the state of the field in the resonator before the atoms entered the resonator. For a review on micromaser physics see [30].

Now we will focus on the special case that the atoms enter the maser in clusters and not individually. We examine the trapped states of the maser, i.e. cyclically stationary states where the atom leaves the resonator in the excited state so that the resonator is not excited. The map (6.16) describes a maser experiment where a cluster of partially or completely excited atoms enter and leave the resonator at the same time. A schematic drawing of this type of experiment is shown in figure 7.1. We assume that the excitation of the atoms is selective on the velocity of the atoms so that only clusters with a certain velocity are pumped into the Rydberg state that interacts with the resonator. Please note that the effects of the mode structure have been neglected. The state of the resonator mode just

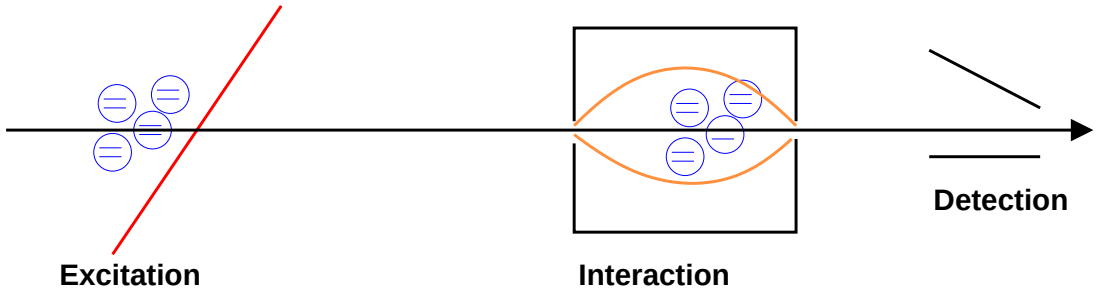

Figure 7.1: Schematic drawing of the maser.

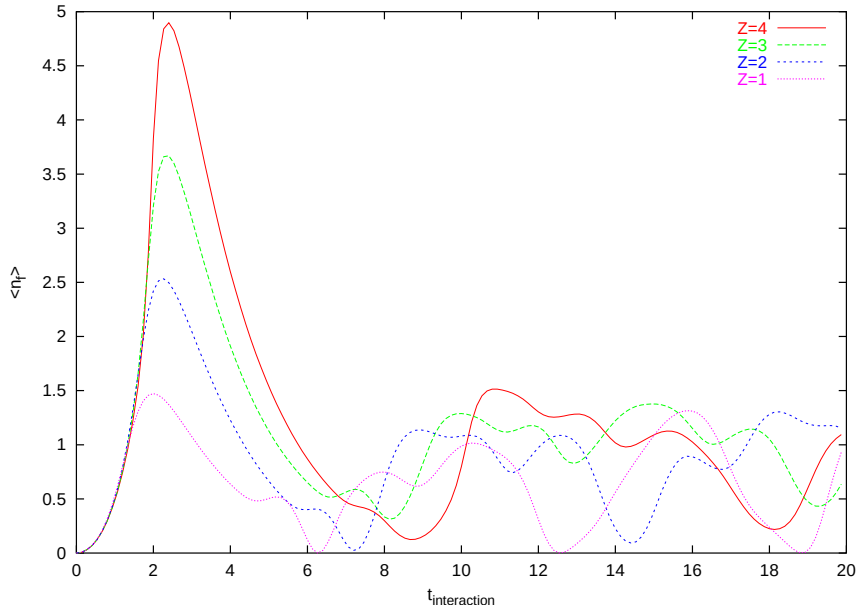

Figure 7.2: Mean photon number $< n_f >$ at $g = 1/\sqrt{Z}$, $A = 0.008$ and $B = 0.004$ and $Z = 1, 2, 3, 4$. The vacuum trapped states do not occur at the same time, therefore the scaling of of g does not hold here.

before one atom enters the resonator is mapped onto the state of the mode just before the next cluster enters the resonator. The eigenstate with eigenvalue 0 of this map therefore describes a cyclically stationary state.

In the following we will examine the properties of these cyclically stationary states.

7.1 All Atoms Initially Excited: Suppression of the Trapped States

If all atoms enter the resonator in their excited state, the pump rate is proportional to the number of atoms. Therefore, the mean photon number is proportional to the number of atoms. With increasing Z the photon number may become quite large in this case. Figure 7.2 shows the stationary photon number at the moment when the cluster enters the resonator for clusters of one to four atoms. The parameters are $g = 1/\sqrt{Z}$, $A = B = 0.004$. The arrival times of the atoms are regularly distributed and the time difference between two arrivals is 60 time units. The time units have been chosen so that the one-atom coupling constant is exactly $1/\sqrt{Z}$. After the interaction a period of pure resonator damping follows. In the interaction picture used in this work the resonator mode

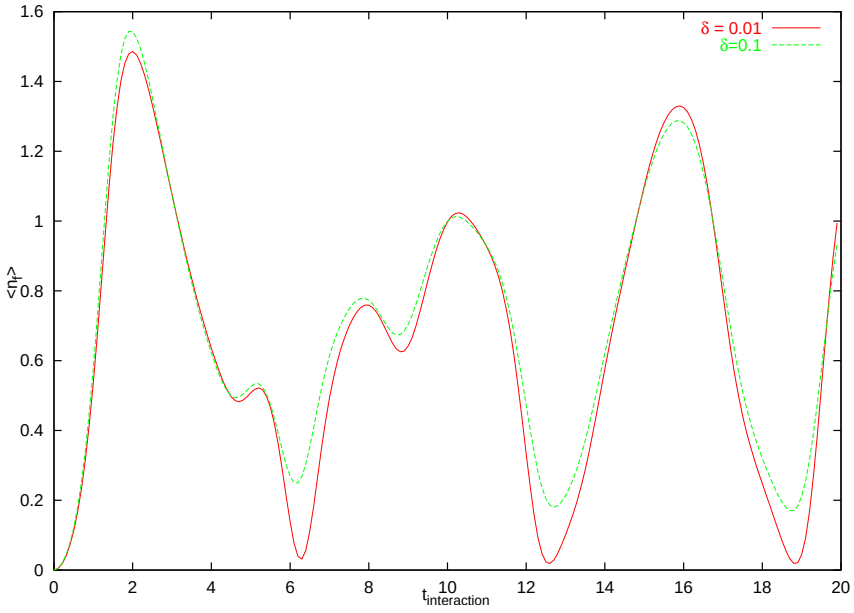

Figure 7.3: The stationary photon number $< n_f >$ at uncertain atom number Z. The atom number is $Z = 1$ with probability $1 - \delta$ and $Z = 2$ with probability δ as a function of the interaction time. All atoms are excited when entering the cavity. For $\delta = 0.05$ even the vacuum trapping states vanish.

has no self-energy. The interaction time of the atoms with the resonator mode is between 0 and 20 time units.

The interaction time at which the maximum and the first minimum of the photon number occurs, depends on the number of atoms. This means that the $\sqrt{Z}$-scaling does not hold in this case. The explanation for this observation is that the scaling behavior of g was derived in Section 3 under the assumption $Z \gg M$. The trapped states vanish for $Z > 2$ as expected, since in this regime many different oscillation frequencies are involved.

7.2 Atom Number Fluctuations

If the number of atoms of the individual cluster cannot be fixed exactly the dependency of the oscillation frequency on the number of atoms causes a broadening and therefore washes out the trapped states. This effect has been already discussed by E. Wehner et al. in [39] using the assumption that the time the atoms need to traverse the resonator is much smaller than the time between two consecutive atomic clusters.

We assume that with probability δ not one but two excited atoms enter the

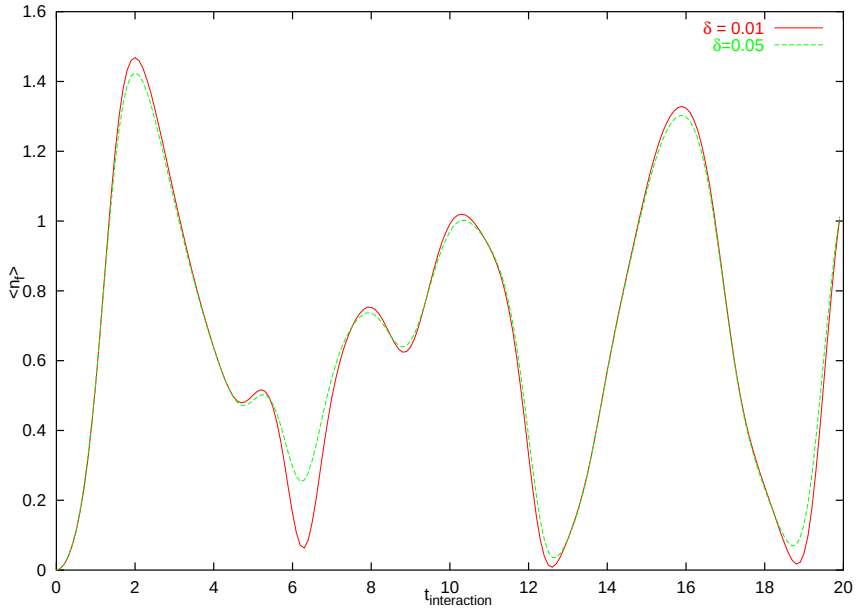

Figure 7.4: The stationary photon number $< n_f >$ at uncertain atom number Z. The atom number is $Z = 1$ with probability $1 - \delta$ and $Z = 2$ with probability δ as a function of the interaction time. In the one-atom events and the two-atom events only one atom is excited For $\delta = 0.05$ the first vacuum trapping states vanishes but the second and third persist.

resonator. In order to model this behavior we replace the map (6.16) with the weighted mean of maps corresponding to different numbers of atoms.

The weighted means are

$$\mathcal{M} = (1 - \delta)\mathcal{M}_{1\,\text{atom}} + \delta\mathcal{M}_{2\,\text{atoms}}, \tag{7.1}$$

if one or two atoms arrive at one point in time respectively

$$\mathcal{M} = (1 - 2\delta)\mathcal{M}_{Z\,\text{atoms}} + \delta\mathcal{M}_{Z+1\,\text{atoms}} + \delta\mathcal{M}_{Z-1\,\text{atoms}}, \tag{7.2}$$

if $Z - 1, Z$ or $Z + 1$ atoms enter the resonator at one point in time. Since clusters where the atom number differs from the mean value by two or more have been neglected, this does not correspond exactly to a poissonian distribution of atomic numbers in the arriving clusters. We assume that all atoms used in one experiment are of the same kind, therefore here we use the same value of g for all atom numbers.

As shown in figure 7.3 even at a small value of $\delta = 0.05$ the vacuum trapped states are washed out if all atoms enter the resonator in the excited state.

The situation is slightly different if only one of the atoms of the two-atom-clusters is excited when it enters the resonator. This means that the pump rate does not

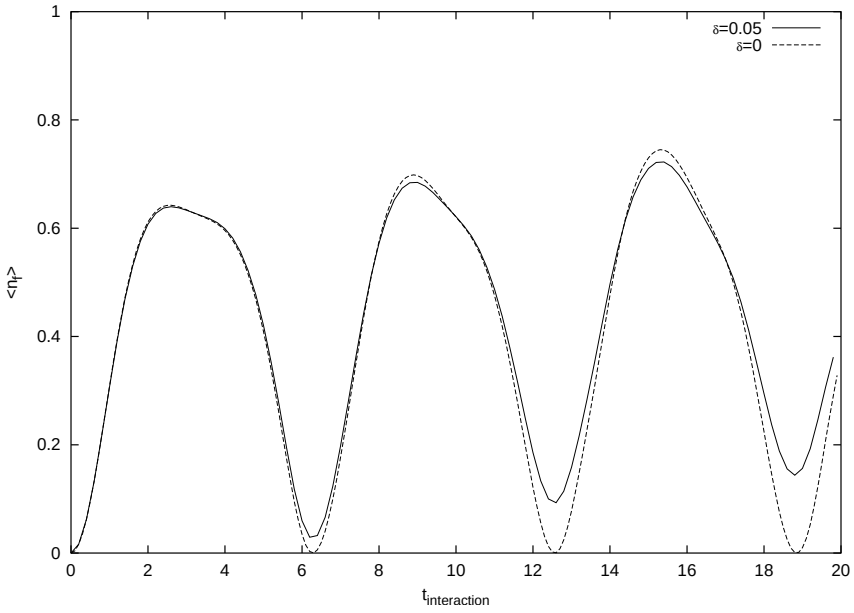

Figure 7.5: The stationary photon number $< n_f >$ at uncertain atom number Z. The atom number is $Z = 3, 4$ and 5 with probability $\delta, 1 - 2\delta$ and δ. The value of δ is for the solid line comparison to fixed atom number $Z = 4$ (broken line). The mean photon number is plotted as a function of the interaction time. The zero-photon trapping states are washed out.

depend on the number of atoms. As figure 7.4 shows the first vacuum trapping state vanishes if two-atom events occur, but the second and the third vacuum trapping state persist. The reason for the different effect on the first and second vacuum trapping state is that the frequency of the Rabi oscillations with two atoms in the resonator is $\sqrt{2}$ times the frequency of the Rabi oscillations with one atom in the resonator. This means that the interaction time of the second vacuum trapping state of the one-atom case is approximately the interaction time of the third vacuum trapping state in the two-atom case.

We do not find this effect in the case of figure 7.5 where the maser is pumped by a clusters containing four atoms with probability 0.9 and three or five atoms with probability 0.05. In this case the trapped states are washed out again.

7.3 One Atom Excited: Scaling and Limiting Behavior

In order to observe quantum behavior of the resonator mode like trapped states, we are interested in small photon numbers. Furthermore, we have seen that the

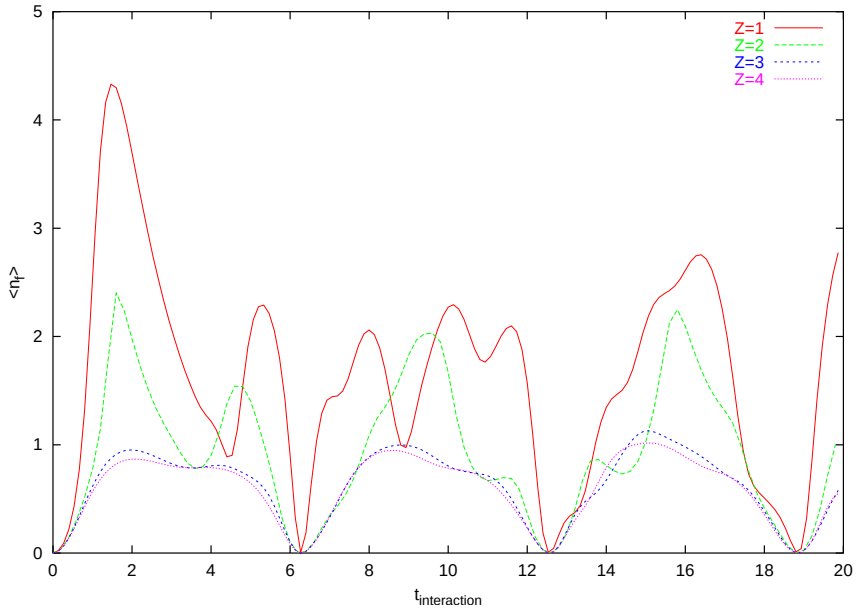

Figure 7.6: Mean photon number $< n_f >$ at $g = 1/\sqrt{Z}$, $A = 0.008$, $B = 0.004$ and $Z = 1, 2, 3, 4$. Only one atom of each cluster is excited. The positions of the vacuum trapping states are predicted accurately by the scaling of g.

suppression of trapped states by multi-atom events is less effective if the clusters enter the resonator only partially excited. Therefore it is useful to consider the case where only one of the many atoms entering the resonator is excited. In this case the maximal photon number of the resonator will not increase with the number of atoms.

Figure 7.6 shows the stationary photon number at the moment when the cluster of atoms enter the resonator for the parameters $g = 1/\sqrt{Z}$, $A = 0.008, B = 0.004$ and $Z = 1, 2, 3, 4$. For small values of Z the curves show a strong dependency on Z, while the curves for $Z = 3$ and $Z = 4$ are very well described by the scaling of g. In contrast to the case of all atoms entering the resonator in their upper state, the trapped states occur at the interaction times predicted by the scaling of g. Even larger numbers of atoms are used in figure 7.7. Here the cluster consists of $Z = 8, 16, 32$ or 64 atoms. The other parameters are the same as in figure 7.6.

For these large values of Z the mean photon number depends periodically on the interaction time. This behavior is completely different from the one-atom case. In this regime the scaling of g is nearly perfect, as can be seen from the fact that the mean photon number for $Z = 32$ and $Z = 64$ are almost the same for any value of the interaction time.

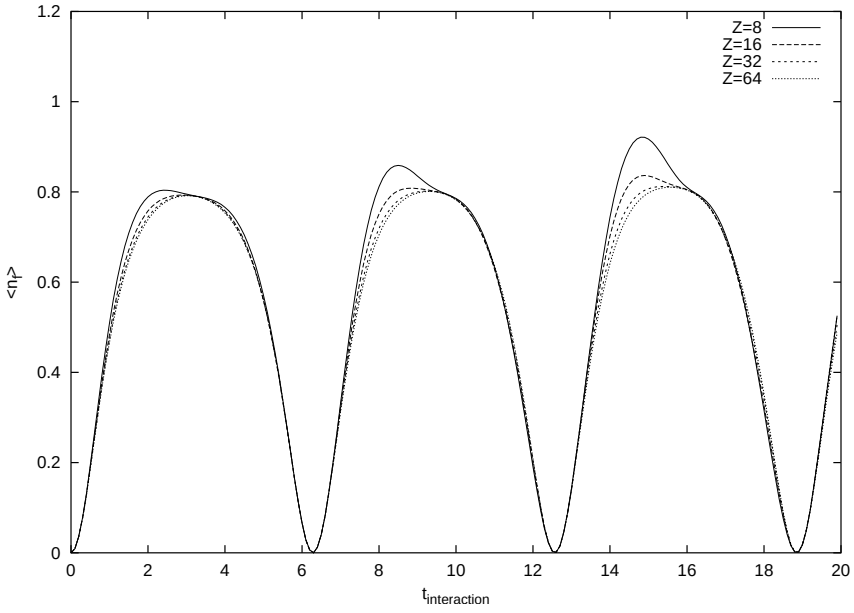

Figure 7.7: Mean photon number $< n_f >$ at $g = 1/\sqrt{Z}$, $A = 0.008$, $B = 0.004$ and $Z = 8, 16, 64$ as a function of the interaction time. Only one atom of the driving cluster is excited. For increasing Z the curves become more and more regular. The positions of the vacuum trapping states and the form of the curves are predicted by the scaling of g.

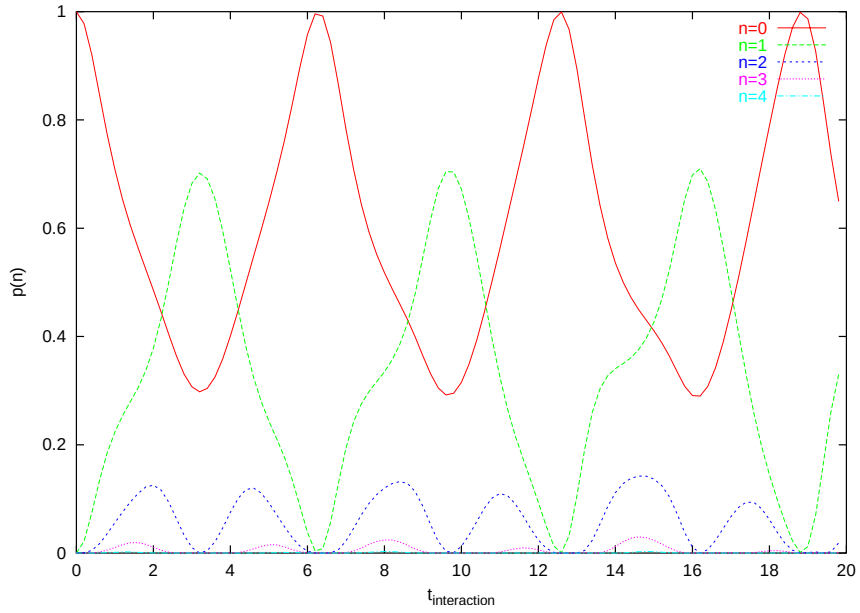

Figure 7.8: Probabilities for finding $n = 0, 1, 2, 3, 4$ photons in the resonator mode as a function of the interaction time. Only one atom of the driving cluster is excited.

7.4 Trapped States

Figure 7.8 shows the stationary resonator mode distribution for $Z = 1, g = 1$ and $A = 0.008, B = 0.004$. At short interaction time one finds contributions of large photon numbers. The dependency on the interaction time is quite irregular. The one-photon trapped state at $t_{interaction} = 5/2\pi$ is completely washed out.

Figure 7.9 shows the stationary resonator mode distribution for $Z = 64, g = 1/8$ and $A = 0.008, B = 0.004$. In contrast to the one-atom-case there is never a significant contribution of states with more than three photons and the interaction time dependency is very regular.

In figure 7.9 the probability for finding one photon in the resonator never approaches unity. In order to demonstrate that this is mainly an effect of the dissipation during the phase between the traversals of the atomic clusters, figure 7.10 shows the photon number distribution in the same system, but immediately after after the atomic cluster has left the resonator. Here, the resonator mode has no time to decay to the vacuum and therefore the peaks corresponding to the one-photon Fock states are much more prominent than in the previous case.

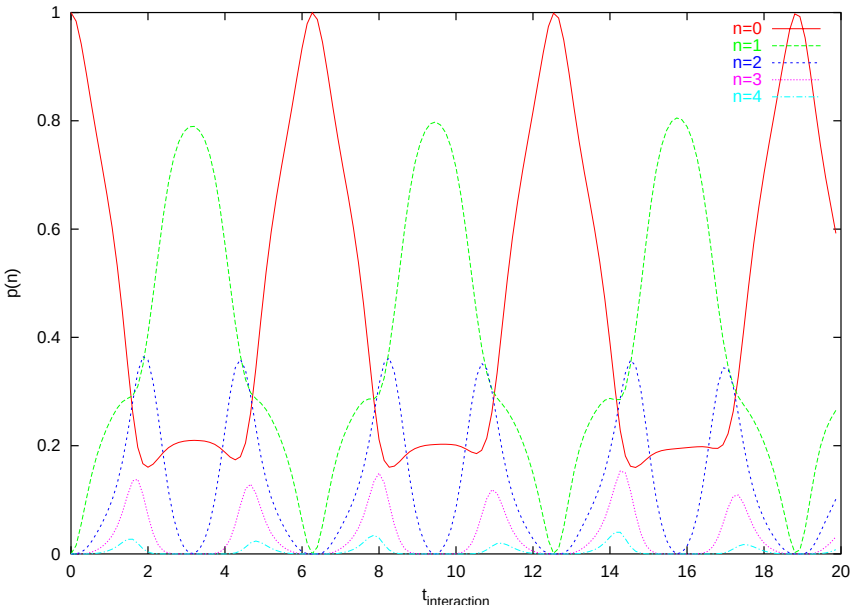

Figure 7.9: Probabilities for finding $n = 0, 1, 2, 3, 4$ photons in the resonator mode as a function of the interaction time. Only one atom of the driving cluster is excited. The probability of finding exactly one photon shows a prominent peak. Here the resonator mode immediately before a new cluster enters the cavity is shown.

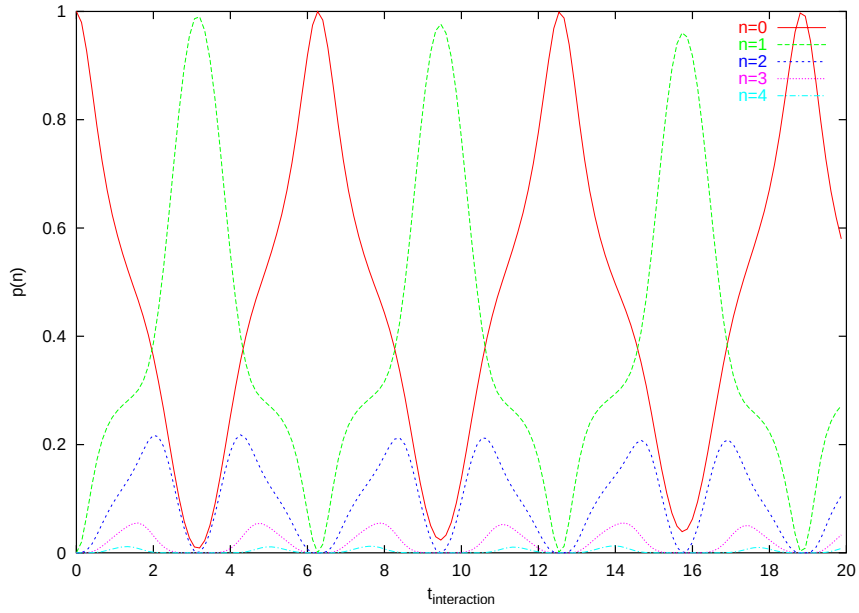

Figure 7.10: Probabilities for finding $n = 0, 1, 2, 3, 4$ photons in the resonator mode as a function of the interaction time. Only one atom of the driving cluster is excited. Here the resonator mode immediately after a new cluster leaves the cavity is shown. The peak of the one-photon Fock state is even more prominent than in the case of Figure 7.9.

Chapter 8

Coherently driven Systems

In order to obtain a nontrivial stationary state in the presence of dissipative processes, we have to include a pump mechanism. In this chapter we assume that classical laser light is coupled into the resonator through one of the mirrors.

The most interesting property of these system is that they can convert light with classical statistic properties, the driving field, into light with nonclassical statistical properties.

The normally-ordered second-order correlation function

$$g^{(2)}(t) = \frac{\left\langle a^\dagger(0)a^\dagger(t)a(t)a(0)\right\rangle}{\left\langle a^\dagger(0)a(0)\right\rangle^2} \tag{8.1}$$

can be measured using fast electronic coincidence counters (see figure 8.1).

8.1 Classical Limits on the Intensity Correlation Function

Following a well-known derivation [14],[37] one can establish a limit on the intensity correlation function of a classical light source.

The classical joint probability distribution for finding the stationary field amplitude α_1 at time t_1 and α_2 at time t_2 is $p_{cl}(\alpha_1, t_1, \alpha_2, t_2)$. Here t_1 is a time when the system has reached its stationary state to sufficient accuracy. Using this probability distribution one finds the classical intensity correlation functions

$$g^{(1)}(t) = \int \mathrm{d}\alpha_1 \int \mathrm{d}\alpha_2 \alpha_1^* \alpha_2 p_{cl}(\alpha_1, t_1, \alpha_2, t_2), \tag{8.2}$$

$$g^{(2)}_{cl}(t) = \frac{1}{|g^{(1)}(0)|^2} \int \mathrm{d}\alpha_1 \int \mathrm{d}\alpha_2 |\alpha_1|^2 |\alpha_2|^2 p_{cl}(I_1, t_1, I_2, t_2), \tag{8.3}$$

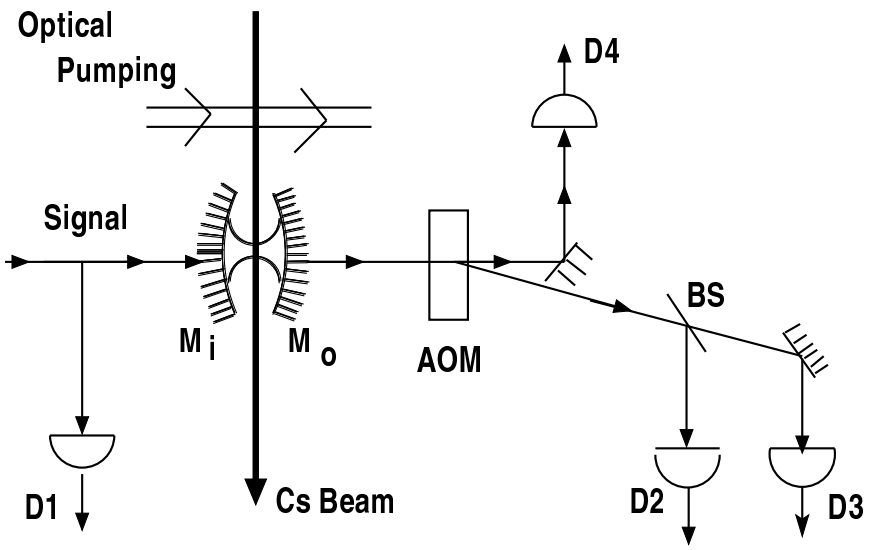

Figure 8.1: The experimental setup of Rempe et al. The cavity was stabilized using the accousto-optic modulator AOM and the detector D4; the beamsplitter BS and and the detectors D2 and D3 were used to measure the coincidence of photon detections and therefore the correlation function.

with $t = |t1 - t2|$. $g^{(1)}(0)$ is the stationary intensity of the field. Since a classical probability distribution is assumed the Cauchy-Schwartz inequality

$$\left\langle |\alpha_1^* \alpha_2|^2 \right\rangle \geq \left\langle \alpha_1^* \alpha_2 \right\rangle^2 \tag{8.4}$$

holds and one obtains the classical limit

$$g^{(2)}(t) \geq \left(\frac{g^{(1)}(t)}{g^{(1)}(0)} \right)^2 . \tag{8.5}$$

A special case of this is $g^{(2)}(0) \geq 1$ for a classical intensity correlation function. This phenomenon is called bunching and indicates a positive correlation of the intensities for small times.

The contrary phenomenon, antibunching, is classically forbidden and hence a pure quantum effect.

Such a coherently driven system has been studied experimentally [32]. The results were, among others, that light with nonclassical properties, namely with antibunched photon counting statistics was emitted. The experimental setup consisted of an atomic beam passing through a high-Q optical cavity. The cavity was excited by a coherent signal beam. The correlation function of the output of the cavity was measured using a coincidence counter. Figure 8.1 shows the principal elements of the experiment.

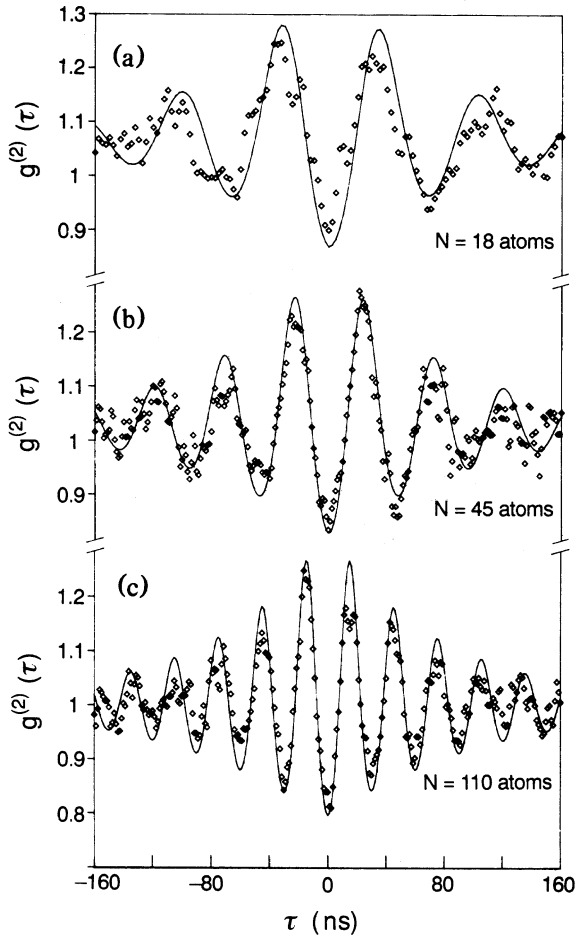

Figure 8.2: Reading points of the intensity correlation function for $Z = 18, 45$ and 110 atoms, as measured by Rempe et al. [32]. The solid line is a fit of a function motivated by the weak-field theory [7]. See the text for a comment on this fit.

The experiment was originally interpreted using a theory which is valid only in the case $\epsilon \ll \kappa$ or equivalently $y \ll \frac{1}{n_s}$ i.e. the weak driving field limit. This is the straight line in figure 8.2. $n_s = \frac{B^2}{8*g^2}$ is the saturation photon number, i.e. the mean photon number of the resonator mode where the mean excitation of one atom interacting with the mode is $\frac{1}{2}$. The atom number Z, the coupling constant g and the damping constants A and B were determined by fitting correlation functions from this approximation to the experimental data. The amplitude of the oscillations in the correlation function was four times the observed amplitude while the frequency of the oscillations was predicted correctly by the approximation.

Figure 8.2 shows the original experimental data of Rempe et al. [32] together

with the scaled curve from the weak-field theory.

The explanation for the need to scale $g^{(2)}(t) - 1$ by a factor of four, that Rempe et al. gave is that [32] used driving fields y which were much stronger than the damping rates, and therefore the weak-field approximation breaks down.

The solution to the many-atom problem presented here supports this explanation and allows us to calculate the value of $g^{(2)}(0)$, as will be shown in the next section.

8.2 Calculation of the Correlation Functions and the Spectrum

If all relevant eigenvalues and eigenstates of the Liouville operator are known, it is possible to calculate dynamical statistical properties of the resonator mode.

The normally ordered intensity correlation function

$$g^{(2)}(t) = \frac{\left\langle a^\dagger(0)a^\dagger(t)a(t)a(0)\right\rangle}{\left\langle a^\dagger(0)a(0)\right\rangle^2} \tag{8.6}$$

can be calculated using the spectral decomposition of the time propagator as a sum over projections on the eigenstates $\check{\rho}_i, \hat{\rho}_i$ multiplied by exponentials of the corresponding eigenvalues λ_i. For any initial value $\rho(0)$ the propagated operator is

$$\rho(t) = \mathrm{e}^{\mathcal{L}t}\rho(0) = \sum_i \hat{\rho}_i \mathrm{e}^{\lambda_i t}\mathrm{tr}\left(\check{\rho}_i\rho(0)\right). \tag{8.7}$$

Although valid for any initial values $\rho(0)$ this formula is particularly useful if $\rho(0)$ is an operator obtained from the stationary state by applying the operators that make up the correlation function. The term $\mathrm{e}^{\mathcal{L}t}$ is a symbolic notation for the propagator. The second equality can be shown by simply inserting the rightmost term of (8.7) into the master equation.

We apply (8.7) to the special case of the correlation function $g^{(2)}(t)$ to express the correlation in terms of eigenvalues λ_i , eigenvectors $\hat{\rho}_i, \check{\rho}_i$ and the stationary state ρ_{stat} of the Liouville operator:

$$\begin{aligned} g^{(2)}(t) &= \frac{\mathrm{tr}\left(a^\dagger(0)a^\dagger(t)a(t)a(0)\rho_{\mathrm{stat}}\right)}{\mathrm{tr}\left(a^\dagger(0)a(0)\rho_{\mathrm{stat}}\right)^2} \\ &= \frac{\mathrm{tr}\left(a^\dagger(0)a(0)\mathrm{e}^{\mathcal{L}t}\left(a(0)\rho_{\mathrm{stat}}a^\dagger(0)\right)\right)}{\mathrm{tr}\left(a^\dagger(0)a(0)\rho_{\mathrm{stat}}\right)^2} \\ &= \sum_i \frac{\mathrm{tr}\left(a^\dagger(0)a(0)\hat{\rho}_i\right)\mathrm{e}^{\lambda_i t}\mathrm{tr}\left(\check{\rho}_i a(o)\rho_{\mathrm{stat}}a^\dagger(0)\right)}{\mathrm{tr}\left(a^\dagger(0)a(0)\rho_{\mathrm{stat}}\right)^2}. \end{aligned} \tag{8.8}$$

The sum runs over all eigenstates of the Liouville operator and λ_i denotes the eigenvalue corresponding to the eigenoperators $\check{\rho}_i, \hat{\rho}_i$.

In practice, this is not possible since there is an infinite number of eigenstates. Therefore, we introduce a maximal photon number well above the mean photon number and one has to cut the eigenstates at that photon number, thus making the problem finite dimensional. The validity of this procedure may be checked by repeating the calculation with different cutoff energies and by requiring that the matrix elements of the stationary state ρ_{stat} vanish at the cutoff energy. This means in practice that the total energy of the stationary state should be significantly lower than the cutoff energy. Some of the eigenstates calculated using the photon number cutoff are not even approximate eigenstates of the Liouville operator if their mean energy of the order of the cutoff energy. These states have the weight zero in the sum 8.8 because their mean photon number differs significantly from the stationary state and therefore their weight $\text{tr}\left(\hat{\rho}_i a(o)\rho_{\text{stat}}a^\dagger(0)\right)$ must be zero.

Since all eigenvalues corresponding to eigenstates other than the stationary state have a negative real part, for large times t all contributions but the one from the stationary state are zero. Because every eigenbasis of $\mathcal{L}$ corresponding to a nonzero eigenvalue is traceless and orthogonal to the dual eigenbasis $\check{\rho}_o$ corresponding to the eigenvalue 0 we conclude that $\check{\rho}_o = 1$. Therefore the correlation function factorises and

$$\lim_{t\to\infty} g^{(2)}(t) = 1. \tag{8.9}$$

This behavior can be used to test the accuracy of the numerical results. The numerical calculations presented here reproduced this behavior exactly.

The fact that system operator correlation functions may be calculated using the propagation of the system operators is known as the quantum regression theorem [14],[37]. We do not use the Quantum regression theorem, since we calculate th correlation functions directly using the eigenstates of $\mathcal{L}$.

The same spectral decomposition may be used to calculate any other correlation function. Since $g^{(1)}(t)$ has the form

$$g^{(1)}(t) = \sum_i \text{tr}\left(a^\dagger\hat{\rho}_i\right)\text{tr}\left(\check{\rho}_i a\rho_o\right)\mathrm{e}^{\lambda_i t} \tag{8.10}$$

the spectrum can be calculated immediately as a sum of lorentzians corresponding

to the different eigenvalues:

$$S(\omega) = \frac{1}{\pi}\Re\left(\int \mathrm{d}t g^{(1)}(t)\mathrm{e}^{i\omega t}\right)$$
$$= \sum_i \mathrm{tr}\left(a^\dagger\hat{\rho}_i\right)\mathrm{tr}\left(\check{\rho}_i a\rho_o\right)\frac{\Re(\lambda_i)}{2\sqrt{2\pi}}$$
$$\left(\frac{1}{\Re(\lambda_i)^2+(\omega+\Im(\lambda_i))}+\frac{1}{\Re(\lambda_i)^2+(\omega-\Im(\lambda_i))}\right). \quad (8.11)$$

The coherent driving field contributes a delta peak at $\omega = 0$ to the spectrum. In the spectra shown throughout this work this peak has been suppressed. The center of the spectra is at the common frequency of the resonator and the atoms.

Since the spectrum is the real part of the Fourier transform of the correlation function $g^{(1)}(t)$ it includes the same information as the correlation functions.

The mean photon number at constant intensity of the driving field depends on the number of atoms in the resonator. This can be understood by considering the energy balance of the system in the stationary state. The cavity gains energy through the driving field and loses energy through the mirrors and spontaneous emission of the atoms, which is unlikely to occur into the resonator mode. Since the atoms interact only with the resonator mode, and not with other atoms, their state is completely determined by the resonator mode. This means that the cavity losses increase with the number of atoms. In order to compensate for the losses the intensity of the driving field must be increased.

We note that another consequence of this argument is that for large numbers of atoms the energy is stored predominantly in the atoms. Therefore, large values of M (number of excited atoms) are possible even if the mean photon number is low. We have to make sure in our numerical calculations that the maximum value of M is large enough, which can be easily controlled by verifying that the stationary state has no occupation probability at the cutoff. Typical values are $M_{\max} = 7$ which is more three hundred times more than the stationary photon number, but only three to six times the mean atomic excitation.

Figure 8.3 shows the intensity correlation function $g^{(2)}(t)$ for $Z = 1, 2, 3, 4$ atoms, coupling constant $g = 1$, $A = 0.28$, $B = 1.6$ and $\epsilon = 0.2$. The values of A and B are taken from [32]. The amplitude of the oscillations in $g^{(2)}(t)$ increases with the number of atoms while the period of the oscillations decreases as a consequence of the scaling of g.

Calculations with different parameter sets have shown that photon antibunching does not happen if B is not significantly larger than A.

The published experimental data of Rempe et al. were obtained for a significantly larger number of atoms. Figure 8.4-8.7 show the intensity correlation function

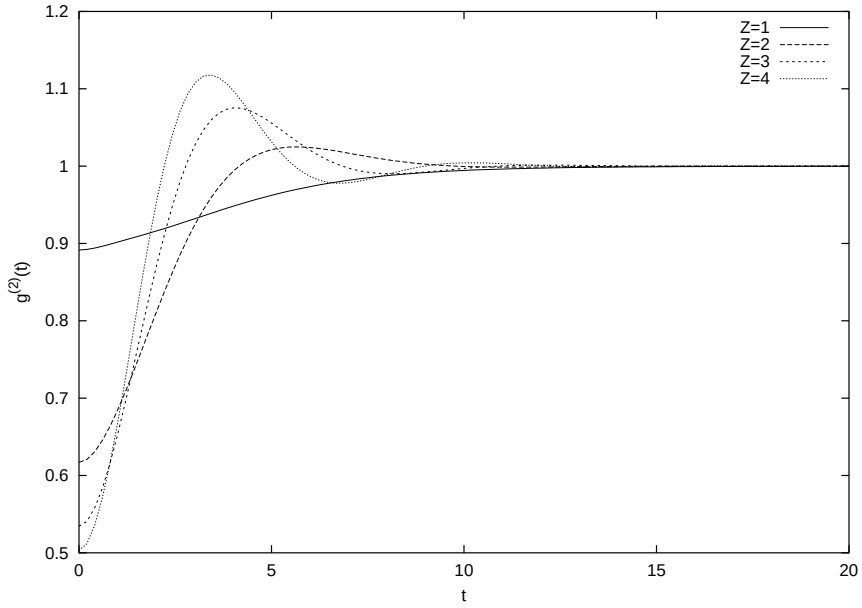

Figure 8.3: The intensity correlation function for $Z = 1, 2, 3, 4$ atoms, coupling constant $g = 1$, $A = 0.28$, $B = 1.6$ and driving field $\epsilon = 0.2$. The value of $g^2(0)$ depends on the number of atoms for low number of atoms, but not for larger numbers of atoms. The frequency of the oscillations increases with the square root of the atom number, as expected.

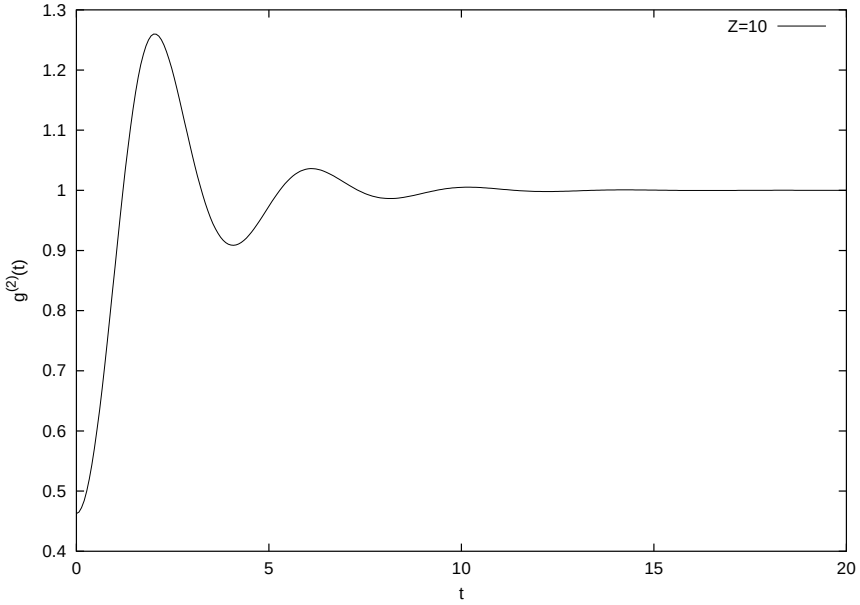

Figure 8.4: The intensity correlation function for $Z = 10$ atoms, coupling constant $g = 1$, $A = 0.28$, $B = 1.6$ and $\epsilon = 0.2$. The frequency of the oscillations increases with the number of atoms while the amplitude does not change considerably.

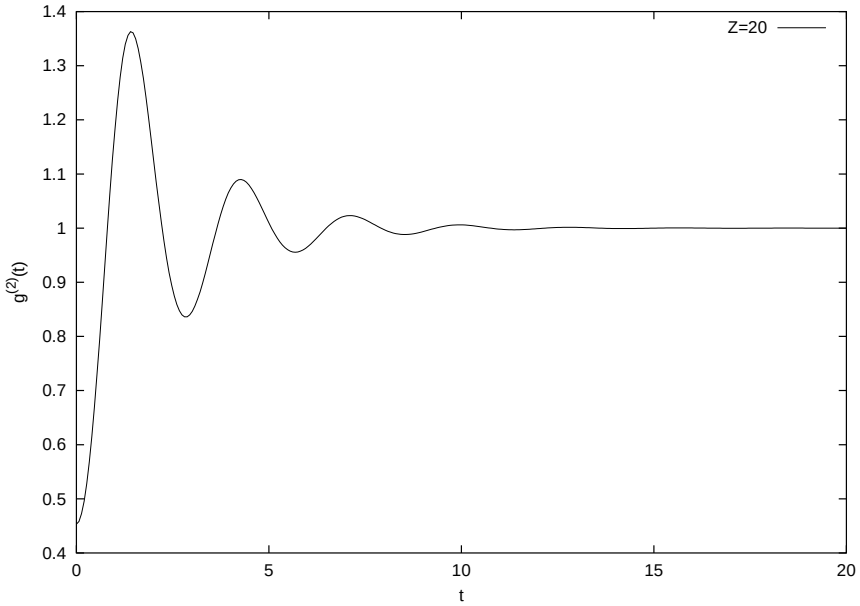

Figure 8.5: The intensity correlation function for $Z = 20$ atoms, coupling constant $g = 1$, $A = 0.28$, $B = 1.6$ and $\epsilon = 0.2$.

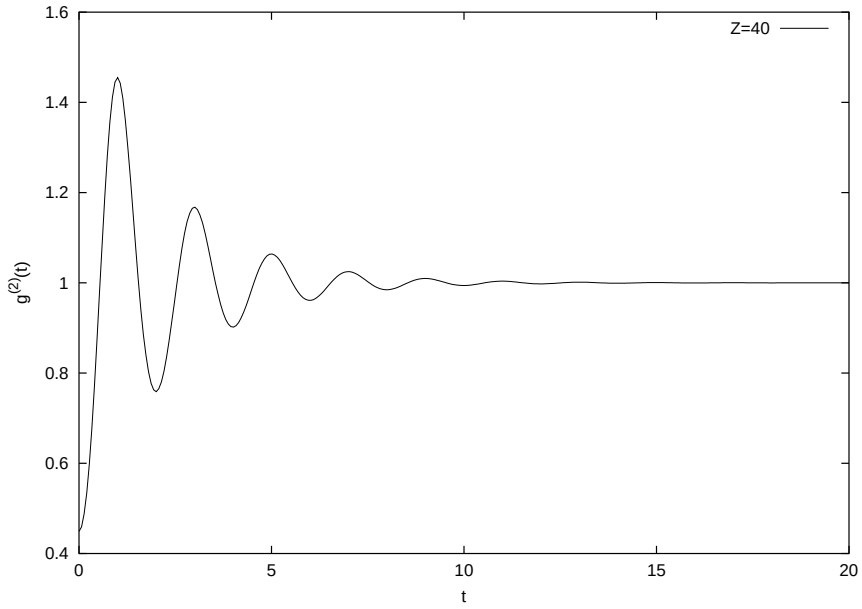

Figure 8.6: The intensity correlation function for $Z = 40$ atoms, coupling constant $g = 1$, $A = 0.28$, $B = 1.6$ and $\epsilon = 0.2$.

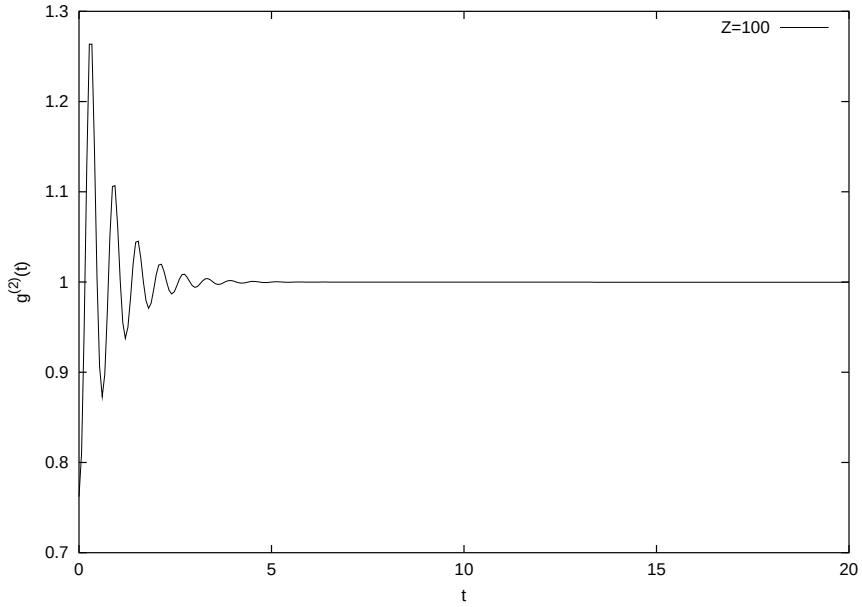

Figure 8.7: The intensity correlation function for $Z = 100$ atoms, coupling constant $g = 1$, $A = 0.28$, $B = 1.6$ and $\epsilon = 0.2$.

$g^{(2)}(t)$ for $Z = 10, 20, 40 and 100$. These values are taken from the experimental data of figure 8.2. The oscillation frequency increases as $\sqrt{Z}$, as expected. In contrast, the value of $g^{(2)}(0)$ depends on the number of atoms only very weakly. This is because in the limit of a very weak driving field the value of $g^{(2)}(0)$ depends only on the saturation photon number [7] which is kept constant in these plots. The envelope of the oscillations does not depend on the number of atoms. The reason for this behavior is that the real parts of the matrix elements (5.34) of the Lindblad operator, which determine the rate of decay of the correlation functions, do not depend on the number of atoms but instead on the number of excited atoms[1].

The experimental results 8.2 of Rempe et al. are not consistent with the weak-field limit $\epsilon \ll A$, because the experimentally measured value of $1 - g^{(2)}(0)$ is four times smaller than calculated under the assumption of a weak driving field.

Rempe et al. have determined the numbers of atoms and the decay rate of $g^{(2)}(t)$ by fits of correlation functions calculated in the weak field limit to the experimental data. Since our results show that the period of the oscillations still depends on $g\sqrt{Z}$ even if ϵ is of the order of A or larger we will still use their values of Z in comparing their experimental data with our results.

In the experiment of Rempe et al. the atoms did not stay permanently in the cavity but crossed the cavity in an atomic beam. Since the inverse of the transit time is much smaller than any of the rates g, A and B effects of the finite transit time are neglected here. Since the experiments were performed at optical frequencies, thermal photons may be neglected.

Figure 8.8 shows that $g^{(2)}(0)$ does depend on the strength of the driving field if the intensity ϵ of the driving field is above a threshold. In our calculations, a value of $\epsilon \approx 2.5$, which still leads to very low mean photon numbers gives the experimentally found correlation function. In the regime $\epsilon < 2$ the driving field does not have any effect on the correlation functions. This is the regime where the weak-field approximation of [7] is appropriate. In the regime $2 < \epsilon < 2.8$ the intensity correlation function is still antibunched, but now depends on the intensity of the driving field. For even larger values of ϵ one observes photon bunching $g^{(2)}(0) > 1$.

Using the results from above, we may show now that the experimental values of Rempe et al. are indeed consistent with the Jaynes-Cummings model if a finite driving field is assumed.

Our calculations gave the same dependency of the oscillation frequency on the number of atoms as the weak-field approximation. Therefore we will use the number of atoms determined from the experimental data using the weak-field

[1]Remember that $m = -\frac{Z}{2}$ if all atoms are in the ground state.

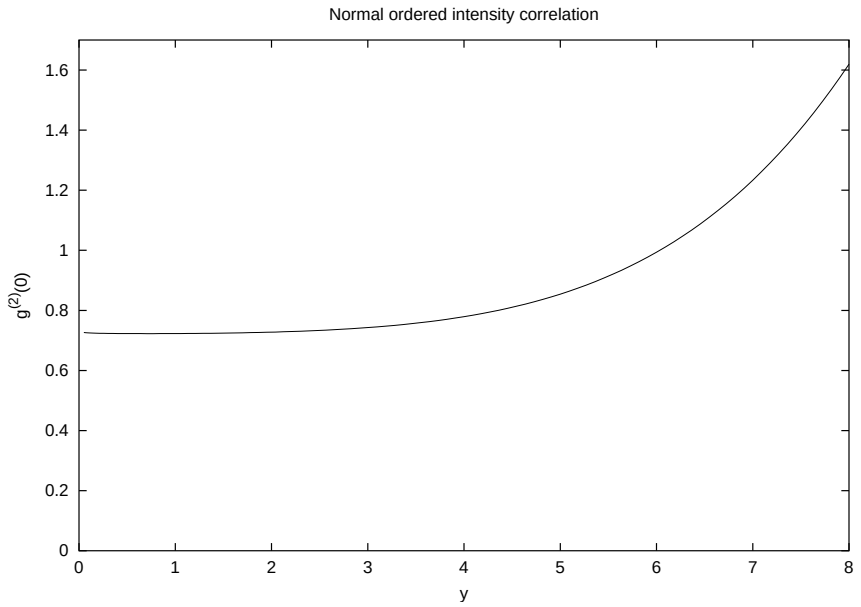

Figure 8.8: The normally ordered intensity correlation $g^{(2)}(0)$ at $Z = 110$, $C = 1.0$ and $n_s = 0.7$. For low values of y the intensity correlation does not depend on y. This is the regime where the weak-field approximation may be used to calculate the intensity correlation function $g^{(2)}$. For larger values of y regime begins where the intensity correlation $g^{(2)}(0)$ increases and finally becomes classical with $g^{(2)}(0) > 1$.

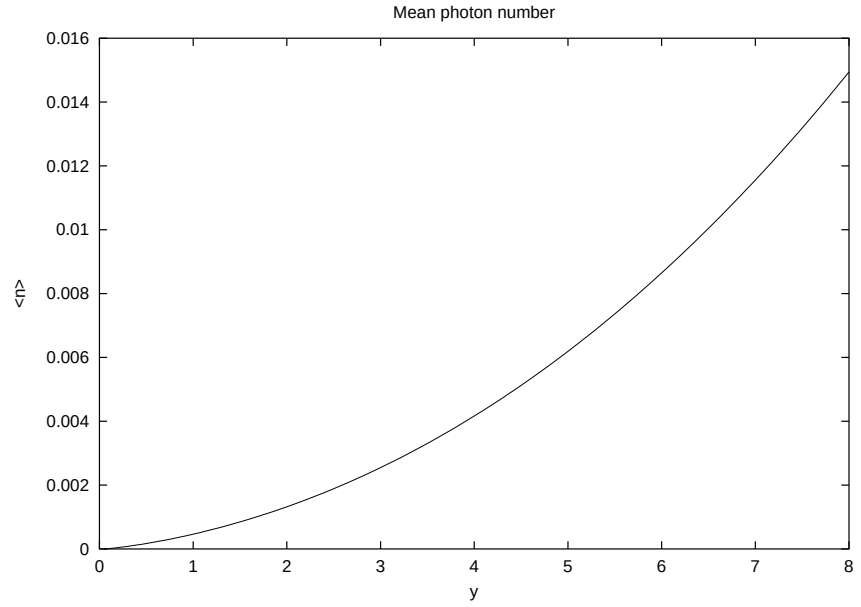

Figure 8.9: The mean photon number at $Z = 110$, $C = 1.0$ and $n_s = 0.7$. The mean photon number depends quadratically on y. The driving field cannot be neglected when calculating the mean photon number.

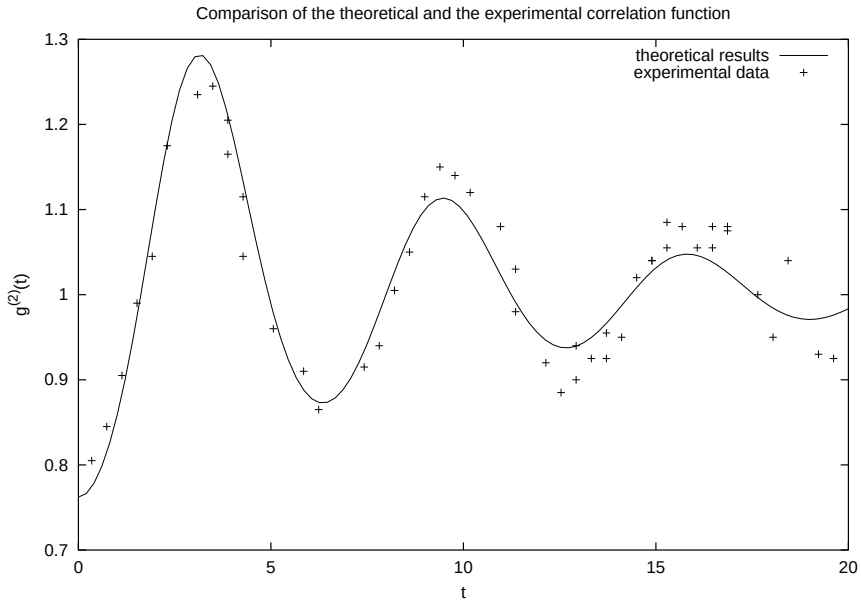

Figure 8.10: The experimental values of the correlation function in comparison with the theoretical results. The data points are taken from figure 8.2. The straight line has been calculated using (8.8). The atom numbers is $Z = 110$ The parameters $C = 1, n_s = 0.6, y = 10$ have been chosen similarly to the values reported in the experimental publication. The theory describes the experiment quite well with the exception that the damping of the theoretical curve is stronger than that of the experimental curve. The time has been scaled by the oscillation period.

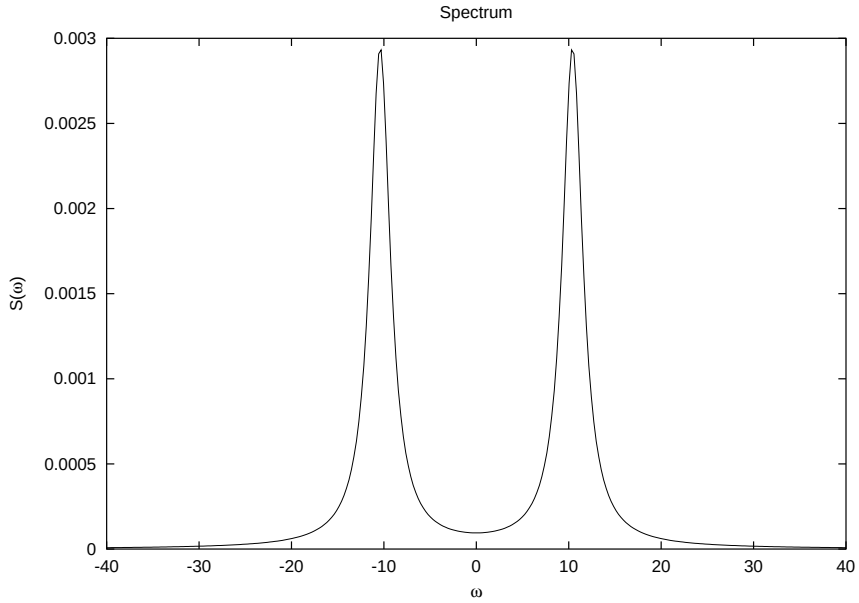

Figure 8.11: The spectrum corresponding to the correlation function of Figure 8.10. The two-peaked form of the spectrum indicates that the 110 atoms here actually behave like one scaled atom.

approximation. At $n_s = 0.6$ and $C = 1.0$ we find a good accordance between experimental and theoretical data, as Figure 8.10 shows. The decay rate of the envelope of the theoretical correlation function is somewhat larger than that of the experimental correlation function. This could not be fixed since this decay rate and $g^{(2)}(0)$ depend mostly on the saturation photon number so that they cannot be changed independently. This observation is consistent with the the weak driving field approximation where in the limit $Z \gg 1$ the same behavior is predicted.

In figure 8.11 the spectrum corresponding to the theoretical correlation function is displayed. The spectrum shows the Rabi splitting expected for a single atom with coupling constant $g\sqrt{Z}$.

The following section will investigate the connection between the spectrum, the number of atoms and the validity of the scaling of the coupling constant in detail.

8.3 Scaling Behavior

Many modern experiments use high-finesse cavities. This means that the damping constant A of the resonator mode can be small in comparison to the atomic damping constant B. This situation allows for adiabatic elimination of the atoms.

The adiabatic elimination of the atoms has been performed in a semiclassical theory where the resonator mode is treated classically [19] as well as in a full quantum theory [13]. In the second case one obtains a simple scaling law that reduces a Z-atom-model to a 1-atom model with a scaled coupling constant. In this section we will compare this scaling law with exact results.

Using adiabatic elimination one obtains the equation of motion

$$\frac{\mathrm{d}}{\mathrm{d}t}\rho(t) = \mathcal{L}_m\rho(t) + Z\mathcal{L}_i\rho(t) \tag{8.12}$$

for the density operator $\rho(t)$ of the resonator mode. Here $\mathcal{L}_i\rho(t)$ contains all terms that result from the interaction between the atoms and the resonator mode. These terms are of the form

$$g^2\left(aa^\dagger\hat{\rho} + a\emptyset a^\dagger P - 2a^\dagger\hat{\rho}a\right) + g^4\left(a^2{a^\dagger}^2\hat{\rho} + a^2{a^\dagger}^2\hat{\rho} - 2{a^\dagger}^2\hat{\rho}a^2\right) + \cdots \tag{8.13}$$

The first term $\mathcal{L}_m\rho(t)$ of (8.12) contains the dissipation of the light mode and the interaction of the light mode with the driving field. The derivation of 8.12 is based on two assumptions: First, at most one of the many atoms is excited, and second, adiabatic elimination of the atoms is possible, i.e. the decay rate of the atoms is fast enough so that the state of the atoms is always determined by the state of the resonator mode.

If we insert in equation 8.12 for the time, the intensity of the driving field, the interaction constant and the mode operators scaled quantities defined by

$$\begin{aligned} t' &= Zt \\ g' &= \sqrt{Z}t \\ \epsilon' &= \frac{1}{\sqrt{Z}}\epsilon \\ a &= \frac{1}{\sqrt{Z}}a \\ a^\dagger &= \frac{1}{\sqrt{Z}}a^\dagger \end{aligned} \tag{8.14}$$

we obtain a new equation of motion

$$\frac{\mathrm{d}}{\mathrm{d}t'}\rho(t') = \mathcal{L}'_m\rho(t) + \mathcal{L}'_i\rho(t) \tag{8.15}$$

which does not contain the number of atoms at all. We can now test the validity of this approach by comparing the exact calculations with expectations from the scaling theory.

Figure 8.12 shows the mean photon number for $Z = 1, 2, 3, 4, 5, 10, 18, 55$ and 110 atoms and a straight line through the origin. The intensity of driving field which is chosen such that at $Z = 110$ approximately 2 atoms are excited.

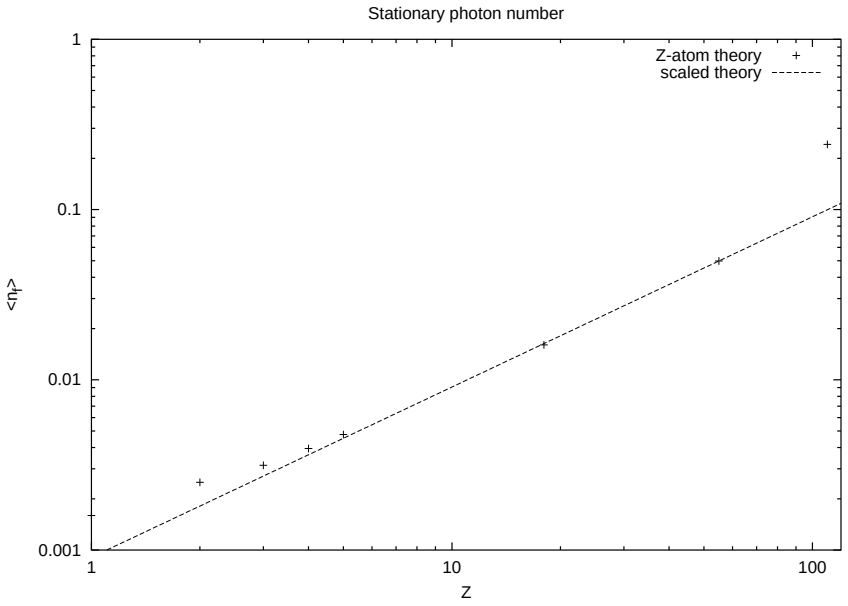

Figure 8.12: Double logarithmic plot of the mean photon number $< n_f >$ for Z=1,2,3,4,5,10,18,55 and 110 atoms. The driving field parameter ϵ and the coupling constant g are scaled according to (8.15). The adiabatic elimination predicts that the mean photon number is proportional to the number of atoms. The plot shows that this is the case if $1 \ll Z \lesssim 100$.If the scaling was exact all points would lie on a straight line. At large atom numbers the scaling theory breaks down because in its derivation it was assumed that at most one atom is excited. This is not the case for large atom numbers.

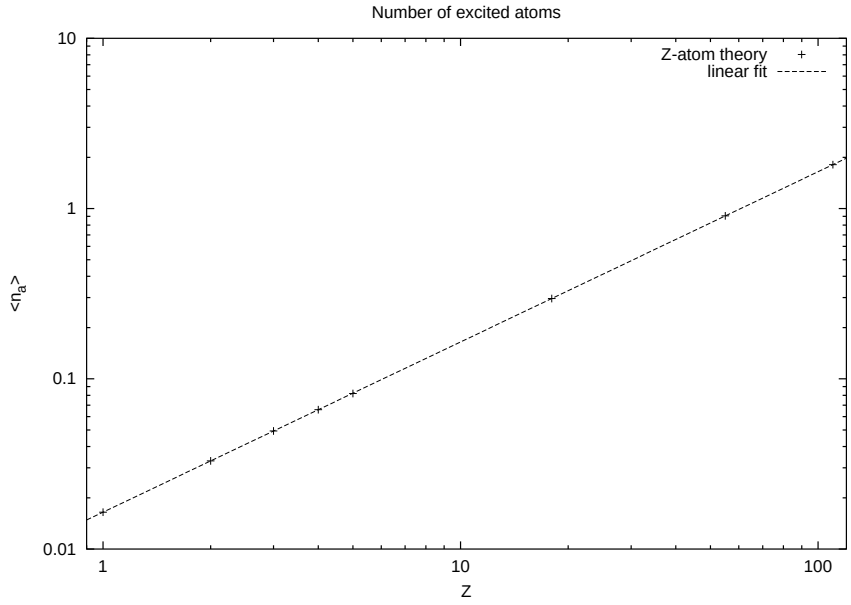

Figure 8.13: Double logarithmic plot of the number $< n_a >$ of excited atoms for Z=1,2,3,4,5,10,18,55 and 110 atoms. The mean number of excited atoms is proportional the number of atoms. This behavior is expected from energy conservation arguments as explained in the text.

The adiabatic approximation 8.12 predicts that the mean photon number is proportional to the number of atoms. For $1 \ll Z \lesssim 100$ atoms this is the case, while for $Z \lesssim 5$ and $Z \gtrsim 5$ the mean photon number is larger than consistent with the scaling behavior. The adiabatic elimination of the atoms is only possible if at most one atom is excited. Since the number of excited atoms increases with the total number of atoms this condition is only met if the number of atoms is smaller than an upper limit that depends on the intensity of the driving field. The number of excited atoms is shown in figure 8.13 for $Z = 1, 2, 3, 4, 5, 10, 18, 55$ and 110. The mean atomic excitation does not depend on the number of atoms. This behavior can be understood if looking at the energy balance of the combined system of resonator mode and atoms: The energy pumped into the system is proportional to the number of atoms, since the intensity $|\epsilon|^2$ of the driving field is proportional to the number of atoms and the resonator losses are predominantly caused by spontaneous emission of the atoms since the total energy is predominantly stored in the atoms. Therefore, the energy losses per atom and hence the mean state of the atoms cannot depend on the number of atoms.

Please note that one cannot determine the mean photon number at large numbers of atoms from the mean photon number at $Z = 1$, as equation (8.12) suggests. Instead it is possible to obtain an approximation for the the mean photon number from the value at another, sufficiently large atom number.

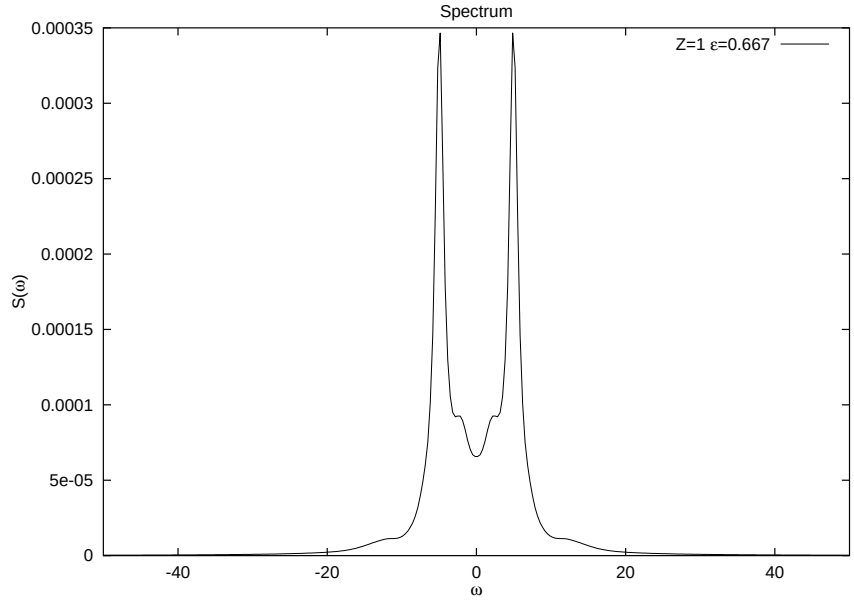

Figure 8.14: Spectrum for 1 atom, $A = 0.422577, B = 2.36643, \epsilon = 0.667$ and $g = 10.48$. The Rabi splitting is clearly visible, but there is also a shoulder and little extra peaks between the two main peaks.

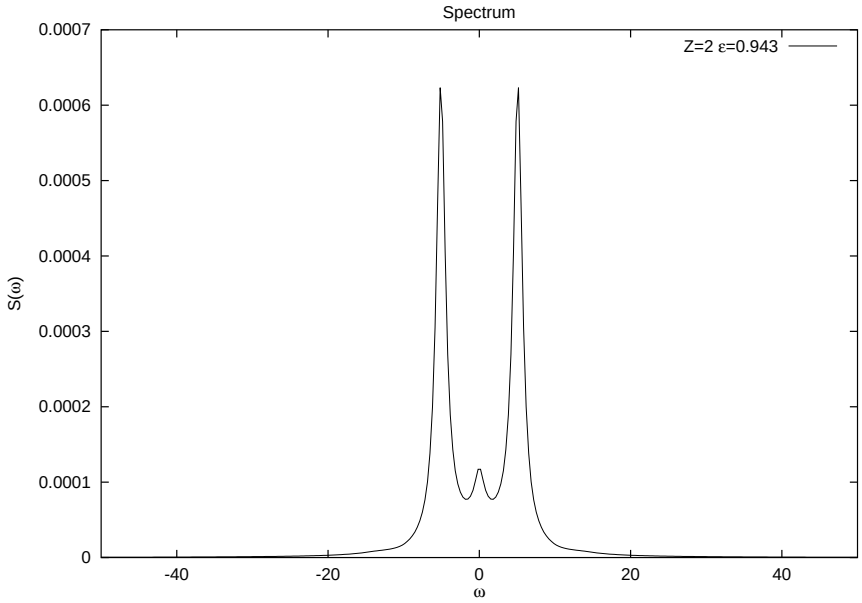

Figure 8.15: Spectrum for 2 atoms, $A = 0.422577, B = 2.36643, \epsilon = 0.943$ and $g = 7.41$. The Rabi splitting is clearly visible. The separation of the peaks is the same as in figure 8.14 because the coupling constant g has been scaled by the square root of the atom number.

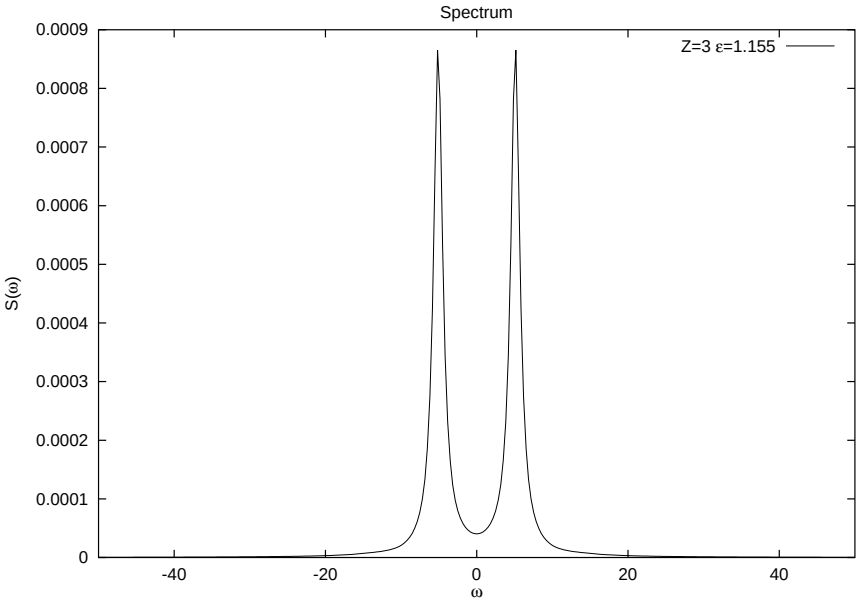

Figure 8.16: Spectrum for 3 atoms, $A = 0.422577, B = 2.36643, \epsilon = 1.155$ and $g = 6.05$.

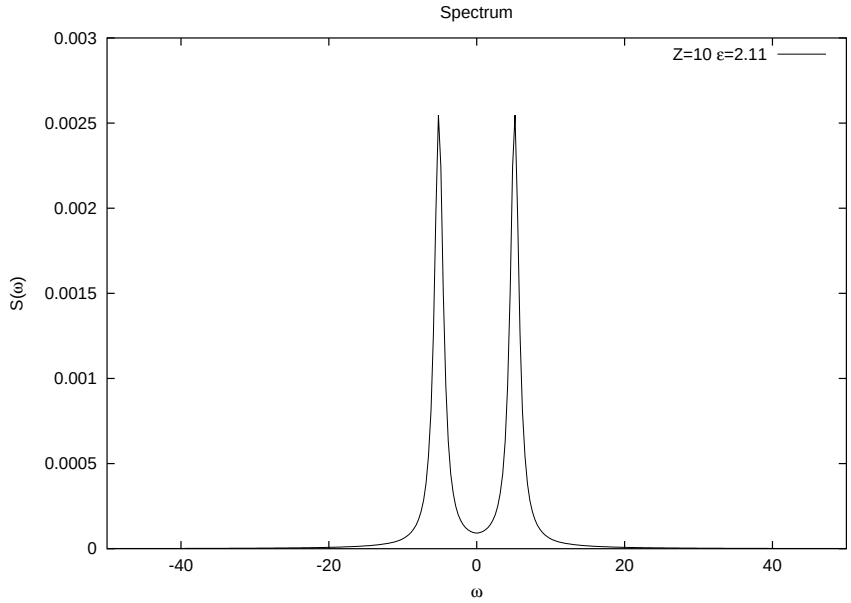

Figure 8.17: Spectrum for 4 atoms, $A = 0.422577, B = 2.36643, \epsilon = 2.11$ and $g = 3.314$.

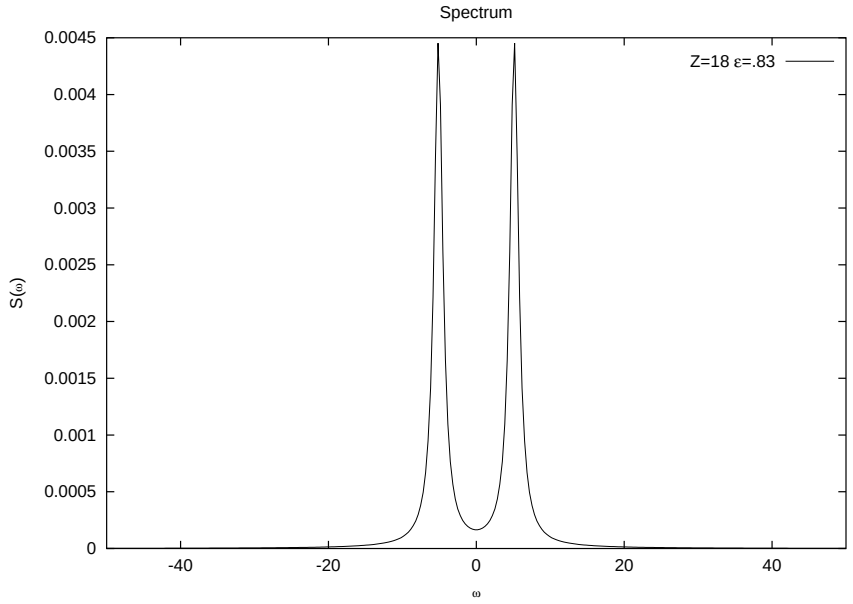

Figure 8.18: Spectrum for 18 atoms, $A = 0.422577, B = 2.36643, \epsilon = 2.83$ and $g = 2.47$.

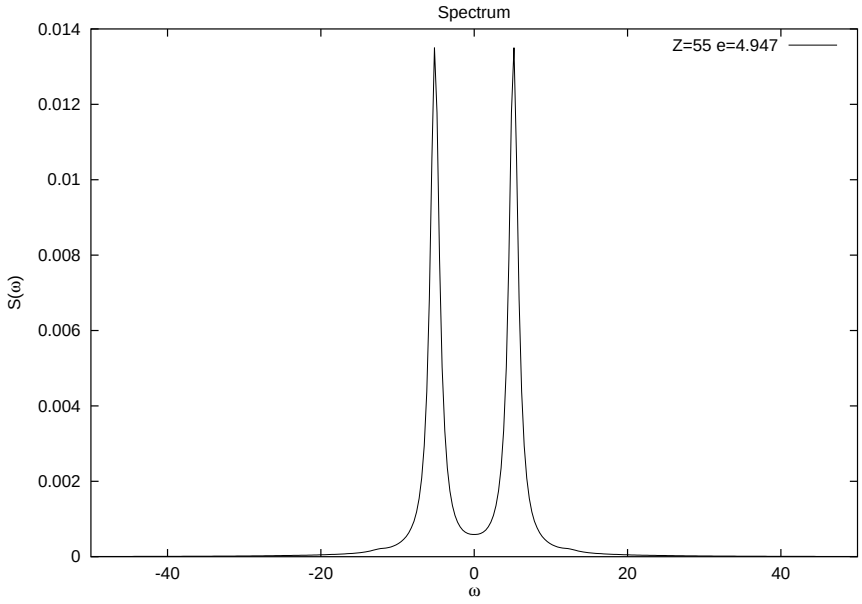

Figure 8.19: Spectrum for 55 atoms, $A = 0.422577, B = 2.36643, \epsilon = 4.947$ and $g = 1.413$.

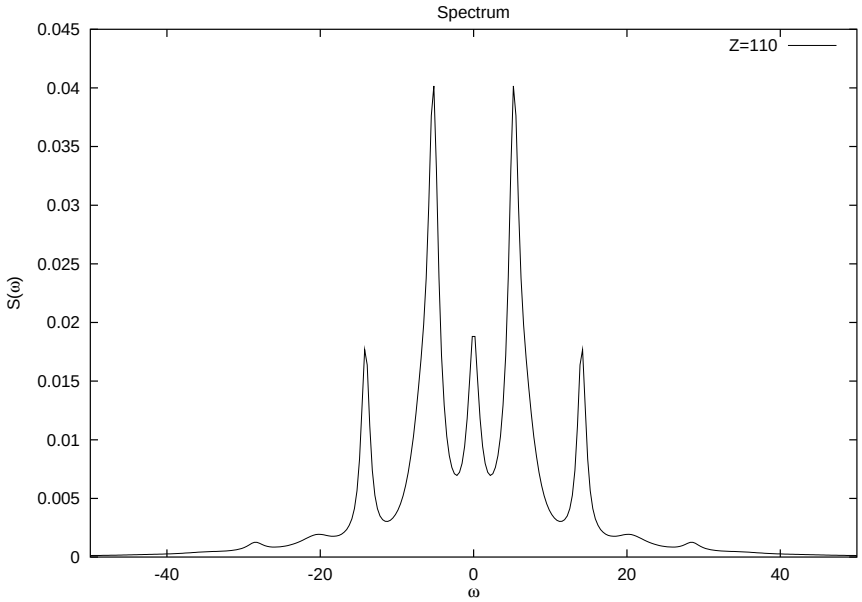

Figure 8.20: Spectrum for 110 atoms, $A = 0.422577, B = 2.36643, \epsilon = 7.0$ and $g = 1.0$. The dominant feature of the spectrum is the Rabi splitting, but there are sidebands indicating that now more than one atom is excited.

The mean photon number and the number of excited atoms is a property of the stationary state only. In contrast, the correlation functions and the spectrum, i.e the Fourier transform of $g^{(1)}$, depend on all eigenvalues and eigenstates and therefore contain dynamical information on the system. The scaling law (8.12) implies that the spectrum does not depend on the number of atoms.

Figure 8.14-8.19 show the spectra corresponding to 8.12 respectively 8.13. At $Z = 1$ and $Z = 2$ the spectra contain significant contributions at $\omega = 0$. The spectra corresponding to higher numbers of atoms have the typical two-peaked form of the Rabi splitting. At $Z = 110$ where the mean number of excites atoms approaches two, sidebands show up. The validity of the scaling law coincides with the two-peaked form of the spectrum.

In order to verify that the upper bound of the validity of the adiabatic approximation results from the large value of ϵ required at large numbers of atoms the mean photon number and mean number of excited atoms has been calculated for larger values the amplitude of the driving field. Again the values of ϵ and g were chosen in accordance with the scaling prescriptions (8.15). The results are shown in the figure 8.22. The deviation at low numbers of atoms now is much larger than with the weaker driving field and the upper bound of the validity of the adiabatic approximation is reached at $Z \approx 20$. At this number of atoms the mean number of excited atom now approaches two, as can be seen from figure

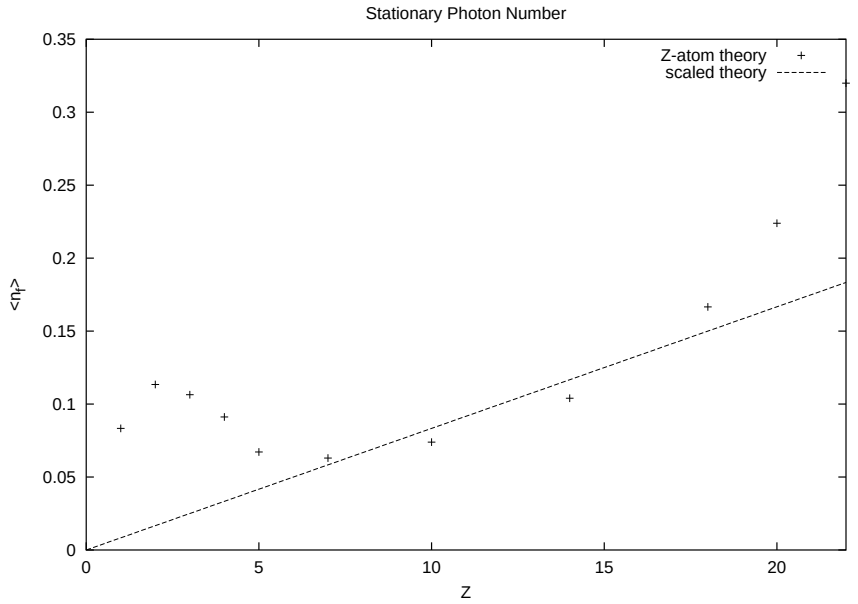

Figure 8.21: Mean photon number $< n_f >$ for $Z = 1, 2, 3, 4, 5, 7, 10, 14, 18$ atoms and a stronger driving field than in figure 8.12. The driving field parameter ϵ and the coupling constant g are scaled according to (8.15). The deviations from the scaling behavior are larger than in figure 8.12.

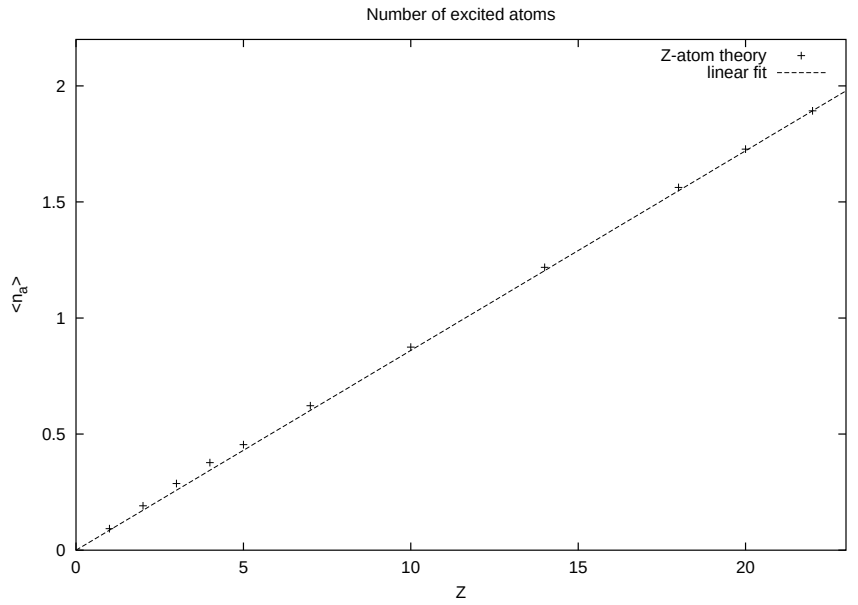

Figure 8.22: Mean number $< n_a >$ of excited atoms for $Z = 1, 2, 3, 4, 5, 7, 10, 14, 18$. The mean number of excited atoms is proportional the number of atoms. This behavior is expected from energy conservation arguments as explained in the text.

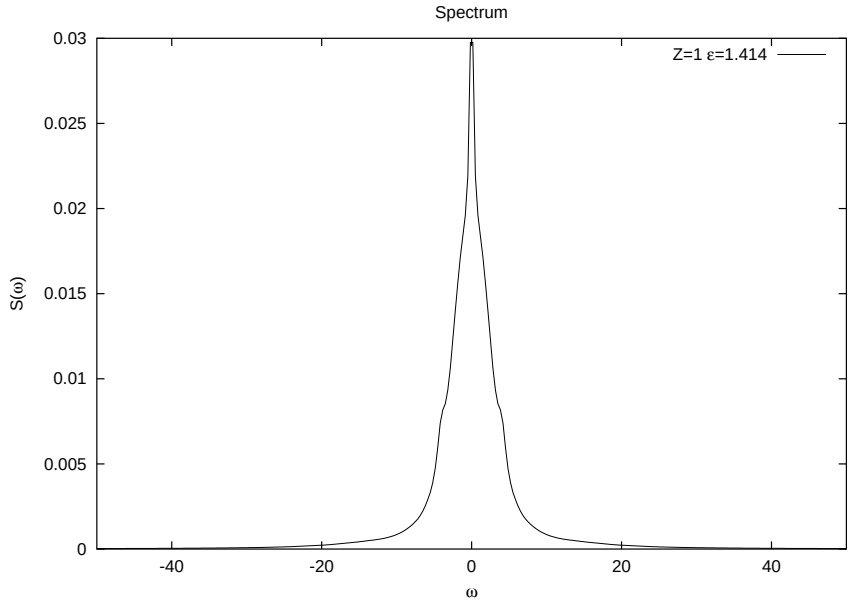

Figure 8.23: Spectrum for 1 atom, $A = 0.422577, B = 2.36643, \epsilon = 1.414$ and $g = 10.48$.

8.22 which displays the number of excited atoms atoms as a function of the number of atoms in the cavity. We conclude that the adiabatic approximation indeed requires that the number of excited atoms is less than two.

For $Z = 4$ atoms the Rabi splitting is clearly visible (8.18), but the central peak is still dominant. The Rabi peaks in the spectrum become dominant at $Z = 7$. This is the number of atoms where the scaling regime begins, as figure 8.21 shows. As in the case of the lower driving field above the scaling behavior coincides with the two-peaked form of the spectrum. Here the driving field is sufficiently large to hide the Rabi splitting completely for $Z = 1$ (figure 8.23) and $Z = 2$ (figure 8.24).

The scaling regime ends at $Z = 18$ where the sidepeaks begin to show up in the spectrum 8.28.

The results presented here do support the validity of the adiabatic approximation if at most one atom is excited and the Rabi splitting is visible. The visibility of the Rabi splitting sets a lower limit to the number of atoms for which the scaling behavior can be observed.

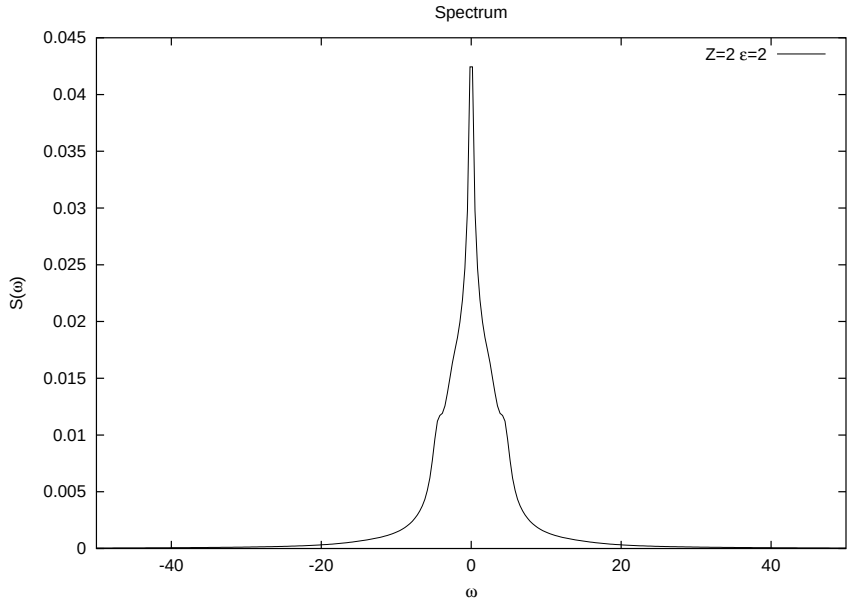

Figure 8.24: Spectrum for 2 atoms, $A = 0.422577, B = 2.36643, \epsilon = 2.0$ and $g = 7.41$.

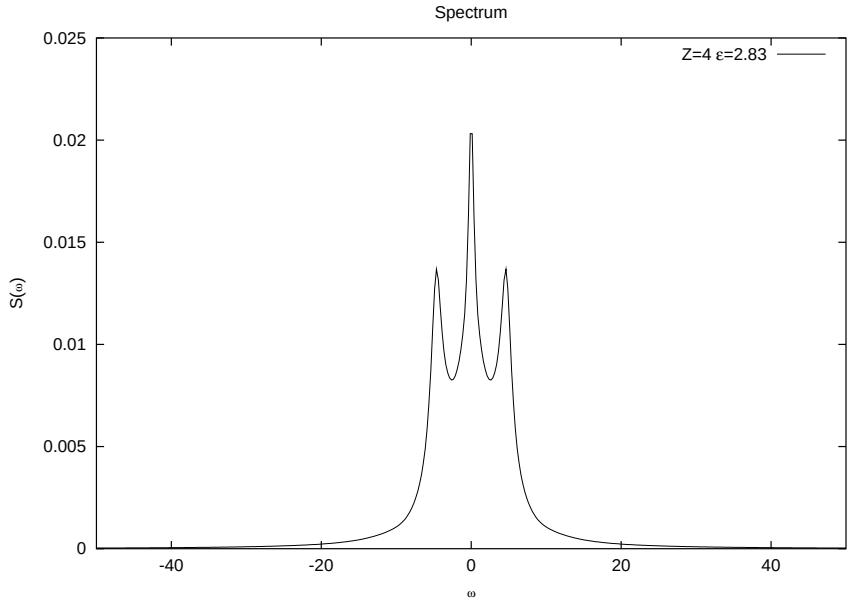

Figure 8.25: Spectrum for 4 atoms, $A = 0.422577, B = 2.36643, \epsilon = 2.0$ and $g = 5.24$.

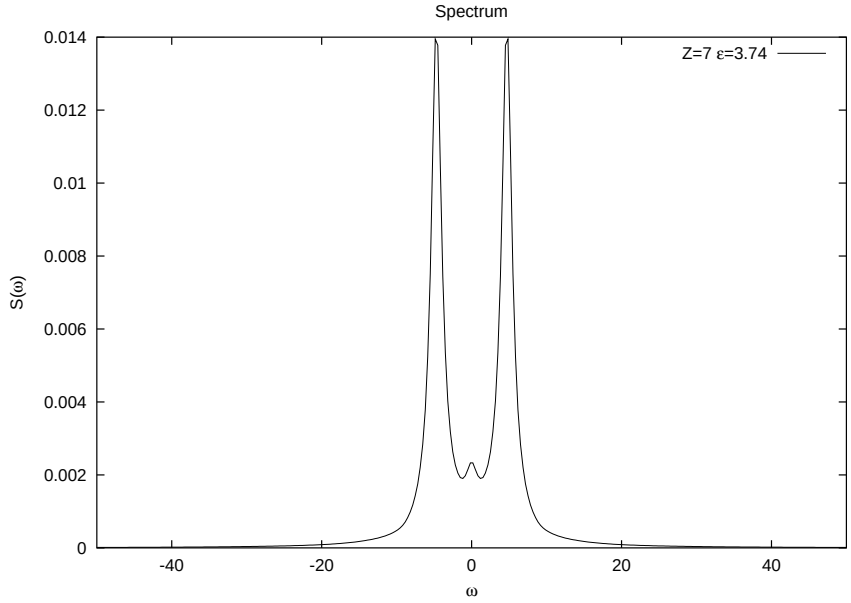

Figure 8.26: Spectrum for 7 atoms, $A = 0.422577, B = 2.36643, \epsilon = 3.74$ and $g = 3.96$.

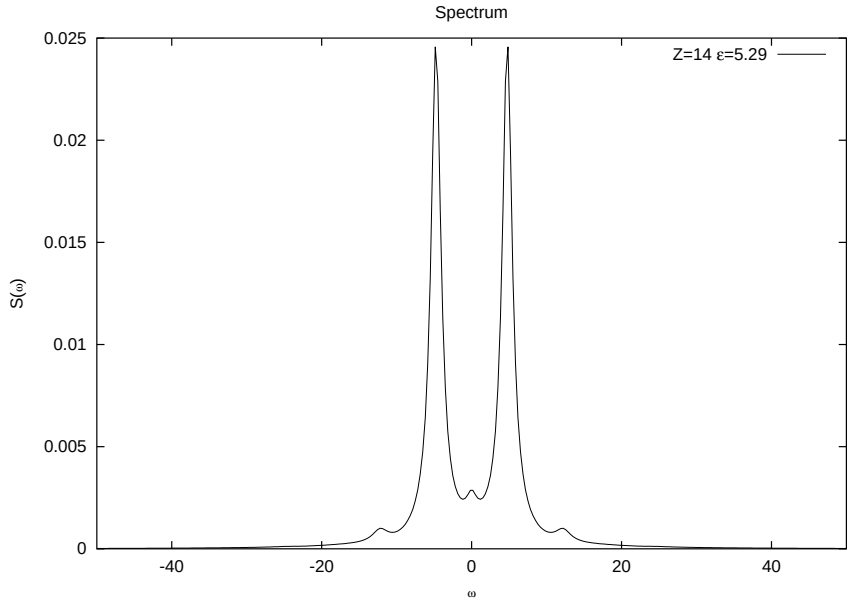

Figure 8.27: Spectrum for 14 atoms, $A = 0.422577, B = 2.36643, \epsilon = 5.29$ and $g = 2.8$. This spectrum is almost two-peaked and correspondingly at $Z = 14$ the mean photon number scales with the number of atoms.

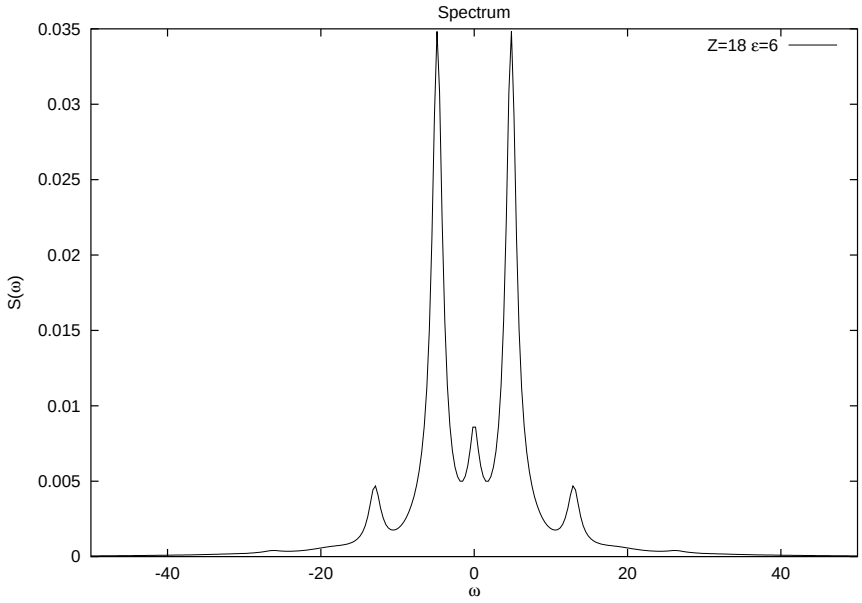

Figure 8.28: Spectrum for 18 atoms, $A = 0.422577, B = 2.36643, \epsilon = 6.0$ and $g = 2.47$.

Chapter 9

Summary

We have studied the interaction of an arbitrary number Z of atoms with a quantized damped resonator mode. In order to reduce the dimension of the system we employed a symmetrized density operator description. These density operators are analogous to angular momentum eigenstates which are usually referred to as Dicke states.

In this symmetric basis the dimension of the atomic system is only $\frac{1}{6}(Z+1)(Z+2)(Z+3)$ in contrast to 4^Z without symmetrization. We have shown that the symmetry is not broken by spontaneous emission. A simple analytical expression for the matrix elements of the complete Liouville operator with respect to the Dicke states was found.

Using these results we are able to study the interaction of the atoms with a resonator mode without any further approximations. In particular, we do not eliminate the atoms.

Two different experimentally motivated systems were examined:

A micromaser which is pumped by clusters of atoms and not by single atoms. If the cluster enter the maser completely excited the pump rate is proportional to the number of atoms and the mean number of photons in the resonator increases accordingly with Z. In this case the zero-photon-trapped states vanish when the number of atoms is increased. If the clusters enter the resonator only partially excited such that any cluster deposits at most one photon in the resonator, the trapped states do not vanish and even one-photon-trapped states appear. The dependence of the mean photon number converges with increasing atom number to a very regular curve in this case.

In the other system the maser pump process was replace by a coherent driving field. For the first time the experimental intensity correlation functions for more than hundred atoms were reproduced. The dependence of the correlation

functions on the number of atoms was studied. The weak-field regime where the correlation function does not depend on the intensity of the driving field was established. The exact results have been compared to an approximation where the atoms are eliminated adiabatically and the number of atoms enters only as a scaling factor. This approximation is neither valid for very low atom numbers nor for very large atom numbers. The range of permissible atom numbers decreases with increasing driving field. The spectra corresponding to different numbers of atoms and driving fields were calculated. It was shown that the adiabatic elimination is only valid if the spectrum has the form of single-atom Rabi splitting.

The Dicke state formalism developed in this work is very general and can be applied to all systems where several atoms interact with one resonator under the only condition that the Liouville operator is symmetric with respect to any permutation of the atoms.

Chapter 10

Outlook

The methods developed in this work allow to find stationary as well as dynamical properties of a system consisting of an arbitrary number of atoms interacting with a resonator mode where each atom is coupled to an individual bath and the resonator dissipates energy through imperfect mirrors. The new method has been applied to a coherently driven system and a maser that is driven by atom clusters instead of single atoms. At least three more applications are possible:

- Lasers: The simplest description of a laser uses an inverted heat bath described by the parameter s in equation (5.34). Therefore, this equation could serve as a starting point into a microlaser theory describing lasers whose active medium consists of several atoms. But please note that the implementation model with a large photon number and a large atom number leads to a very large state space. The numerical solution of this problem requires computers which large amounts of memory. One feature of the atomic pump mechanism is advantageous when compared to the driving field used in this work: The off-diagonal matrix elements remain zero for all times. Since the failure of the adiabatic approximation at large numbers of atoms can be attributed to the strong classical driving field that this approximation requires at large numbers of atoms it is quite possible that a laser theory with adiabatically eliminated atoms will not show this behavior. Hence we expect that the scaling works better in conjunction with this pump process.

- Finite Temperatures: Finite temperatures are already contained in the model, but at finite temperatures it is no longer possible to obtain the eigenvalues from the matrix $\mathcal{M}$ only but from the complete Liouville operator.

- Generalization of the two-state atom model: The Dicke states served as a motivation to introduce the symmetrized description of the atomic degrees

of freedom and were used in many steps of the derivation of equation (5.34). Nevertheless, the most important assumption was the exchange symmetry of the atoms. This symmetry could be reformulated in the case of realistic multilevel atoms.

- Criteria for nonrelevant dimensions: The numerical calculations show that not all basis states $\hat{\xi}_{Z,l,m,m'}$ have a relevant contribution to the correlation function $g^{(2)}(t)$. Therefore, one probably may find a way to suppress these irrelevant states, thus reducing the numerical complexity of the calculations, if one is only interested in the two-point features only.

- Atomic correlation functions: Since the far field emitted from an atom is proportional to its dipole moment there is a connection between atomic and mode correlation functions which can be used to express one of theses by the other one. Nevertheless, it is possible to take one atom out of the symmetrization collective and couple it individually to its own bath and the field mode. This leads to a state space of four times the size of the symmetric state space and makes it possible to calculate atom-atom correlation functions.

- Mode structure: One of the basic assumptions was that the frequencies g, A and B are the same for all atoms. In the case of a ring resonator, this assumption is justified, but in order to describe atoms interacting with a standing wave one has to take into account the mode structure of the wave. If it is possible to group the atoms into cluster experiencing approximately the same interaction strength the methods developed in this work still apply to those clusters.

- Decoupling of decoherence and interaction time scale: Since spontaneous emission and coherent interaction of atoms with resonator modes are fundamentally the same process these two processes happen on the same time scale. One possibility to separate these time scales is to use high-Q cavities that enhance a selected mode. Since the correlation functions show that the frequency of the collective dynamics may scale like the square root of the number of atoms while the decay rate remains independent of the number of atoms, clusters of atoms should be considered as a possibility to separate interaction and decoherence time scales.

Bibliography

[1] K. An, J. J. Childs, R. R. Dasari, and M. S. Feld. Microlaser: A laser with one atom in an optical resonator. *Physical Review Letters*, 73(25):3375, 1994.

[2] A. Barenco, A. Berthiaume, D. Deutsch, and A. Ekert. Stabilisation of quantum computations by symmetrisation. *quant-ph/9604028*, 1996.

[3] R. J. Brecha, P.R. Rice, and M. Xiao. N two-level atoms in a driven optical cavity: Quantum dynamics of forward photon scattering for weak incident fields. *Physical Review A*, 59(2):2392, 1999.

[4] H.J. Briegel and B.G. Englert. Quantum optical master equations: The use of damping bases. *Physical Review A*, 47(3):3311, 1993.

[5] D. M. Brink and G. R. Satchler. *Angular Momentum.* Oxford University Press, 1994.

[6] M. Brune, J.M. Raimond, P. Goy, L. Davidovich, and S. Haroche. Realization of a two-photon maser oscillator. *Phys. Rev. Lett.*, 59:1899, 1987.

[7] H.J. Carmichael, R.J. Brecha, and P.R. Rice. Quantum interference and collapse of the wave function in cavity QED. *Optics Communications*, 82(1,2):73, 1991.

[8] F. Casagrande, A. Lulli, and S. Ulzega. Collective effects and trapping states by a quantum-trajectory treatment of micromaser dynammics. *Physical Review A*, 60:1582, 1999.

[9] C. Cohen-Tannoudji, J. Dupont-Roc, and G. Grynberg. *Photons and atoms.* Wiley interscience, 1989.

[10] D. Meschede and H. Walther and G. Müller. One-atom maser. *Phys. Rev. Lett.*, 54:551, 1985.

[11] R. Dicke. Coherence in spontaneous radiation processes. *Physical Review*, 93:99, 1954.

[12] E.B. Davies. Exact dynamics of an infinite-atom Dicke maser model. *Comm. Math. Phys*, 33, 1973.

[13] M. Fleischhauer. Relation between N-atom laser and the one-atom laser. *Physical Review A*, 50, 1994.

[14] C.W. Gardiner. *Quantum Noise*. Springer, 1991.

[15] K. M. Gheri, P. Horak, and H. Ritsch. Two-atom microlaser. *Journal of Modern Optics*, 44(3):605, 1997.

[16] C. Ginzel, H-J. Briegel, U. Martini, B-G. Englert, and A. Schenzle. Quantum optical master equations: The one-atom laser. *Phys Rev A*, 48:732–738, 1993.

[17] R. J. Glauber. Coherent and incoherent states of the radiation field. *Phys. Rev*, 131, 1963.

[18] R. J. Glauber. The quantum theory of optical coherence. *Phys. Rev*, 130, 1963.

[19] H. Haken. *Laser Theory*. Springer, 1970.

[20] E.T. Jaynes and F.W. Cummings. Comparison of quantum and semiclassical radiation theory with application to the beam maser. *Proc IEEE*, page 51, 1963.

[21] J.T.Höffges, H.W. Baldauf, T. Eichler, S.R. Helmfried, and H. Walther. Heterodyne measurement of the fluorescent radiation of a single atom. *Optics Communications*, 133:170, 1997.

[22] M.I. Kolobov and F. Haake. Collective effects in the mircolaser. *Physical Review A*, 55:3033, 1997.

[23] M. Kozierowski, S.M. Chumakov, J. Swiatlowski, and A.A. Mamedov. Collective collapses and revivals in spontaneous emission of a partially inverted system of 2-level atoms - analytical solution. *Physical Review*, 46(11):7220, 1992.

[24] G. Lindblad. On the generators of quantum dynamical semigroups. *Commun. Math. Phys*, 48:119, 1976.

[25] R. Loudon. *The quantum theory of light*. Clarendon, Oxford, 1973.

[26] U. Martini, C. Ginzel, and A. Schenzle. Optical bistability and nonclassical photon counting statistics. *Optics Communications*, 102:379, 1993.

[27] P. Meystre and M. Sargent III. *Elements of quantum optics*. Springer, Berlin, 1990.

[28] S. Nakajima. *Progr. Theor. Physics*, 20:948, 1958.

[29] P.Filipowicz, J. Javanainen, and P. Meystre. Theory of a microscopic maser. *Phys. Rev. A*, 34:3077, 1986.

[30] G. Raithel, C. Wagner, H. Walther, L.M. Narducci, and M.O. Scully. The micromaser: A proving ground for quantum physics. In P.R. Berman, editor, *Cavity Quantum Electrodynamics*. Academic, New York, 1994.

[31] M. Reed and B. Simon. *Functional Analysis*. Academic Press, 1990.

[32] G. Rempe, R.J. Thompson, W.D. Lee, and H.J. Kimble. Optical bistability and photon statistics in cavity quantum electrodynamics. *Physical Review Letters*, 67(13):1727, 1991.

[33] G. Rempe, R.J. Thompson, R.J.Brecha, and P.R. Rice. *Optics Communications*, 82:73, 1991.

[34] A.M. Smith and C.W. Gardiner. Phase space method without large n scaling for the laser and optical bistability. *Phys Rev. A*, 38:4073, 1988.

[35] A.M. Smith and C.W. Gardiner. Three-level atom laser model with results ans applications. *Phys Rev. A*, 41:2730, 1990.

[36] M. Tavis and F.W. Cummings. Exact Solution for an N-Molecule-Radiation Field. *Physical Review*, 2:170, 1968.

[37] Werner Vogel and Dirk-Gunnar Welsch. *Lectures on Quantum Optics*. Akademie Verlag, 1998.

[38] H. Walther. Laser spectroscopy and quantum optics. *Reviews of modern Physics*, 71(2), 1999.

[39] E. Wehner, R. Seno, N. Sterpi, B.-G. Englert, and Herbert Walther. Atom pairs in the micromaser. *Optics Communications*, 110, 1994.

[40] P. Zanardi and F. Rossi. Quantum information in semiconductors: Noiseless encoding in a quantum-dot-array. *quant-ph/9804016*, 1998.

[41] R. Zwanzig. Ensemble method in the theory of irreversibility. *J. Chem. Phys.*, 33:1338, 1963.

Acknowledgement

In the first place I wish to thank Axel Schenzle for introducing me to the field of quantum optics and the granted support over the years. In our discussions he helped me to find the physical meaning behind the formal derivations of this work. Hans Briegel, Michael Fleischhauer and Berthold-Georg Englert contributed important suggestions. I appreciated very much the motivating atmosphere at the institute for theoretical physics of the Ludwig-Maximilians-Universität.

Finally I wish to thank my parents and the *Studienstiftung des deutschen Volkes* for the support during my course of studies.

Curriculum Vitae

Education

1972-1976 Primary school

1976-1985 Secondary school

1985 Abitur

1987-1993 Ludwig-Maximilians-University, Munich

1989 Intermediate diploma, Ludwig-Maximilians-University

1993 Diploma in physics, Ludwig-Maximilians-University

1993-2000 Dissertation, Ludwig-Maximilians-University

Employments

1985-1987 Civil service

since 1993 Ludwig-Maximilians-University, Technical University Munich

Grants

1990-1993 Studienstiftung des deutschen Volkes